

**CHARACTERIZATION AND FUNCTIONAL ANALYSIS OF A NOVEL
MULTICOPPER OXIDASE AND ASSOCIATED POLYKETIDE
BIOSYNTHESIS GENE CLUSTER OF *ASPERGILLUS FUMIGATUS***

**A THESIS SUBMITTED TO
THE GRADUATE SCHOOL OF NATURAL AND APPLIED SCIENCES
OF
MIDDLE EAST TECHNICAL UNIVERSITY**

BY

BANU METİN

**IN PARTIAL FULFILLMENT OF THE REQUIREMENTS
FOR
THE DEGREE OF DOCTOR OF PHILOSOPHY
IN
FOOD ENGINEERING**

OCTOBER 2007

Approval of the thesis:

**CHARACTERIZATION AND FUNCTIONAL ANALYSIS OF A NOVEL
MULTICOPPER OXIDASE AND ASSOCIATED POLYKETIDE
BIOSYNTHESIS GENE CLUSTER OF *ASPERGILLUS FUMIGATUS***

submitted by **BANU METİN** in partial fulfillment of the requirements for the degree
of **Doctor of Philosophy in Food Engineering Department, Middle East
Technical University** by,

Prof. Dr. Canan Özgen
Dean, Graduate School of **Natural and Applied Sciences**

Prof. Dr. Zümrüt B. Ögel
Head of Department, **Food Engineering**

Prof. Dr. Zümrüt B. Ögel
Supervisor, **Food Engineering Dept., METU**

Prof. Dr. Ufuk Bakır
Co-Supervisor, **Chemical Engineering Dept., METU**

Examining Committee Members:

Prof. Dr. Haluk Hamamcı
Food Engineering Dept., METU

Prof. Dr. Zümrüt B. Ögel
Food Engineering Dept., METU

Prof. Dr. Serap Emre
Medical Biology Dept., HU

Prof. Dr. Gülay Özcengiz
Biology Dept., METU

Assoc. Prof. Dr. G. Candan Gürakan
Food Engineering Dept., METU

Date: 25.10.2007

I hereby declare that all information in this document has been obtained and presented in accordance with academic rules and ethical conduct. I also declare that, as required by these rules and conduct, I have fully cited and referenced all material and results that are not original to this work.

Name, Last name : Banu Metin

Signature :

ABSTRACT

CHARACTERIZATION AND FUNCTIONAL ANALYSIS OF A NOVEL MULTICOPPER OXIDASE AND ASSOCIATED POLYKETIDE BIOSYNTHESIS GENE CLUSTER OF *ASPERGILLUS FUMIGATUS*

Metin, Banu

Ph.D., Department of Food Engineering

Supervisor: Prof. Dr. Zümürüt B. Ögel

Co-supervisor: Prof. Dr. Ufuk Bakır

October 2007, 154 pages

In this study, novel polyketide biosynthesis gene cluster of *Aspergillus fumigatus* was characterized and functionally analyzed. Analysis of the newly sequenced *A. fumigatus* genome for laccases, which are involved in melanin biosynthesis and detoxification in fungi, resulted in several putative laccase and multicopper oxidase gene sequences, one of which, Afu4g14490 (*tpnJ*), was selected for further characterization. The predicted amino acid sequence TpnJp showed 63% identity with the dihydrogeodin oxidase of *Aspergillus terreus*, which is involved in the biosynthesis of the antifungal geodin. When the genome region of *tpnJ* was investigated, the presence of a polyketide biosynthesis gene cluster containing 13 genes, hypothesized to be responsible for the production of trypacidin and monomethylsulochrin, was realized. By a comparative genomics approach, a putative geodin biosynthesis gene cluster containing 13 genes, including dihydrogeodin oxidase, in *A. terreus* and a putative trypacidin biosynthesis gene cluster containing 13 genes in *N. fischeri* were established. Targeted deletions of the polyketide synthase (*tpnC*) and multicopper oxidase (*tpnJ*) genes confirmed the hypothesis that

TpnCp, a three-domain minimal polyketide synthase, is involved in trypacidin and monomethylsulochrin biosynthesis in *A. fumigatus*. TpnCp is the first fungal minimal polyketide synthase whose functional role was experimentally identified. Moreover, the fact that LC-MS analysis of $\Delta tpnJ$ strain showed the absence of trypacidin and the presence of a higher amount of monomethylsulochrin in $\Delta tpnJ$ strain, confirmed the hypothesis that TpnJp is involved in the oxidation of monomethylsulochrin into trypacidin. This novel multicopper oxidase having high substrate specificity is given the name monomethylsulochrin oxidase.

Keywords: *Aspergillus fumigatus*, trypacidin, monomethylsulochrin, polyketide synthase, monomethylsulochrin oxidase.

ÖZ

***ASPERGILLUS FUMIGATUS*'UN YENİ BİR POLİKETİT BİYOSENTEZİ GEN KÜMESİNİN FONKSİYONEL ANALİZİ VE KARAKTERİZASYONU**

Metin, Banu

Doktora, Gıda Mühendisliği Bölümü

Tez Danışmanı: Prof. Dr. Zümrüt B. Ögel

Yardımcı Tez Danışmanı: Prof. Dr. Ufuk Bakır

Ekim 2007, 154 sayfa

Bu çalışmada, *Aspergillus fumigatus*'un yeni bir poliketit biyosentezi gen kümesinin karakterizasyonu ve fonksiyonel analizi gerçekleştirilmiştir. Dizilimi yeni açıklanan *A. fumigatus* genomunun melanin biyosentezinde ve detoksifikasyonda rol oynadığı bilinen lakkazlar yönünden analizi, çeşitli olası lakkaz ve çoklu bakır oksidaz gen dizilimlerinin bulunmasıyla sonuçlanmış; bunlardan bir tanesi, Afu4g14490 (*tpnJ*), daha detaylı karakterizasyon için seçilmiştir. *TpnJp*'nin tahmin edilen amino asit dizilimi, *A. terreus*'un bir antifungal olan geodinin biyosentezinde rol alan dihidrogeodin oksidazında % 63 benzerlik göstermiştir. Genomda *tpnJ*'nin bulunduğu alan incelendiğinde, tripasidin ve monometilsulokrin biyosentezinde görev aldığı düşünülen, 13 genlik bir poliketit gen kümesini tespit edilmiştir. Karşılaştırmalı genomic bir yaklaşımla, *A. terreus*'ta, dihidrogeodin oksidazı da içeren, 13 genlik bir olası geodin biyosentez gen kümesi, *N. fischeri*'de de yine 13 genlik bir olası tripasidin gen kümesi saptanmıştır. Poliketit sentaz (*tpnC*) and çoklu bakır oksidaz (*tpnJ*) genlerinin hedefli yokedilmeleri, üç domainli minimal bir yapıya sahip olan *TpnCp*'nin tripasidin ve monometilsulokrin biyosentezinde rol aldığı hipotezini doğrulamıştır. *TpnCp*, fonksiyonel rolü deneysel olarak açığa

kavuşturulmuş ilk fungal minimal poliketit sentazdır. Ayrıca, $\Delta tpnJ$ suşunun LC-MS analizi sonucunda tripasidin üretiminin yok olması ve monometilsulokrinin daha fazla üretildiğininin saptanması, TpnJ'nin monometilsulokrinin tripasidine oksidasyonunda görev aldığını doğrulamıştır. Bu yeni çoklu bakır oksidaza, yüksek bir substrat spesifisitesine sahip gözüktüğünden monometilsulokrin oksidaz ismi verilmiştir.

Anahtar Kelimeler: *Aspergillus fumigatus*, tripasidin, monometilsulokrin, poliketit sentaz, monometilsulokrin oksidaz.

To my parents

ACKNOWLEDGMENTS

I would like to extend thanks to my supervisor Prof. Dr. Zumrut Ogel and my co-supervisor Prof. Dr. Ufuk Bakir for their guidance in this study.

I would like to express sincere thanks to Prof. Gillian Turgeon from the Department of Plant Pathology, Cornell University. Being far away from home would not have been easy without her kindness, help and friendship. Without spending four months in her lab, I would not have completed this thesis.

I would like to express special thanks to Dr. Berna Arapaslan for her invaluable support and encouragement, which played a very important role in the realization of this thesis.

I also want to thank my labmates, Betul, Alper, Gokhan, Sumeyra, Ozlem, Yonca, Elife, Nansilma, Ayla, Abdulvali, Bengu, Tunca and Meltem for their support and friendship throughout these years.

I would also like to thank my labmates from Cornell, Patrik, Gianna, Kathryn, JinYuan and Schinichi for their help and friendship.

I would like to extend sincere thanks to Hatice, who was always with me during my Ithaca days. She did everything she could to feel myself at home.

Special thanks go to my dear friends, Ceren, Betul, Ozlem, and Filiz. Thank you for everything that you do for me... I cannot imagine a world without you.

At last, but not the least, I would like to express sincere thanks to my parents, my sisters, Bilge and Betul, and my husband, Semih. You have always been there with your love, support and faith. I am so lucky to have all of you.

TABLE OF CONTENTS

ABSTRACT	iv
ÖZ	vi
DEDICATION	viii
ACKNOWLEDGMENTS	ix
TABLE OF CONTENTS	x
LIST OF TABLES.....	xv
LIST OF FIGURES	xvi
CHAPTER	
1. INTRODUCTION	1
1.1. The Genus <i>Aspergillus</i>	1
1.2. <i>Aspergillus fumigatus</i>	2
1.2.1. Biology of <i>A. fumigatus</i>	2
1.2.2. Genome Sequence of <i>A. fumigatus</i>	4
1.3. Fungal Secondary Metabolism	10
1.3.1. Classes of fungal Secondary Metabolites	11
1.3.1.1. Polyketides	11
1.3.1.1.1. Biosynthesis of Polyketides: Polyketide Synthases	13
1.3.1.1.2. Fungal Polyketide Synthases	17
1.3.1.2. Non-Ribosomal Peptides.....	21
1.3.1.3. Terpenes	25
1.3.1.4. Indole alkaloids	27
1.3.2. Gene Cluster Concept of Secondary Metabolites	27
1.4. Multicopper Oxidases.....	29
1.4.1. Enzymology of Multicopper Oxidases	29
1.4.2. Multicopper Oxidases in Secondary Metabolite Biosynthesis	32
1.5. Aim of the Study	35

2. MATERIALS and METHODS	37
2.1. Materials	37
2.1.1. Fungal Strains.....	37
2.1.2. Bacterial Strains	37
2.1.3. Plasmids	37
2.1.4. Chemicals and Enzymes	38
2.1.5. Growth Media, Buffers and Solutions.....	38
2.2. Methods	38
2.2.1. Maintenance and Cultivation of Strains	38
2.2.2. Nucleic Acid Isolation Techniques	39
2.2.2.1. Genomic DNA Isolation	39
2.2.2.2. Plasmid DNA Isolation	40
2.2.2.3. Total RNA Isolation.....	41
2.2.2.4. Recovery of DNA from Agarose Gel	42
2.2.2.5. Recovery of DNA from PCR reaction.....	43
2.2.3. The Polymerase Chain Reaction (PCR) and Reverse Transcriptase Polymerase Chain Reaction (RT-PCR).....	43
2.2.4. Agarose Gel Electrophoresis and Visualization of DNA and RNA	4Error! Bookmark not defined.
2.2.5. Restriction Enzyme Digestion of DNA	45
2.2.6. Ligation.....	45
2.2.7. Transformation of <i>E. coli</i> XL1 Blue MRF'	46
2.2.8. Sequencing.....	47
2.2.9. Transformation of <i>Aspergillus sojae</i>	47
2.2.9.1. <i>A. sojae</i> Strain Used for Heterologous Expression.....	47
2.2.9.2. Selection Plasmid.....	47
2.2.9.3. Expression vectors	47
2.2.9.4. <i>Aspergillus sojae</i> Transformation Protocol.....	48
2.2.10. Southern Blot.....	49
2.2.10.1. Labeling of Probe DNA	50
2.2.10.2. Blot Assembly	50
2.2.10.3. Hybridization	51

2.2.10.4. Detection	52
2.2.11. Enzyme Assays.....	53
2.2.12. SDS-PAGE.....	53
2.2.12.1. Gel Plate Assembly.....	53
2.2.12.2. Gel Pouring.....	54
2.2.12.3. Sample Preparation and Electrophoresis.....	54
2.2.12.4. Silver Staining	56
2.2.13. Split Marker Method for Targeted Gene Deletion	56
2.2.14. Transformation of <i>Aspergillus fumigatus</i> AfS28	58
2.2.15. Detection of Monomethylsulochrin and Trypacidin from <i>Aspergillus</i> <i>fumigatus</i>	60
3. RESULTS and DISCUSSION.....	61
3.1. Experimental Strategy	61
3.2. Analysis of <i>A. fumigatus</i> Genome for Laccase Genes	63
3.2.1. Characterization of Afu4g14490 Gene.....	63
3.2.2. Bioinformatic Analysis of the Gene Cluster Containing Afu4g14490	68
3.3. Heterologous Expression Studies of <i>tpnJ</i> in <i>Aspergillus sojiae</i>	80
3.3.1. Primer Design.....	80
3.3.2. Amplification of <i>tpnJ</i> by Genomic PCR	81
3.3.3. Ligation of the PCR Products onto pAN52-1 and pAN52-4 Expression Vectors.....	82
3.3.5. Sequencing of Plasmids pTPNJ52-1 and pTPNJ52-4	86
3.3.6. Transformation of <i>A. sojiae</i> with pTPNJ52-1 and pTPNJ52-4.....	87
3.3.7. Analysis of Transformant Strains.....	87
3.3.7.1. Analysis of Transformant Strains by PCR	87
3.3.7.1.1. Primer Design to Amplify <i>tpnJ</i> Gene	87
3.3.7.1.2. PCR with TpnJinF and TpnJinR.....	88
3.3.7.2. Analysis of Transformant Strains by Southern Blotting.....	89
3.3.7.3. Analysis of <i>tpnJ</i> Transcription by RT-PCR	90
3.3.7.3.1. Preparation of RNA Samples	90
3.3.7.3.2. RT-PCR.....	91

3.3.7.4. Enzyme Assays with <i>A. sojae</i> TPNJ52-1#3, <i>A. sojae</i> TPNJ52-4#1 and <i>A. fumigatus</i>	94
3.4. Characterization of the Putative Trypacidin Gene Cluster.....	98
3.4.1. Targeted Deletions of <i>tpnC</i> (Afu4g14550, Polyketide Synthase) and <i>tpnJ</i> (Afu4g14490, Multicopper Oxidase-Monomethylsulochrin Oxidase) ..	98
3.4.1.1. The <i>A. fumigatus</i> Strain for Targeted Gene Deletion	99
3.4.1.2. PCR to Amplify <i>hygB</i> (Hygromycin B Phosphotransferase) Split Marker Fragments	100
3.4.1.3. Targeted <i>tpnC</i> Deletion.....	102
3.4.1.3.1. Primer Design for <i>tpnC</i> Deletion	102
3.4.1.3.2. First Round PCR.....	103
3.4.1.3.3. Second Round PCR.....	104
3.4.1.3.4. Transformation of <i>A. fumigatus</i> AfS28 with <i>tpnC</i> Split Marker Fragments.....	105
3.4.1.3.5. Analysis of $\Delta tpnC$ Transformants by PCR.....	105
3.4.1.3.6. Analysis of $\Delta tpnC$ Transformants by Southern Blot	107
3.4.1.4. Targeted <i>tpnJ</i> Deletion.....	108
3.4.1.4.1. Primer Design for <i>tpnJ</i> Deletion.....	108
3.4.1.4.2. First Round PCR.....	109
3.4.1.4.3. Second Round PCR.....	110
3.4.1.4.4. Transformation of <i>A. fumigatus</i> AfS28 with <i>tpnJ</i> Split Marker Fragments.....	111
3.4.1.4.5. Analysis of $\Delta tpnJ$ Transformants by PCR	112
3.4.1.4.6. Analysis of $\Delta tpnJ$ Transformants by Southern Blotting	114
3.4.2. Detection of Metabolites from <i>A. fumigatus</i> AfS28, $\Delta tpnC1$, and $\Delta tpnJ2$ by Liquid Chromatography Mass Spectrometry	116
3.4.3. Phenotypic Assays.....	120
3.4.3.1. Analysis of the Effect of Carbon Sources	120
3.4.3.2. Analysis of the Effect of Nitrogen Sources.....	122
3.4.3.3. Analysis of the Effect of Temperature.....	123
3.4.3.4. Analysis of the Effect of Oxidative and Osmotic Stress on Growth	123

3.4.3.5. Analysis of the Effect of Cell Wall Inhibitor Agents on Growth	124
3.4.3.6. Analysis of the Effect of Antifungal Agents on Growth	124
4. CONCLUSION AND FUTURE WORK.....	126
REFERENCES	128
APPENDICES	
A. CHEMICALS, ENZYMES AND THEIR SUPPLIERS	141
B. PREPARATIONS OF GROWTH MEDIA, BUFFERS AND SOLUTIONS.	143
C. PLASMID MAPS	149
VITA	150

LIST OF TABLES

TABLE

Table 1.1. Infrageneric taxa of the genus <i>Aspergillus</i>	2
Table 1.2. Ascomycetous genera with an <i>Aspergillus</i> anamorph	2
Table 1.3. Properties of the <i>Aspergillus fumigatus</i> Af293 genome	6
Table 1.4. Secondary metabolite gene types in <i>A. fumigatus</i> , <i>A. nidulans</i> and <i>A. oryzae</i>	7
Table 1.5. Genome statistics	9
Table 1.6. Secondary metabolites detected from species in section <i>Fumigati</i>	12
Table 1.7. NRPS genes of <i>A. fumigatus</i> , with hypothetical NRPS domain architecture based on in silico analysis	23
Table 2.1. Separating Gel Preparation	55
Table 2.2. Stacking Gel Preparation	55
Table 3.1. Bioinformatic analysis of the putative proteins encoded by genes in the cluster containing Afu4g14490	69
Table 3.2. Features of the primers designed for heterologous expression	81
Table 3.3. Features of the primers designed for amplification of <i>tpnJ</i>	87
Table 3.4. Determination of RNA yield and purity by spectrophotometer.....	91
Table 3.5. Features of the primers amplifying <i>hygB</i>	100
Table 3.6. Features of the primers designed for <i>tpnC</i> deletion.....	102
Table 3.7. PCR products that can be obtained with <i>A. fumigatus</i> AfS28, Δ <i>tpnC</i> knock-out strain and a strain with a possible ectopic integration.....	105
Table 3.8. Features of the primers designed for <i>tpnJ</i> deletion.....	109
Table 3.9. PCR products that can be obtained with <i>A. fumigatus</i> AfS28, Δ <i>tpnJ</i> knock-out strain and a strain with a possible ectopic integration.....	113

LIST OF FIGURES

FIGURE

Figure 1.1. Scanning electron microscope image of an <i>Aspergillus fumigatus</i> conidiophore.....	4
Figure 1.2. <i>Aspergillus fumigatus</i> chromosomes.....	5
Figure 1.3. Phylogenetic tree of 5 <i>Aspergillus</i> species	9
Figure 1.4. Examples of polyketide secondary metabolites.....	13
Figure 1.5. Common acyl-CoA thioesters used for chain initiation and elongation by PKSs.....	14
Figure 1.6. Posttranslational modification of ACP domains by phosphopantetheinyltransferases	15
Figure 1.7. β -Carbon processing in PKSs	16
Figure 1.8. Examples for non-reducing (NR: PksA, Pks1, WA), partially reducing (PR: 6-MSAS), and highly reducing (HR: LDKS, MlcB, SQTKS, LNKS, MlcA) PKS, and their domain architectures.....	18
Figure 1.9. Basic mechanism of fungal polyketide biosynthesis	18
Figure 1.10. Melanin biosynthesis gene cluster of <i>A. fumigatus</i>	20
Figure 1.11. Sporulating cultures of the <i>A. fumigatus</i> wild-type strain and six single-gene deletants.....	20
Figure 1.12. ACV synthetase, a trimodular non-ribosomal peptide synthetase	22
Figure 1.13. Terpene biosynthetic pathway	26
Figure 1.14. (a) Three-dimensional structure, (b) copper binding sites of <i>Melanocarpus albomyces</i> laccase.....	31
Figure 1.15. Copper binding regions of multicopper oxidases showing high degree of homology	32
Figure 1.16. Biosynthesis of (+)-geodin in <i>A. terreus</i> and astrictic acid in <i>P. frequentans</i>	33

Figure 2.1. Split marker strategy for gene deletion	57
Figure 3.1. Experimental strategy flow chart	62
Figure 3.2. The alignment of the predicted protein sequence of Afu4g14490 and dihydrogeodin oxidase gene of <i>A. terreus</i>	65
Figure 3.3. Predicted Afu4g14490 sequence both at the DNA and amino acid level.....	67
Figure 3.4. Comparison the laccase signature sequences developed by Suresh Kumar <i>et al.</i> (2003) to the corresponding residues in DHGO and the predicted amino acid sequence of Afu4g14490.....	67
Figure 3.5. The 21.8 kb-gene cluster containing Afu4g14490.....	68
Figure 3.6. Conserved domain architecture analysis of the polyketide synthase of <i>A. fumigatus</i> , Afu4g14560	70
Figure 3.7. Genealogy of fungal type I PKSs.....	71
Figure 3.8. Biosynthesis of geodin	72
Figure 3.9. Chemical structures of geodin (a) and trypacidin (b).....	72
Figure 3.10. Comparison of the putative trypacidin (a) and geodin (b) gene clusters from <i>A. fumigatus</i> and <i>A. terreus</i> , respectively, identified by a comparative genomics approach in this study.....	74
Figure 3.11. Comparison of the putative trypacidin gene clusters from <i>A. fumigatus</i> (a) and <i>N. fischeri</i> (b) identified by a comparative genomics approach in this study	75
Figure 3.12. Putative enzymatic steps for conversion of VA to DMST	76
Figure 3.13. Reaction scheme for questin to desmethylsulochrin conversion proposed by Henry and Townsend (2005).....	77
Figure 3.14. (a) Conversion dihydrogeodin to geodin in <i>A. terreus</i> (Fujii <i>et al.</i> (1987); (b) conversion of sulochrin to bisdechlorogeodin in <i>P.frequentans</i> (Huang <i>et al.</i> , 1996); (c) proposed conversion of monomethylsulochrin to trypacidin in <i>A. fumigatus</i>	79
Figure 3.15. Possible gene products in the biosynthesis of geodin	79
Figure 3.16. Proposed biosynthesis of trypacidin and monomethylsulochrin	80

Figure 3.17. Annealing sites of the primers designed to amplify <i>tpnJ</i> . S denotes the signal peptide region	81
Figure 3.18. Amplification of <i>tpnJ</i> using the primer pairs P5-P6 (lane 1) and P7-P8 (lane 2)	82
Figure 3.19. Isolation of (a) pAN52-1, lane 1, 5733 bp and (b) pAN52-4, lane 2, 5760 bp.....	83
Figure 3.20. (a) Recombinant plasmid pTPNJ52-1, 7892 bp, lane 1; (b) Restriction digestion of pTPNJ52-1 with <i>NcoI</i> leading to 5733 bp vector and 2159 bp insert (lane 2)	84
Figure 3.21. (a) Recombinant plasmid pTPNJ52-4, 7839 bp, lane 1; (b) Restriction digestion of pTPNJ52-4 with <i>BamHI</i> leading to 5760 bp vector and 2079 bp insert (lane 2)	84
Figure 3.22. Maps of recombinant pTPNJ52-1 (a) and pTPNJ52-1 (b) plasmids.	85
Figure 3.23. Analysis of amino acid sequences of TpnJp and TpnJp with A16P mutation by SOSUisignal program	86
Figure 3.24. Annealing sites of the primers TpnJinF and TpnJinR.....	88
Figure 3.25. PCR with TpnJinF and TpnJinR using transformant, <i>A. sojae</i> and <i>A. fumigatus</i> DNAs	89
Figure 3.26. Analysis of <i>A. sojae</i> TPNJ52-1#3, <i>A. sojae</i> TPNJ52-4#1, <i>A. fumigatus</i> and <i>A. sojae</i> host strains by genomic Southern Blotting	90
Figure 3.27. Total RNA isolation from the 3 rd cultivation day of <i>A. sojae</i> strains and 3 rd and 5 th cultivation day of <i>A. fumigatus</i>	92
Figure 3.28. Analysis of transcription of <i>tpnJ</i> in <i>A. sojae</i> strains by RT-PCR using primers TpnJinF and TpnJinR	93
Figure 3.29. Analysis of transcription of <i>tpnJ</i> in <i>A. fumigatus</i> by RT-PCR using primers TpnJinF and TpnJinR	93
Figure 3.30. Thin layer chromatography (TLC) of sulochrin reactions.....	95
Figure 3.31. TLC of control reaction with commercial laccase (from <i>Trametes versicolor</i>) and sulochrin.....	95
Figure 3.32. TLC of reactions performed with cell extracts and sulochrin	96
Figure 3.33. TLC of reactions performed with dihydrogeodin (DHG) using (a) supernatants (b) cell extracts	97

Figure 3.34. SDS-PAGE of proteins from pAMDSPYRG transformed <i>A. sojae</i> host strain, <i>A. sojae</i> TPNJ52-1#3 and <i>A. sojae</i> TPNJ52-4#1	98
Figure 3.35. Annealing sites of the primers to amplify <i>hygB</i>	101
Figure 3.36. Amplification of the overlapping marker fragments.....	101
Figure 3.37. Annealing sites of the primers for <i>tpnC</i> deletion	103
Figure 3.38. First round PCR for <i>tpnC</i> deletion (a) PCR showing 5' and 3' flank fragments, (b) Annealing sites of the primers used in first round PCR.....	103
Figure 3.39. Second round PCR for <i>tpnC</i> deletion	104
Figure 3.40. The annealing sites of the primers designed on DNA from <i>A. fumigatus</i> AfS28, from a knock-out strain and from a strain with ectopic integration.....	106
Figure 3.41. Analysis of <i>A. fumigatus</i> AfS28 and $\Delta tpnC$ transformants by PCR.....	106
Figure 3.42. The restriction sites on the <i>tpnC</i> locus of <i>A. fumigatus</i> AfS28 and on a possible knock-out strain.....	107
Figure 3.43. Analysis of <i>A. fumigatus</i> AfS28 and transformants $\Delta tpnC1$, $\Delta tpnC2$ and $\Delta tpnC3$ by Southern Blot.....	108
Figure 3.44. Annealing sites of the primers for <i>tpnJ</i> deletion.....	109
Figure 3.45. First round PCR for <i>tpnJ</i> deletion	110
Figure 3.46. Second round PCR for <i>tpnJ</i> deletion.....	111
Figure 3.47. The annealing sites of the designed primers on <i>A. fumigatus</i> AfS28 DNA, on the DNA from a knock-out strain and on the DNA from a strain with ectopic integration	112
Figure 3.48. Analysis of <i>A. fumigatus</i> AfS28 $\Delta tpnJ$ transformants by PCR.....	113
Figure 3.49. The restriction sites on the <i>tpnJ</i> locus of <i>A. fumigatus</i> AfS28 and on a possible knock-out strain.....	115
Figure 3.50. Analysis of <i>A. fumigatus</i> AfS28 and transformants $\Delta tpnJ2$ and $\Delta tpnJ3$ by Southern Blotting and hybridization	115
Figure 3.51. Chromatograms of <i>A. fumigatus</i> AfS28, $\Delta tpnC1$, and $\Delta tpnJ2$ extracts when searched for the presence of tryptacidin having a molecular weight of 344117	
Figure 3.52. Mass spectrum of the compound eluted at 23.4 min.....	118

Figure 3.53. Chromatograms of <i>A. fumigatus</i> AfS28, $\Delta tpnC1$, and $\Delta tpnJ2$ extracts when searched for the presence of monomethylsulochrin having a molecular weight of 346.....	119
Figure 3.54. Mass spectrum of the compound eluted at 24.7 min.....	120
Figure 3.55. Effects of different carbon sources on growth of <i>A. fumigatus</i> AfS28 and deletion strains	121
Figure 3.56. Effects of different nitrogen sources on growth of <i>A. fumigatus</i> AfS28 and deletion strains	122
Figure 3.57. Effect of temperature on growth of <i>A. fumigatus</i> AfS28 and deletion strains	123
Figure 3.58. Effect of oxidative and osmotic stress on growth, the medium was supplemented with H ₂ O ₂ (2 mM) and NaCl (1.5 M), respectively.....	124
Figure 3.59. Effect of cell wall inhibitor agents, SDS and congo red, on growth	125
Figure 3.60. Effect of antifungal agents, voriconazole and amphotericin B on growth	125
Figure C1. Map of pAN52-1	149
Figure C2. Map of pAN52-4	150
Figure C3. Map of pUCATPH	151

CHAPTER 1

INTRODUCTION

1.1. The Genus *Aspergillus*

The genus *Aspergillus* has a worldwide distribution and is one of the most common of all groups of fungi. They are possibly the greatest contaminants of natural and man-made organic products, and a few species can cause infections in man and animals. The aspergilli are also one of the most important mycotoxin-producing groups of fungi when growing as contaminants of cereals, oil seeds, and other foods. Not all aspergilli are viewed as troublesome contaminants, however, as several species have had their metabolic capabilities harnessed for commercial use (Smith, 1994).

The genus contains more than 180 species, with about 70 named teleomorphs. Samson, 1999 subdivided the genus *Aspergillus* into six subgenera and 18 sections as shown in Table 1.1. Group names following the classification of Raper and Fennel, 1965 are given in parentheses (Samson, 1999).

Aspergillus has teleomorphs placed in nine genera (Table 1.2). The most common teleomorph genera are *Eurotium*, *Neosartorya* and *Emericella*. Some genera such as *Hemicarpaceles* and *Warcupiella* have been found to be distantly related to other *Aspergillus* teleomorphs (Samson, 1999).

Table 1.1. Infrageneric taxa of the genus *Aspergillus* (Samson, 1999)

Subgenus	Section
<i>Aspergillus</i>	<i>Aspergillus</i> (<i>A. glaucus</i> group), <i>Restricti</i> (<i>A. restrictus</i> group)
<i>Fumigati</i>	<i>Fumigati</i> (<i>A. fumigatus</i> group), <i>Cervini</i> (<i>A. cervinus</i> group)
<i>Ornati</i>	(<i>A. ornatus</i> group)
<i>Clavati</i>	<i>Clavati</i> (<i>A. clavatus</i> group)
<i>Nidulantes</i>	<i>Nidulantes</i> (<i>A. nidulans</i> group), <i>Versicolor</i> (<i>A. versicolor</i> group), <i>Usti</i> (<i>A. ustus</i> group), <i>Terrei</i> (<i>A. terreus</i> group), <i>Flavipedes</i> (<i>A. flavipes</i> group)
<i>Circumdati</i>	<i>Wentii</i> (<i>A. wentii</i> group), <i>Flavi</i> (<i>A. flavus</i> group), <i>Nigri</i> (<i>A. niger</i> group), <i>Circumdati</i> (<i>A. ochraceus</i> group), <i>Candidi</i> (<i>A. candidus</i> group), <i>Cremai</i> (<i>A. cremeus</i> group), <i>Sparsi</i> (<i>A. sparsus</i> group)

Table 1.2. Ascomycetous genera with an *Aspergillus* anamorph (Samson, 1999)

Section <i>Aspergillus</i> :	<i>Eurotium</i> , <i>Dichlaena</i> , <i>Edyuillia</i>
Section <i>Fumigati</i> :	<i>Neosartorya</i>
Subgenus <i>Ornati</i> :	<i>Warcupiella</i> , <i>Sclerocleista</i> , <i>Hemicarpenoteles</i>
Section <i>Nidulantes</i> :	<i>Emericella</i>
Section <i>Flavipedes</i> :	<i>Fennellia</i>
Section <i>Circumdati</i> :	<i>Petromyces</i>
Section <i>Cremai</i> :	<i>Chaetosartorya</i>

1.2. *Aspergillus fumigatus*

1.2.1. Biology of *A. fumigatus*

A. fumigatus is by far the most important pathogenic *Aspergillus* species known and until recently this was the only species that was considered pathogenic

from *Aspergillus* section *Fumigati* (Samson *et al.*, 2006). However, *Neosartorya pseudofischeri* was also reported as a potential human pathogen (Padhye *et al.*, 1994; Peterson, 1992; Jarv *et al.*, 2004) and recently *A. lentulus* was described as a pathogen related to *A. fumigatus* (Balajee *et al.*, 2005).

Geiser *et al.*, 1998 found that *A. fumigatus* and *N. fischeri* show a very close relationship, indicated by their molecular data but also by the production of the same secondary metabolites as reported by Larsen *et al.*, 2007. However, DNA-DNA reassociation values less than 70% were found for *A. fumigatus* and *Neosartorya*, proving conclusively that *Neosartorya* is not the teleomorph form of *A. fumigatus* (Peterson, 1992). Other analyses using different methods produced identical results (Girardin *et al.*, 1995). Unlike *A. nidulans*, which has a well-characterized sexual cycle, no sexual cycle has been described for *A. fumigatus* (Brakhage and Langfelder, 2002).

A. fumigatus is a saprophytic fungus that plays an essential role in recycling environmental carbon and nitrogen. Its natural ecological niche is the soil, wherein it survives and grows on organic debris. Although this species is not the most prevalent fungus in the world, it is one of the most ubiquitous of those with airborne conidia. It sporulates abundantly, with every conidial head producing thousands of conidia. The conidia released into the atmosphere have a diameter small enough to reach the lung alveoli (Latge, 1999). *A. fumigatus* conidia are continuously inhaled by humans but rarely have any adverse effects as they are eliminated efficiently by the innate immune response. However, the harmless status of *A. fumigatus* has changed over the past 10-20 years, owing to the increasing number of immunosuppressed patients and an increase in the severity of immunosuppressive therapies (Latge, 2001). Diseases caused by *A. fumigatus* can be divided into three categories: (a) allergic reactions and (b) colonization with restricted invasiveness are observed in immunocompetent individuals, whereas (c) systemic infections with high mortality rates occur in immunocompromised patients (Brakhage and Langfelder, 2002).

A. fumigatus conidia are gray-green in color and only 2.5-3 μm in diameter. Conidia contain a single haploid nucleus. The conidiophore extends from a foot cell at right angles to the mycelium and culminates in a broadly clavate vesicle (20-30 μm in diameter). A single layer of cells (phialides) is attached to the apical side of

the vesicle. The conidia result from a constriction of an elongated portion of the phialide (Figure 1.1) (Brakhage and Langfelder, 2002).

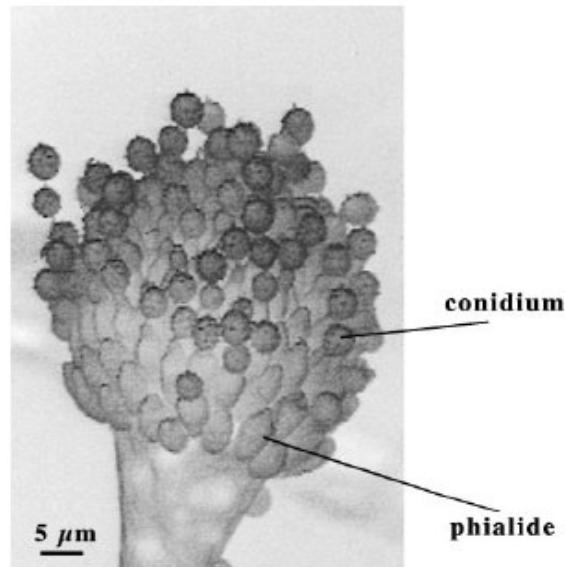


Figure 1.1. Scanning electron microscope image of an *Aspergillus fumigatus* conidiophore (Brakhage and Langfelder, 2002).

A. fumigatus is able to grow rapidly on minimal agar plates containing a carbon source, a nitrogen source and trace elements. In addition to being relatively flexible with regard to growth medium, *A. fumigatus* is also able to withstand high temperatures. Growth occurs up to 55°C, and conidia are able to survive at temperatures up to 70°C (Brakhage and Langfelder, 2002).

1.2.2. Genome Sequence of *A. fumigatus*

The genome of the fully pathogenic clinical *A. fumigatus* isolate Af293 was sequenced by the whole genome random sequencing method and augmented by

optical mapping for sequence assembly confirmation (Nierman et al., 2005a and 2005b). The completed Af293 genome consists of eight chromosomes with estimated optical map sizes of: Chromosome 1, 4.9 Mb; 2, 4.8 Mb; 3, 4.0 Mb; 4, 3.9 Mb; 5, 3.9 Mb; 6, 3.6 Mb; 7, 2.0 Mb; and 8, 1.8 Mb, for a total size of 29.2 Mb (Figure 1.2). The 31,892 bp mitochondrial genome contains 16 protein-coding genes and 25 tRNAs.

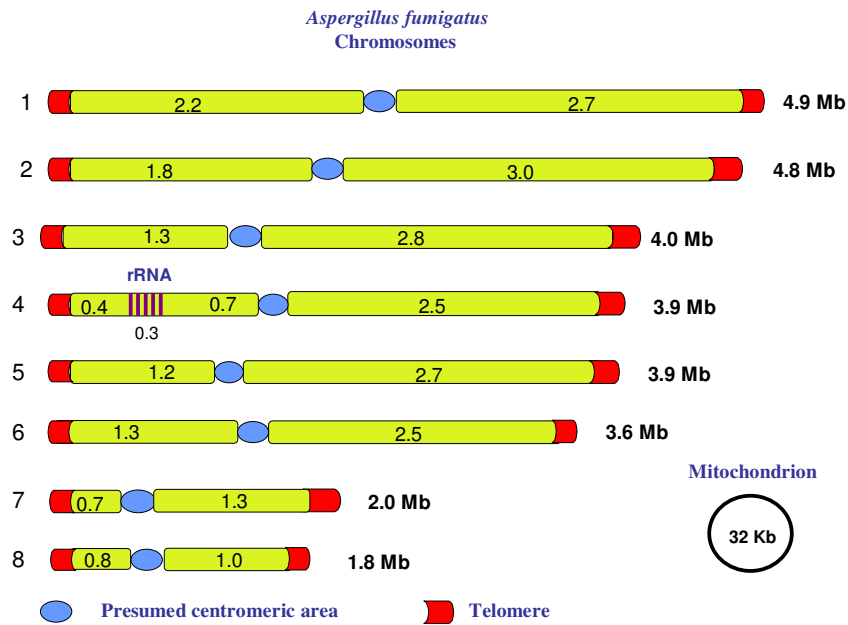


Figure 1.2. *Aspergillus fumigatus* chromosomes (Nierman *et al.*, 2005a). The 8 chromosomes of *A. fumigatus* are represented from largest to smallest, short arm to long arm. The size presented to the right of each chromosome representation is the optical map estimated size. The numbers superimposed on each arm is the size of that arm in Mb by sequence content. The location of the rRNA repeat cluster is represented by the brown vertical bars. The number of repeats is estimated to be 35 by the optical map. The direction of the repeat telomeric to centromeric is 28S to 18S. The 33 copies of 5S rRNA are dispersed in the genome. No centromere is completely sequenced. There are also physical gaps at the rDNA repeats on Chromosome 4 as well as at a subtelomeric location on Chromosome 6.

The nuclear genome of *A. fumigatus* contains 9,926 identified protein coding sequences, 3,288 of which code for proteins with unknown functions (Table 1.3). The protein-coding genes and other genome features were identified by an automated annotation pipeline coupled with manual review (Nierman *et al.*, 2005a).

Table 1.3. Properties of the *Aspergillus fumigatus* Af293 genome (Nierman *et al.*, 2005a).

Genome	Value
Nuclear genome	
General information	
Size (Mb)	29.4
G+C content (%)	49.9
Gene number	9,926
Mean gene length (bp)	1,431
Per cent coding	50.1
Per cent genes with introns	77.0
Genes of unknown function	3,288
Exons	
Mean number per gene	2.8
Mean length (bp)	516
G+C content (%)	54.0
Introns	
Mean number per gene	1.8
Mean length (bp)	112
G+C content (%)	46.3
Intergenic regions	
Mean length (bp)	1,226
G+C content (%)	46.0
RNA	
tRNA number	179
5S rRNA number	33
Mitochondrial genome	
Size (bp)	31,892
G+C content (%)	25.4
Gene number	16
Mean gene length (bp)	1,189
Per cent coding	44.1
Per cent genes with introns	6.2
tRNA number	33

A. fumigatus virulence may be augmented by its numerous secondary metabolites. Genes controlling fungal secondary metabolites are generally organized in clusters, many of which are species-specific. The *A. fumigatus* genome contains 26 such clusters with polyketide synthase, nonribosomal peptide synthase and/or dimethylallyl tryptophan synthase genes. Only 13 of the 26 clusters have orthologues in *A. oryzae* and/or *A. nidulans*, and ten of these orthologous clusters are missing many or most of the genes present in the *A. fumigatus* clusters. The unique clusters of *A. fumigatus* are dispersed in the genome with a bias towards telomeric locations. Many of these clusters contain regulatory genes, genes associated with resistance such as transporters involved in efflux, and genes with no obvious role in production of the metabolite. Fifteen of the clusters contain 22 transcriptional regulators, which are probably specific to their cluster because they do not have strong similarity to other proteins in the databases. In contrast to these regulators within the clusters, other global regulators of secondary metabolite synthesis are dispersed in the *A. fumigatus* genome. The genome also contains one copy of *laeA* encoding a global regulator of *Aspergillus* secondary metabolites (Nierman *et al.*, 2005a).

Table 1.4 summarizes the numbers of different classes of secondary metabolite genes for *A. fumigatus* (Nierman *et al.*, 2005a), *A. nidulans* (Galagan *et al.*, 2005) and *A. oryzae* (Machida *et al.*, 2005).

Table 1.4. Secondary metabolite gene types in *A. fumigatus*, *A. nidulans* and *A. oryzae* (Nierman *et al.*, 2005a).

Gene type	<i>A. fumigatus</i>	<i>A. nidulans</i>	<i>A. oryzae</i>
Polyketide synthase	14	27	30
Non-ribosomal peptide synthetase	14*	14*	18
Sesquiterpene cyclase	-	1	1
Dimethylallyl tryptophan synthase	7	2	2

*Includes one hybrid peptide/polyketide synthase

The publication of the genomes of *Aspergillus fumigatus*, a human pathogen, *Aspergillus oryzae*, important in food production, and *Aspergillus nidulans*, a genetic model organism, represents a milestone for the *Aspergillus* research community, expanding knowledge of fungal physiology and mechanisms of gene regulation. Although members of the same genus, phylogenetic analysis of these species revealed that the three aspergilli differ considerably in their genome sequences. Predicted orthologs shared by all three species display an average of only 68% amino acid identity, comparable to that between mammals and fish. The three species also differ considerably in genome size and show extensive structural reorganization (Galagan *et al.*, 2005; Wortman *et al.*, 2006).

Given the large evolutionary distance between the sequenced aspergilli, three additional genome projects are being funded by the National Institute of Allergy and Infectious Disease, National Institutes of Health (NIAID, USA) with the goal of better elucidating the genome of pathogenic *A. fumigatus*: *Neosartorya fischeri* (*Aspergillus fischerianus*), *Aspergillus clavatus* and *Aspergillus terreus*. The objectives in sequencing these three genomes are to use comparative genomics to improve annotation in the sequenced *Aspergillus* genomes, to provide new targets for experimental studies, to identify differences in gene content and/or regulatory elements that might contribute to pathogenicity, and to facilitate vaccine component selection with the ultimate goal of preventing invasive aspergillosis. The genomes of *N. fischeri* and *A. clavatus* are being sequenced by The Institute for Genomic Research (TIGR) and *A. terreus* is being sequenced by the Broad Institute (Wortman *et al.*, 2006).

The assembled genomic sequences of *N. fischeri* and *A. clavatus* are available to the public and a first round of automated annotation has allowed the investigation of the genome structure and gene content of these species in comparison to the published *A. fumigatus* Af293. The genome sequence of a second *A. fumigatus* strain (CEA10) was also made available by Merck & Co (Rahway, NJ, USA). The assembled genome sizes are similar, as seen in Table 1.5, with *N. fischeri* approximately 10% larger. Gene numbers are approximate, as they reflect the raw output of the automated pipeline without manual review and modification, with the exception of *A. fumigatus* which was manually improved prior to publication. Due to

issues with missing and merged gene predictions, it is expected that the gene number for *A. clavatus*, in particular, will increase. The average protein identity between *A. fumigatus* and *N. fischeri* orthologs is 94%, while that between *A. fumigatus* and *A. clavatus* is 80% (Wortman *et al.*, 2006). As described by Galagan *et al.*, 2005, the average protein identity between *A. fumigatus* and *A. oryzae* is 70%, and that between *A. fumigatus* and *A. nidulans* is 66%. A set of 1000 orthologs between these five species were used by Wortman *et al.*, 2005 to generate an inclusive phylogeny (Figure 1.3).

Table 1.5. Genome statistics (Wortman *et al.*, 2006).

	<i>A. fumigatus</i> Af293	<i>A. fumigatus</i> CEA10	<i>N. fischeri</i>	<i>A. clavatus</i>
Size (Mb)	29.4	29.2	32.0	27.7
GC content	49.9	49.4	49.6	49.2
Genes	9926	10099	10929	8653
Mean gene length (bp)	1431.0	1425.2	1434.3	1436.8

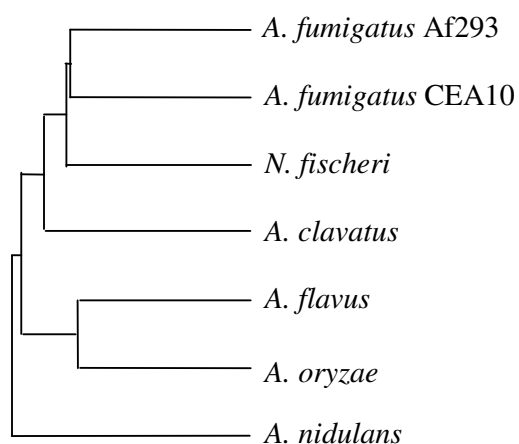


Figure 1.3. Phylogenetic tree of 5 *Aspergillus* species (Wortman *et al.*, 2006).

A. fumigatus isolates Af293 and CEA10 display variation in their genome structure, with smallscale insertions/deletions and rearrangements. Careful inspection of the Af293 and CEA10 genomes revealed a number of unique, strain-specific genes (2%), located predominantly in non-syntenic subtelomeric blocks. A few strain-specific regions contain putative gene clusters involved in secondary metabolism, osmotolerance, or arsenic resistance, highlighting the potential role of the subtelomeric regions in maintaining species variability (Wortman *et al.*, 2006).

An initial examination of the genome sequences and predicted proteomes of *A. fumigatus*, *N. fischeri* and *A. clavatus* by Wortman *et al.* (2006) reveals extensive conservation of gene content and order. The core chromosome regions encode predominantly highly conserved housekeeping genes, whereas strain- and lineage-specific genes are found in subtelomeric regions. Breaks in synteny between these genomes are often flanked by repeats and transposable elements. Wortman *et al.* (2006) pointed that further characterization of strain and species-specific genes, polymorphisms and differential regulation will foster our understanding of mechanisms of pathogenicity, environmental adaptation and resistance to anti-fungal treatments.

1.3. Fungal Secondary Metabolism

The fungal kingdom includes many species with unique and unusual biochemical pathways. The products of these pathways include important pharmaceuticals such as penicillin, cyclosporin and statins; potent poisons, including aflatoxins and trichothecenes; and some interesting metabolites that are both toxic and pharmaceutically useful, such as the Ergot alkaloids. All of these natural products, along with many other low-molecular-weight fungal metabolites, are classified together as secondary metabolites (Keller *et al.*, 2005). Secondary metabolites are not essential to the basic metabolism of the fungus. They are often bioactive, usually of low molecular weight, and are produced as families of related compounds at restricted parts of the life cycle, with production often correlated with a specific stage of morphological differentiation. Secondary metabolites share the enigmatic properties of cellular dispensability (producer organisms can grow without

synthesizing these metabolites) and restricted taxonomic distribution (only a small group of organisms produces each metabolite) (Keller *et al.*, 2005; Bennett *et al.*, 1989).

Aspergillus fumigatus has been reported to produce a large number of secondary metabolites (Turner, 1971; Turner and Aldrich, 1983; Cole and Cox, 1981; Cole and Schweikert, 2003a and 2003b; Cole *et al.*, 2003; Rementeria *et al.*, 2005) including the very toxic metabolite gliotoxin, which seems to be implicated in the *A. fumigatus* infection process (Rementeria *et al.*, 2005; Bok *et al.*, 2005). It is less clear whether other secondary metabolites are involved in pathogenesis (Mitchell *et al.*, 1997). In the study by Larsen *et al.* (2007), major metabolites produced in *Aspergillus* section *Fumigati*, comprising *A. fumigatus*, *A. lentulus*, *N. fisheri*, *N. pseudofischeri* and the two newly described species *A. novofumigatus* and *A. fumigatiaffinis* were determined by LC DAD-MS (Table 1.6). A major finding was detection of gliotoxin from *N. pseudofischeri*, a species not previously reported to produce this mycotoxin. Gliotoxin was also detected from *A. fumigatus* together with fumagillin, fumigaclavine C, fumitremorgin B and C, fumiquinazolines, pseurotin, trypacidin, monomethylsulochrin, TR-2, verruculogen, helvolic acid and pyripyropenes. Major compounds from *A. lentulus* were cyclopiazonic acid, terrein, neosartorin, auranthine and pyripyropenes A, E and O.

1.3.1. Classes of Fungal Secondary Metabolites

1.3.1.1. Polyketides

The polyketide natural products (Figure 1.4) are a remarkable class of compounds found in bacteria, fungi and plants. In addition to exhibiting a wide range of functional and structural diversity, they boast a wealth of medicinally important activities, including antibiotic, anticancer, antifungal, antiparasitic and immunosuppressive properties (Staunton and Weissman, 2001; Shen, 2003).

Table 1.6. Secondary metabolites detected from species in section *Fumigati* (Larsen *et al.*, 2007)

Compound	<i>A. fumigatus</i>	<i>A. lentulus</i>	<i>A. novofumigatus</i>	<i>A. fumigatiaffinis</i>	<i>N. fischeri</i>	<i>N. pseudofischeri</i>
Auranthine		+		+		
Cyclopiazonic acid		+				
<i>Epi</i> -aszonalenin A			+			
<i>Epi</i> -aszonalenin A			+			
Fumagillin	+					
Fumigaclavine C	+					
Fumiquinazoline D	+					
Fumiquinazoline F/G	+					
Fumitremorgin A					+	
Fumitremorgin B	+				+	
Fumitremorgin C	+					
Gliotoxin	+					+
Helvolic acid	+		+	+	+	
Monomethylsulochrin	+					
Neosartorin		+	+	+	+	
Pseurotin A or D	+					
Pseurotin A or D	+					
Pyripyropene A		+		+		+
Pyripyropene E		+		+		+
Pyripyropene O		+		+		+
Pyripyropene S	+	+		+	+	+
Terrein		+	+			
Trypacidin	+				+	
TR-2	+				+	
Verruculogen	+				+	

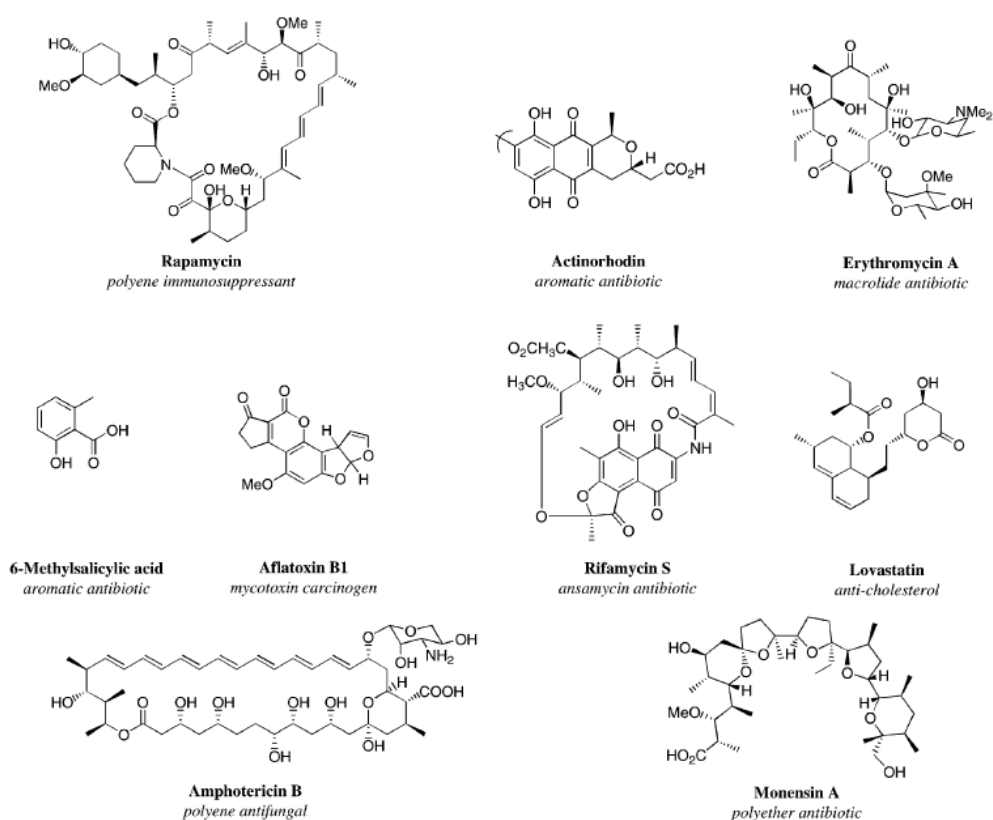


Figure 1.4. Examples of polyketide secondary metabolites. The type of polyketide and its primary biological activity are indicated (Staunton and Weissman, 2001).

1.3.1.1.1. Biosynthesis of Polyketides: Polyketide Synthases

Despite having such diverse structures and biological properties, the biosynthesis of these natural products follows a common mechanistic rule. Polyketide synthases (PKSs) are multi-enzyme complexes on which a polyketide chain is assembled by a stepwise condensation reaction of simple organic acids activated as coenzyme A (CoA) thioesters (Figure 1.5) in a similar fashion to the chain elongation steps of classical fatty acid biosynthesis. Malonyl-CoA and methylmalonyl-CoA comprise the great bulk of monomer units incorporated during chain elongation. The chain starter units can be the thioesters of monoacyl groups

such as acetyl-, propionyl-, and benzoyl-CoAs, or structural variants, such as malonamyl-CoA or methoxymalonyl-CoA (Fischbach and Walsh, 2006).

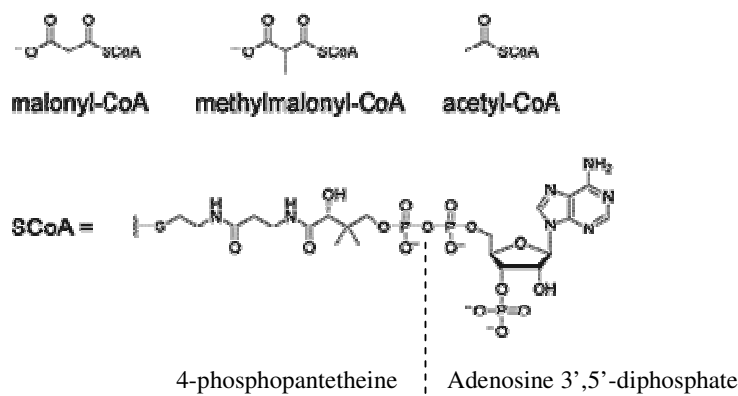


Figure 1.5. Common acyl-CoA thioesters used for chain initiation and elongation by PKSs (Fischbach and Walsh, 2006).

Chain elongation proceeds via “covalent tethering” of all the substrates, intermediates, and products. Acyl carrier protein (ACP) domains, which bear a covalently attached phosphopantetheinyl “arm”, are the points of attachment of the activated monomers and growing acyl chains. For enzymatic assembly lines to become functional, each ACP domain must be posttranslationally modified with a phosphopantetheinyl arm, derived from coenzyme A (Figure 1.6) (Fischbach and Walsh, 2006).

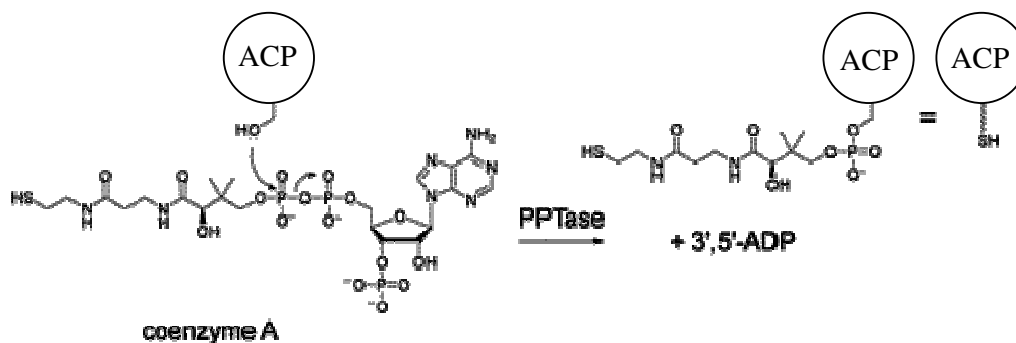


Figure 1.6. Posttranslational modification of ACP domains by phosphopantetheinyltransferases. Members of this enzyme class catalyze the transfer of phosphopantetheine from coenzyme A to a conserved serine in the ACP domain (Fischbach and Walsh, 2006).

Two catalytic domains, ketosynthase (KT) and acyltransferase (AT), and ACP domain comprise the minimal set of domains present in PKS enzymatic machinery (Figure 1.7). ACP domain provides a thiol on which substrate and intermediate acyl chains are covalently tethered during chain elongations. AT domains select either malonyl-CoA or methylmalonyl-CoA as substrates and thereby act as gatekeepers for specificity. They transfer the C3 or C4 acyl group to the thiolate terminus of the pantetheinyl arm on an ACP domain. The KS is the C-C bond-forming catalyst. Each catalytic cycle of a KS domain results in a net addition of two carbons (from a malonyl unit) or three carbons (from a methylmalonyl unit) to the growing acyl chain (Fischbach and Walsh, 2006).

Additional common optional catalytic domains present in PKSs are ketoreductase (KR), dehydratase (DH), and enoylreductase (ER) domains. They operate in the sequence KR→DH→ER, initially reducing the β -ketoacyl- arising from KS-mediated condensation to the β -hydroxyacyl- (KR action), then dehydrating to form the α,β -enoyl- (DH action), and finally reducing the conjugated olefin to the saturated acyl- (ER action) (Fischbach and Walsh, 2006).

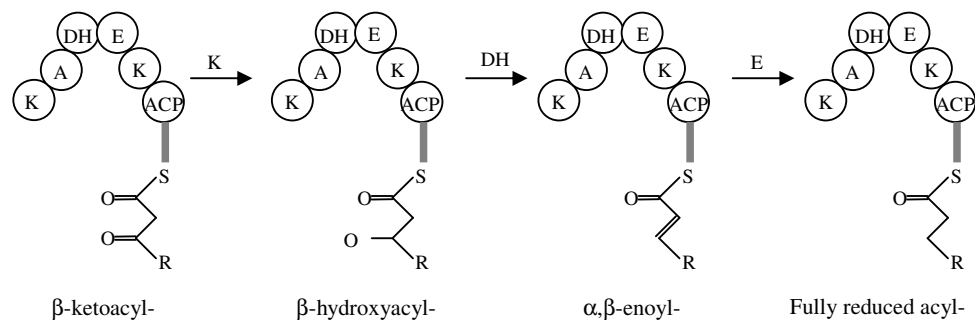


Figure 1.7. β -Carbon processing in PKSs. The β -ketoacyl- condensation product is reduced by the ketoreductase (KR) domain to form β -hydroxyacyl-, subsequent dehydration by the dehydratase (DH) domain yields an α,β -enoyl-S-T, and reduction of this species by the enoyl reductase (ER) domain gives the fully saturated acyl- (Fischbach and Walsh, 2006).

PKSs are classified as Type I, II and III according to their architecture. Type I PKSs can be subdivided into iterative, which use the same set of catalytic sites in a repetitive manner and modular, where a specific set of catalytic sites exist for each round of chain elongation. Iterative type I PKSs, which are commonly found in fungi, use each active site of the multifunctional enzyme repeatedly during assembly of the carbon chain. Well-known polyketide examples biosynthesized by these enzymes are lovastatin and 6-methylsalicylic acid. In contrast, in modular type I PKSs, one distinct group of active sites, called a module on a single polypeptide is used to initiate and extend the carbon chain. The active sites present in each module are used only once during product assembly and determine the choice of starter and extender units plus the level of reduction or dehydration for that particular extension cycle. The length of the polyketide carbon chain and the sequence of steps by which it is built are determined by the number and order of modules in the polypeptides constituting the PKS. Such modular PKSs control the biosynthesis of well-known antibiotics such as erythromycin A and rifamycin as well as the immunosuppressant

rapamycin. Type II PKSs constitute the next class, where each catalytic site is present on a separate polypeptide and various polypeptides work by forming non-covalent complexes. The type III PKSs, which includes the chalcone synthases common in higher plants, differ from other PKSs in that the substrates and intermediates remain attached to coenzyme A instead of being transferred to an acyl carrier protein. (Gokhale *et al.*, 2007; Hutchinson *et al.*, 2000; Reeves, 2003)

1.3.1.1.2. Fungal Polyketide Synthases

The biosynthesis of fungal polyketides is governed by type I PKSs. Fungal polyketide synthases consist of a minimal set of ketosynthase (KS), acyl transferase (AT), and acyl carrier protein (ACP) domains. In addition, optional β -keto processing reactions may be catalyzed by keto reductase (KR), dehydratase (DH) and enoyl reductase (ER) domains. Further optional accessory domains are represented by cyclase (CYC) (Fujii *et al.*, 2001) and methyl transferase (MT) activities (Hutchinson *et al.*, 2000) (Fig. 1.8). It should be noted that in fungal polyketide biosynthesis no methylmalonyl elongation units are employed, as opposed to numerous examples in bacterial polyketide biosynthesis involving modular type I PKS. Fungal iterative PKS can use each active site in an iterative way during chain assembly, and determine the degree of reduction and C-methylation within each elongation round (Fujii *et al.*, 1998; Rawlings, 1999). To date it has remained a mystery how a single set of catalytic domains determines chain length, degree of reduction, and timing of C-methylation at a particular step in the pathway (Schümann and Hertweck, 2006).

Common to all fungal polyketides is their biosynthetic origin. They are produced by repetitive Claisen condensations of an acyl-coenzyme A (CoA) starter with malonyl-CoA elongation units in a fashion reminiscent of fatty acid biosynthesis (Figure 1.9). One of the major differences between both metabolic pathways is that polyketides can differ in the degree of β -keto processing. Some are not or only partially reduced, resulting in the formation of (poly-)cyclic aromatic compounds. Alternatively, they may be partially or largely reduced, which usually gives rise to linear or macrocyclic, non-aromatic carbon frameworks (Rawlings, 1999; Staunton and Weissman, 2001, Schümann and Hertweck, 2006).

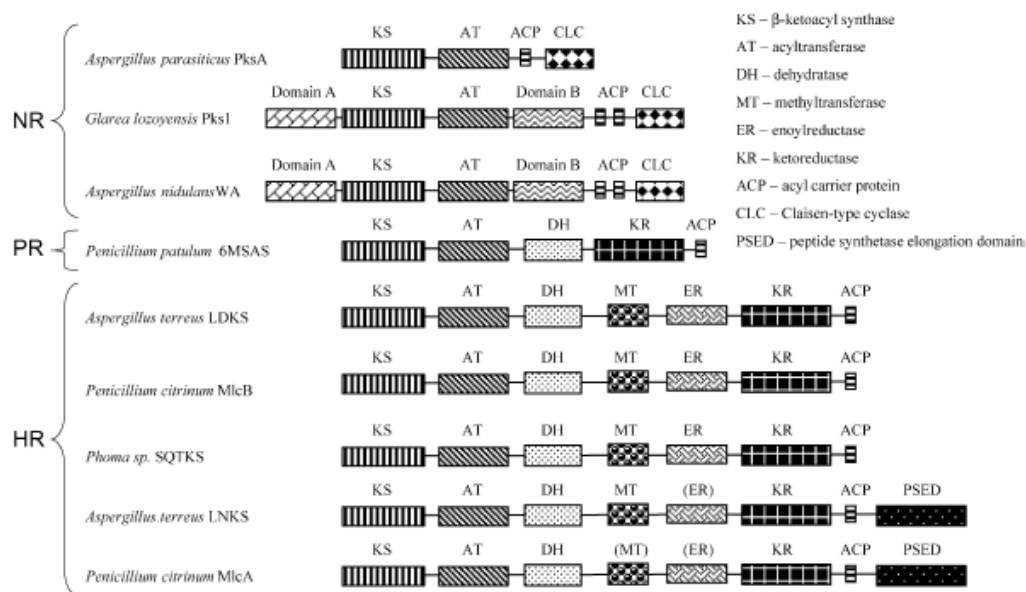


Figure 1.8. Examples for non-reducing (NR: PksA, Pks1,WA), partially reducing (PR: 6-MSAS), and highly reducing (HR: LDKS, MlcB, SQTKS, LNKS, MlcA) PKS, and their domain architectures (Schümann and Hertweck, 2006).

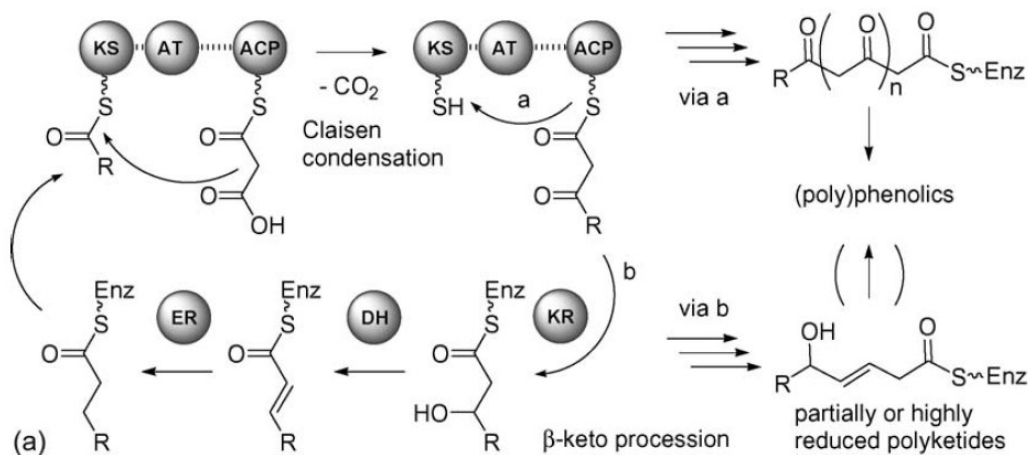


Figure 1.9. Basic mechanism of fungal polyketide biosynthesis (Schümann and Hertweck, 2006)

According to their architecture and the presence or absence of additional β -keto processing domains, fungal PKSs are grouped into non-reducing or aromatic, partially reducing, and highly reducing PKSs (Schümann and Hertweck, 2006). Kroken *et al.* (2003) showed that amino acid sequences of fungal KS domains cluster according to the degree of reduction of their products in reducing PKS (additional reductive domains: KR, ER, DH) and non-reducing PKS (no reductive domains), each type further divided into four subclades.

In addition to the chain length, the degree of β -keto processing and cyclization, the large structural diversity of polyketides derives from derivatization of the polyketide carbon skeleton by alkylation, acylation, and oxygenation, by so-called post-PKS or tailoring reactions. From analyses of the few PKS gene loci that have been investigated to date it appears that all genes necessary for fungal polyketide biosynthesis are clustered, i.e. PKS genes, genes encoding enzymes involved in tailoring reactions, as well as genes required for regulation and resistance (Schümann and Hertweck, 2006).

A. fumigatus genome contains at least 14 PKS genes/gene clusters. Although *A. fumigatus* has been found to produce a number of polyketides including orsellinic acid (Packter, 1966), fumigatin (Packter and Glover, 1965), fumiquinones and spinulosin (Pettersson, 1964; Hayashi *et al.*, 2007), anthraquinones (Yamamoto *et al.*, 1968), monomethylsulochrin, trypacidin (Turner, 1965) and melanin, only one polyketide synthase gene that involve in the biosynthesis of melanin was characterized.

Lanfelder *et al.* (1998) obtained a mutant *A. fumigatus* strain lacking conidial pigmentation and showing smooth surface morphology. This mutant also showed reduced virulence in a murine animal model. By complementation, the mutant gene was identified and designated as *pksP* (polyketide synthase involved in pigment biosynthesis). Simultaneously, Tsai *et al.* (1998) identified the same polyketide synthase gene by complementation of a pigmentless mutant of *A. fumigatus* and named the gene as *alb1* (albino 1). They showed that expression of *alb1* is developmentally regulated and expressed only during the conidiation stage. Additionally, *alb1* mutation blocked 1,3,6,8-tetrahydroxynaphthalene production, indicating that *alb1* is involved in dihydroxynaphthalene-melanin biosynthesis.

Similar to Langfelder *et al.* (1998), they also showed that *alb1* disruptant had a significant loss of virulence in a murine model. Later, Tsai *et al.* (1999) identified a six-gene cluster involved in conidial pigment biosynthesis in *A. fumigatus* including *alb1* (Figure 1.10). Involvement of the six genes in conidial pigmentation was confirmed by the altered conidial color phenotypes that resulted from disruption of each gene (Figure 1.11). Although fungal polyketide melanins are often derived from a pentaketide 1,8-dihydroxynaphthalene, studies by Watanabe *et al.* (2000) and Tsai *et al.* (2001) later showed that *alb1* codes for a heptaketide synthase, the product of which is then converted to the pentaketide 1,3,6,8-tetrahydroxynaphthalene (1,3,6,8-THN) by Ayl1p encoded by *ayg1* from the melanin gene cluster.

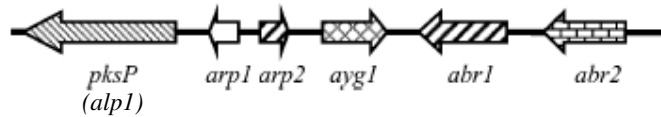


Figure 1.10. Melanin biosynthesis gene cluster of *A. fumigatus*

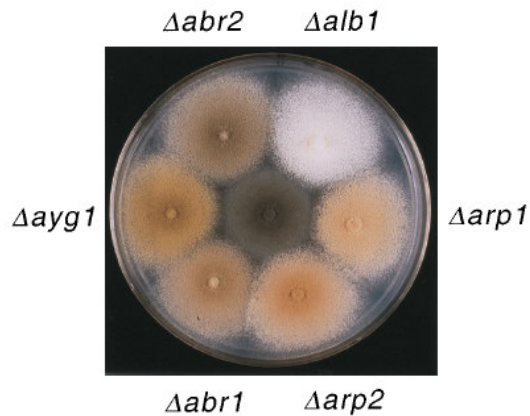


Figure 1.11. Sporulating cultures of the *A. fumigatus* wild-type strain and six single-gene deletants (Tsai *et al.*, 1999). The wild-type strain, producing bluish green conidia, is at the center of the plate. Each gene deletant is designated by the name of the deleted gene .

1.3.1.2. Non-Ribosomal Peptides

Nonribosomal peptide synthesis is a key mechanism responsible for the biosynthesis of bioactive metabolites in bacteria and fungi (Stack *et al.*, 2007; Mootz *et al.*, 2002; Reiber *et al.*, 2005). Non-ribosomal peptides are derived from both proteinogenic amino acids and non-proteinogenic amino acids by multidomain, multi modular enzymes named non-ribosomal peptide synthetases (NRPSs) (Keller *et al.*, 2005). Each module in an NRPS contains several domains: adenylation (A) for substrate activation, peptidyl carrier protein (P) for covalent loading and condensation (C) domain for peptide bonding (Stack *et al.*, 2007; Finking and Marahiel, 2004). Each module is responsible for the recognition (via the A domain) and incorporation of a single amino acid into the growing peptide product (Stack *et al.*, 2007). A terminal domain such as a thioesterase (TE) domain releases the full-length peptide chain from the enzyme complex (Mootz *et al.*, 2002; Stack *et al.*, 2007).

The first fungal NRPS identified, δ -(*L*- α -aminoadipyl)-*L*-cysteinyl-*D*-valine synthetase (ACVS), catalyses the first committed step in the biosynthesis of the β -lactam antibiotics penicillin and cephalosporin. ACVS condenses *L*- α -aminoadipic acid, *L*-cysteine and *L*-valine, and epimerizes *L*-valine to *D*-valine to form a linear peptide (ACV) that is subsequently cyclized to isopenicillin N by the action of isopenicillin N synthase (Keller *et al.*, 2005; Smith *et al.*, 1990a; Kallow *et al.*, 2000).

The significance of *A. fumigatus* as a potential reservoir of bioactive, nonribosomally synthesized, peptides has been consolidated by the observation that at least 14 NRPS genes/gene clusters are found within the *A. fumigatus* genome (Stack *et al.*, 2007) (Table 1.7).

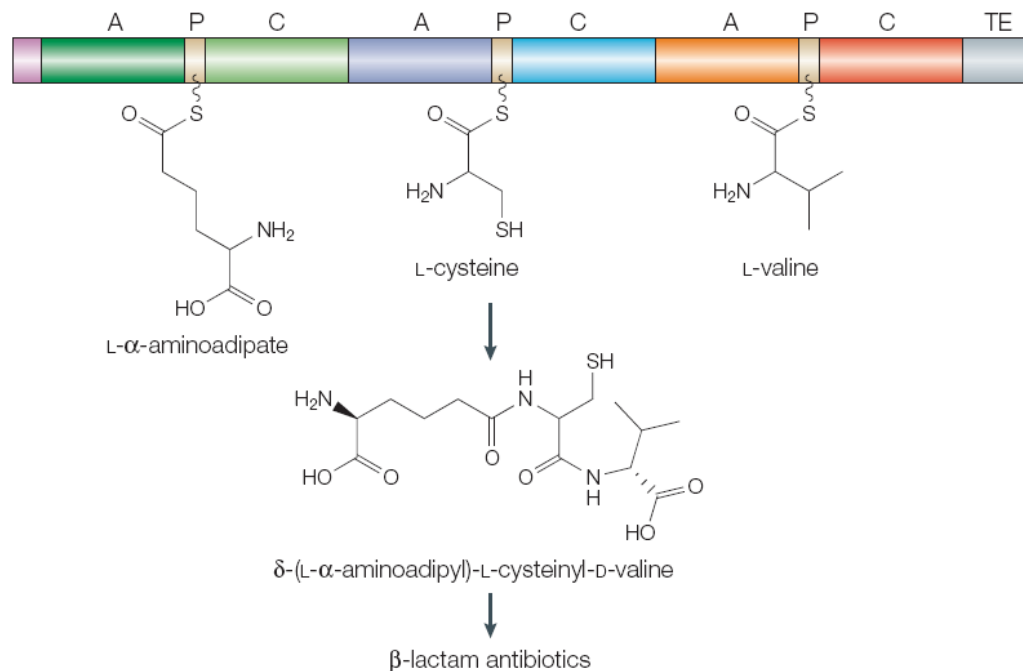


Figure 1.12. ACV synthetase, a trimodular non-ribosomal peptide synthetase (Keller *et al.*, 2005). δ -(L- α -aminoadipyl) L-cysteinyl-D-valine (ACV) synthetase catalyses the first committed step in penicillin and cephalosporin biosynthesis. Each amino acid is recognized and activated by the cognate adenylation domain (A), and attached as a thioester at the peptidyl carrier domain (P). Peptide bonds are formed with the involvement of the condensation domain (C). The final tripeptide, attached to the peptidyl carrier domain of the C-terminal module, is released by the integrated thioesterase domain (TE), with the L-valine isomerized to D-valine. The tripeptide is subsequently cyclized to isopenicillin N.

Table 1.7. NRPS genes of *A. fumigatus*, with hypothetical NRPS domain architecture based on in silico analysis (Stack *et al.*, 2007).

NRPS gene	Domain architecture*	ID*	Reference
<i>pesI (pesB)</i>	APECACACAPECPCP	Afu1g10380	Neville <i>et al.</i> , 2005; Nierman <i>et al.</i> , 2005; Reeves <i>et al.</i> , 2006
<i>sidC</i>	APCAPCAPCPCPC	Afu1g17200	Reiber <i>et al.</i> , 2005; Nierman <i>et al.</i> , 2005
<i>sidE</i>	APCAPC	Afu3g03350	Reiber <i>et al.</i> , 2005; Nierman <i>et al.</i> , 2005
<i>sidD</i>	APCAPC	Afu3g03420	Reiber <i>et al.</i> , 2005; Nierman <i>et al.</i> , 2005
<i>pesF</i>	APCAPCP	Afu3g12920	Nierman <i>et al.</i> , 2005
<i>pesG</i>	APC	Afu3g13730	Nierman <i>et al.</i> , 2005
<i>pesH</i>	ACAPC	Afu3g15270	Nierman <i>et al.</i> , 2005
<i>pesI</i>	APCAPECAPCEPCAPCAPCAPEC	Afu5g12730	Nierman <i>et al.</i> , 2005; Cramer <i>et al.</i> , 2006b
<i>pesJ</i>	C*APC	Afu6g09610	Nierman <i>et al.</i> , 2005
<i>pesK (gliP)</i>	APCAPCP	Afu6g09660	Nierman <i>et al.</i> , 2005; Cramer <i>et al.</i> , 2006a; Kupfahl <i>et al.</i> , 2006
<i>pesL</i>	APC	Afu6g12050	Nierman <i>et al.</i> , 2005
<i>pesM</i>	APCAPCEAPC(TE)	Afu6g12080	Nierman <i>et al.</i> , 2005
<i>pesN (ftmA)</i>	APCAPC	Afu8g00170	Nierman <i>et al.</i> , 2005; Maiya <i>et al.</i> , 2006; Sheppard <i>et al.</i> , 2005
<i>pesO</i>	PKS-NNCAP(DH)	Afu8g00540	Nierman <i>et al.</i> , 2005; Sheppard <i>et al.</i> , 2005

Key: A, adenylation domain; P, peptidyl carrier domain; C, condensation domain; E, epimerase domain; TE, thioesterase domain; DH, putative dehydrogenase domain of multifunctional NRPS; C, partial condensation domain; PKS, polyketide synthetase; N, incomplete domain, not identifiable. Afu6g09660, gliotoxin precursor synthetase (Cramer *et al.*, 2006a; Kupfahl *et al.*, 2006); Afu8g00170, brevianamide F synthetase (Maiya *et al.*, 2006); Afu8g00540 appears to be a hybrid PKS/NRP synthetase.

To date, only two *A. fumigatus* NRPSs have been definitively shown to produce specific non-ribosomal peptide products. Firstly, a bimodular NRPS (*ftmA*; ID: Afu8g00170; Table 1.7) from *A. fumigatus* has been shown to encode the dipeptide brevianamide F (cyclo-L-Trp-L-Pro), which is a precursor of bioactive prenylated alkaloids (e.g. fumitremorgins A, B and C and tryprostatin B) (Maiya et al., 2006; Stack *et al.*, 2007). Secondly, Gardiner And Howlett (2005) identified a cluster of 12 genes in *A. fumigatus* by a comparative genomics approach, and demonstrated that the genes were co-regulated and that the timing of expression correlated with gliotoxin production. It has since been conclusively demonstrated that the gene cluster directs gliotoxin biosynthesis since disruption of the transcriptional regulator (*gliZ*) eliminates expression of the entire cluster and prevents gliotoxin production (Bok *et al.*, 2006). This unambiguously confirms the role of the hypothetical gliotoxin gene cluster in gliotoxin formation. The *gliP* gene (ID: Afu6g09660; Table 1.7), encoding the bimodular NRPS responsible for the biosynthesis of the dipeptide L-Phe-L-Ser, a precursor of gliotoxin, has been identified by gene disruption whereby a *gliP* mutant failed to produce gliotoxin (Cramer *et al.*, 2006a; Kupfahl *et al.*, 2006).

NRP synthesis represents an important mechanism for the biosynthesis of extra- and intracellular iron-chelating siderophores which aid fungal growth. In *A. fumigatus*, studies have identified the expression of three NRPS genes (*sidC*, *D* and *E*) (Table 1.7) which are, to varying extents, susceptible to regulation by the level of free iron present in the culture medium. Based on gene expression analysis, protein identification and siderophore detection, Stack *et al.* (2007) hypothesized that the NRP synthetases SidC, D and E potentially biosynthesize siderophores responsible for iron acquisition by *A. fumigatus* – although direct proof of this remains outstanding.

Significantly, a *pes1* deletion mutant in *A. fumigatus* ($\Delta pes1$) exhibits altered conidial morphology and increased sensitivity to oxidative stress due to H₂O₂ presence (Reeves *et al.*, 2006; Table 1.7). Work is currently under way to identify the nature of the *Pes1*-encoded peptide product.

In summary, although at least 14 NRPS genes are present in *A. fumigatus*, the function of most of this coding potential (i.e. the biochemical nature of resulting NRP products) remains unknown. In addition, the function of most additional ORFs, associated with NRPS genes in clusters, remains to be fully elucidated (Stack *et al.*, 2007).

1.3.1.3. Terpenes

The best-known terpenes are odoriferous plant metabolites such as camphor and turpentine, but fungi also synthesize several important terpenes, including the aristolochenes, carotenoids, gibberellins, indole-diterpenes and trichothecenes. All terpenes are composed of several isoprene units, can be linear or cyclic, saturated or unsaturated, and can be modified in various ways (Keller *et al.*, 2005) (Figure 1.13).

Common classes of terpenes include the monoterpenes, which are generated from geranyl pyrophosphate (also known as geranyl diphosphate); sesquiterpenes, which are generated from farnesyl pyrophosphate (also known as farnesyl diphosphate); and diterpenes and carotenoids, which are generated from geranylgeranyl pyrophosphate (also known as geranylgeranyl diphosphate). The defining enzyme in terpene synthesis is terpene cyclase, which is essential for the production of different terpenes from different diphosphates (Keller *et al.*, 2005).

Bioinformatic analysis of the *Aspergillus* genomes has revealed few terpene biosynthetic genes. *A. nidulans* and *A. oryzae* have one terpene cyclase homologue but no obvious terpene cyclase is detectable in *A. fumigatus* (Nierman *et al.*, 2005a).

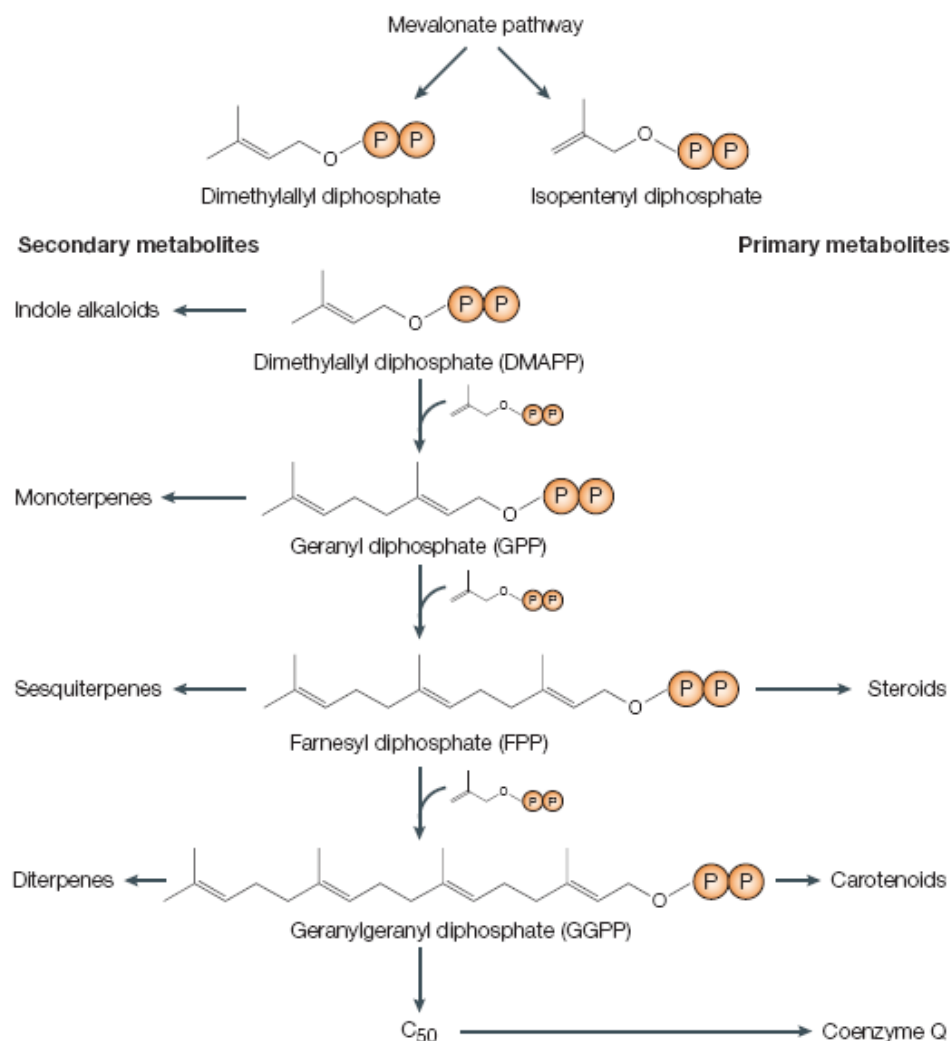


Figure 1.13. Terpene biosynthetic pathway (Keller *et al.*, 2005). Isopentenyl diphosphate and its isomer dimethylallyl diphosphate (DMAPP), products of the mevalonate pathway, are the building blocks (5C isoprene units) for the linear polyprenyl diphosphates, which are precursors of steroids, carotenoids and coenzyme Q in many species. A family of isoprenyl diphosphate synthases is responsible for chain elongation. DMAPP and the isoprenoid intermediates are also the starting points for a wide range of secondary metabolites, including indole alkaloids, monoterpenes, sesquiterpenes and diterpenes. The terpenes are produced by cyclization of the isoprenoids. For example, farnesyl diphosphate is cyclized to produce a large variety of sesquiterpenes, depending on the cyclase structure and function. DMAPP can be added as a side chain to various aromatic compounds. For example, ergotamine is derived from dimethylallyl tryptophan.

1.3.1.4. Indole alkaloids

Indole alkaloids are usually derived from tryptophan and dimethylallyl pyrophosphate, although sometimes amino acids other than tryptophan are used as precursors. The best-understood pathway is ergotamine synthesis in *Claviceps purpurea* and related species (Tudzynski, 1999). The first committed step is the prenylation of tryptophan by dimethylallyl tryptophan synthetase (DMATS). Following methylation of dimethylallyl tryptophan, a series of oxidation steps proceed through agroclavine to lysergic acid. Lysergic acid is then activated by a single-module NRPS, condensed with a tripeptide that is produced by a second NRPS, and released as ergotamine (Keller *et al.*, 2005).

A. fumigatus has been reported to produce fumitremorgins, which are tremorgenic mycotoxins (Yamazaki *et al.*, 1971; Horie and Yamazaki, 1981). Fumitremorgins are members of a group of prenylated indole alkaloids derived from tryptophan and proline (Maiya *et al.*, 2006). This group includes other compounds detected in *A. fumigatus* extracts, such as tryprostatins, cyclotryprostatins and spirotryprostatins (Cui *et al.* 2006a and 2006b), and it has been postulated that these compounds are derived from the diketopiperazine cyclo-L-Trp-L-Pro, known as brevianamide F (Williams, 2000). Brevianamide F was found to be synthesised by a dimodular NRPS present within a gene cluster. It is hypothesized that fumitremorgens B and C, and tryprostatins from *A. fumigatus* are derived from brevianamide F by diverse pathways that require various oxidases, methylases and prenyl transferases (Maiya *et al.*, 2006). The details of these pathways are yet to be elucidated.

1.3.2. Gene Cluster Concept of Secondary Metabolites

The advent of recombinant DNA methodologies in the 1980s enabled dramatic progress in the genetics and biochemistry of fungal secondary metabolism. This rapid progress was facilitated by what is now considered a hallmark characteristic of secondary metabolic biosynthetic pathways - the grouping of pathway genes in a contiguous cluster. Metabolic gene clustering was not predicted

by the fungal research community. In fact, in the era between the discovery of the bacterial operon and the advent of large-scale eukaryotic gene cloning, it had become dogma that eukaryotic genes that are involved in functionally related pathways are not linked. By 1990 however, this belief had been abandoned owing to the almost routine discovery of gene clusters in fungi for phenotypes as varied as nutrient use, mating type, pathogenicity and secondary metabolism (Keller and Hohn, 1997; Keller *et al.*, 2005). In less than a decade, it was shown that the genes for the production of a broad range of secondary metabolites were located adjacent to one another; in addition, a pathway-specific regulatory gene was often embedded in these gene clusters. Fungal secondary metabolite clusters characterized by gene cloning include aflatoxins (Yu *et al.*, 2004), cephalosporin (Gutierrez *et al.*, 1992), compactin (Abe *et al.*, 2002), ergot alkaloids (Tudzynski *et al.*, 1999), fumonisin (Proctor *et al.*, 2003), gibberellins (Tudzynski, 1999), HC toxin (Ahn *et al.*, 2002), lovastatin (Kennedy *et al.*, 1999), melanin (Kimura and Tsuge, 1993; Tsai *et al.*, 1999), paxillin (Young *et al.*, 2001), penicillin (Smith *et al.*, 1990b; Brakhage, 1998), sterigmatocystin (Brown *et al.*, 1996), sirodesmin (Gardiner *et al.*, 2004) and trichothecenes (Trapp *et al.*, 1998).

The evolution and maintenance of gene clusters has received a great deal of attention in bacteria (Lawrence and Roth, 1996; Lawrence, 1997; Lawrence, 1999) and fungi (Rosewich and Kistler, 2000; Walton, 2000; Keller and Hohn, 1997). Evidence for horizontal transfer of the penicillin cluster from bacteria to fungi was met with great excitement, as it suggested a reason for both the origin and maintenance of metabolic clustering (Rosewich and Kistler, 2000; Walton, 2000; Smith *et al.*, 1992). However, other functionally conserved metabolites, such as gibberellin production in the fungus *G. fujikuroi* and in plants, are unlikely to have arisen from horizontal transfer between kingdoms (Tudzynski *et al.*, 2001), and it is likely that several evolutionary mechanisms account for the presence of secondary metabolite clusters. Although a unifying model to explain the clustering of secondary metabolite genes in fungi is lacking, the preservation of clusters, now known to be extensive by examination of fungal genomes, might indicate an underlying advantage to maintaining clustering (Keller *et al.*, 2005).

An exciting advance in support of a global requirement for fungal secondary metabolite gene clustering has arisen from identification of an *Aspergillus* methyltransferase, LaeA (Bok and Keller, 2004). Deletion and overexpression of *laeA* in *A. nidulans*, *A. fumigatus* and *A. terreus* strains either silences or increases, respectively, the production of several secondary metabolites and the expression of their respective genes. Sequence analysis of *laeA* and analysis of the encoded protein indicated that it is a protein methyltransferase. The highest sequence similarity is to histone and arginine methyltransferases, which have important roles in the regulation of gene expression (Keller *et al.*, 2005). Although LaeA functions are not yet fully characterized, it was speculated by Keller *et al.* (2005) that this protein is involved in chromatin modification. Methylation is involved in both gene repression and activation of heterochromatic and euchromatic regions of eukaryotic chromosomes (Lee *et al.*, 2005), so one model of LaeA-mediated regulation of clusters invokes a role in heterochromatin repression (Keller *et al.*, 2005).

1.4. Multicopper Oxidases

1.4.1. Enzymology of Multicopper Oxidases

Multicopper oxidases (MCOs) are a family of enzymes belonging to the highly diverse group of blue copper proteins which contain from one to six copper atoms per molecule (Hoegger *et al.*, 2006). The currently well-defined multicopper oxidases are laccase, ascorbate oxidase, and ceruloplasmin. Recently several new additional ones have been isolated and characterized: phenoxazinone synthase, bilirubin oxidase, dihydrogeodin oxidase, sulochrin oxidase, and FET3 (Solomon *et al.*, 1996).

Historically, copper atoms coordinated in proteins have been classified into three types (type 1, type 2 and type 3) based on their spectroscopic properties. In the UV-visible spectrum, type 1 copper (blue copper) shows maximum absorption around 610 nm, and type 3 copper (coupled binuclear copper) shows maximum absorption around 330 nm. Type 1 and type 2 (normal copper) coppers are EPR

(electron paramagnetic resonance) detectable, while the binuclear type 3 coppers are EPR silent (Nakamura and Go, 2005).

Laccase, ascorbate oxidase, and ceruloplasmin exhibit EPR features, indicating the presence of a combination of type 1 and type 2 centers, and have an additional EPR inactive, antiferromagnetically coupled type 3 center. The type 2 plus type 3 centers were originally shown on laccase to form a trinuclear copper cluster (Figure 1.14a), and this has also been determined by crystallography for ascorbate oxidase and ceruloplasmin. The function of the type 1 copper site within the enzyme is longrange intramolecular electron transfer, shuttling electrons from the substrate to the trinuclear cluster. The trinuclear cluster is the site of dioxygen binding and reduction (Figure 1.14b) (Solomon *et al.*, 1996).

The type 1 copper-binding site consists of two histidines, one cysteine, and one methionine (Figure 1.14b, Figure 1.15). The first three residues are essential for the blue copper-binding site and form a tight trigonal coordination with the copper ion, while the coordination of the fourth residue, an axial methionine, is rather distant and weaker, and this residue can be replaced with different amino acids, such as leucine or phenylalanine (Nakamura and Go, 2005). The type 2 and type 3 copper sites form a trinuclear cluster the peptide ligands of which are eight histidines that occur in a highly conserved pattern of four HXH motifs (Figure 1.15). In one, X is the cysteine bound to the type 1 copper and each of the histidines binds to one of the type 3 coppers. About 35-75 residues upstream of this is another HXH motif. Close to the N-terminal end are two more HXHs separated by about 35-60 residues. (Solomon *et al.*, 1996).

Suresh Kumar *et al.* (2003) developed 4 signature sequences for laccases corresponding to the 4 copper binding regions shown in Figure 1.15:

1. H-W-H-G-X₉-D-G-X₅-Q-C-P-I
2. G-T-X-W-Y-H-S-H-X₃-Q-X-C-D-G-L-X-G-X-(F/L/I/M)
3. H-P-X-H-L-H-G-H
4. G-(P/A)-W-X-(L/F/V)-H-C-H-I-(D/A/E)-X-H-X₃-G-(L/M/F)-X₃-(L/F/M)

Although the sequences were designed specifically for laccases, they show significant similarities to other multi-copper oxidases containing 4 copper atoms.

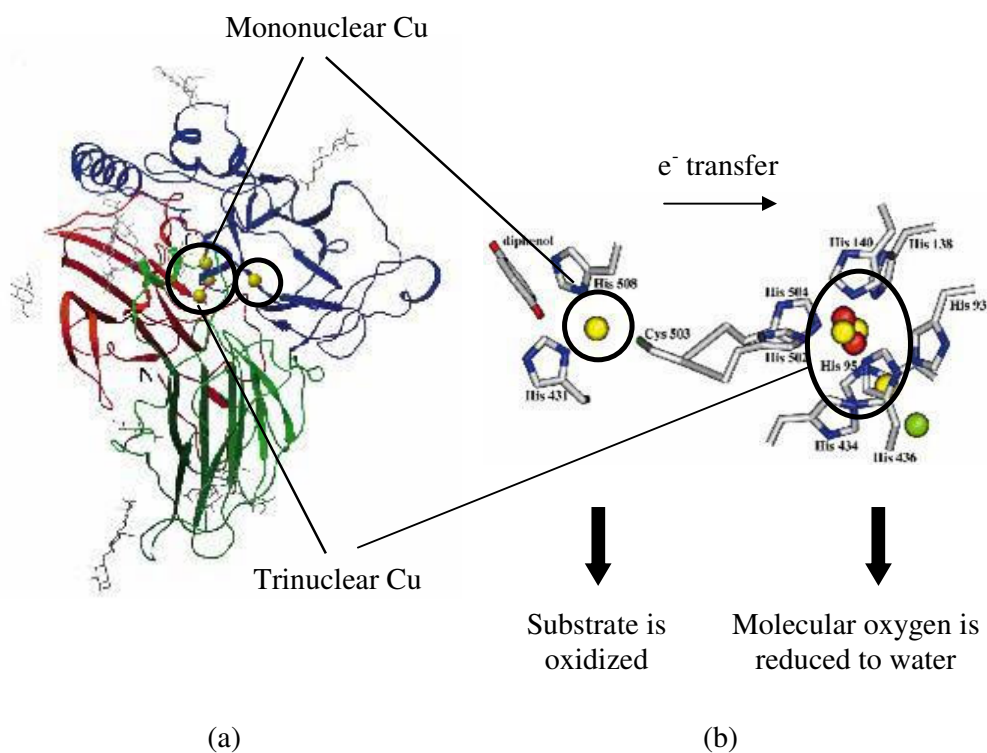


Figure 1.14. (a) Three-dimensional structure, (b) copper binding sites of *Melanocarpus albomyces* laccase (Hakulinen *et al.*, 2002). (a) Domain A (red) includes residues that participate in the binding of coppers at the trinuclear site. Domain B (green) contains residues that take part in the substrate binding. Domain C (blue) contains residues that participate in the binding of coppers at the mononuclear and the trinuclear site, as well as in substrate binding. The mononuclear site is located entirely in domain C, and the trinuclear site is located at the interface between domains A and C. The diphenolic substrate-binding site is located in the cleft between domains B and C. (b) The mononuclear site is on the left and the trinuclear site is on the right. Oxygen atoms are represented by red balls; a chlorine atom, by a green ball.

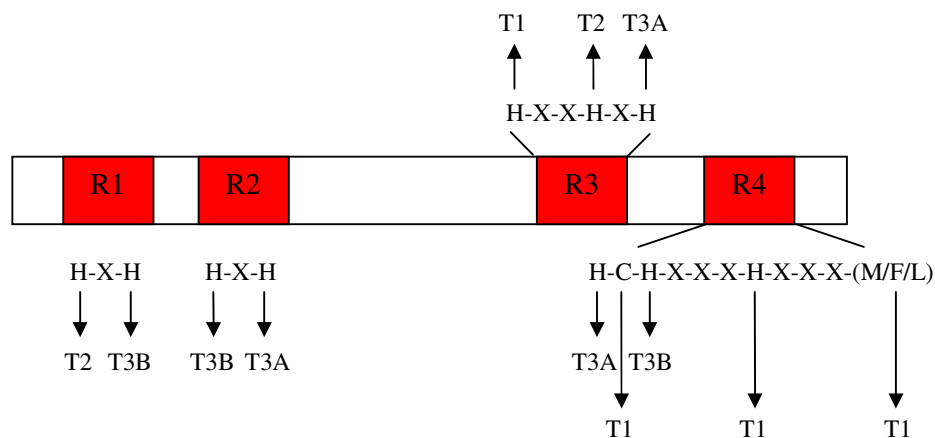


Figure 1.15. Copper binding regions of multicopper oxidases showing high degree of homology. R and T denotes for region and copper type, respectively. T3A: type 3 copper A, T3B: type 3 copper B.

The interactions of the multicopper oxidases with substrates can be broadly divided into two categories: enzymes with low substrate specificity and enzymes with high specificity. The plant and fungal laccases fall into the former category. They can oxidize diphenols, aryl diamines, and aminophenols, indicating that there is probably no binding pocket for substrate and that the oxidation is strictly outersphere. The other multicopper oxidases possess a significant degree of substrate specificity, implying a substrate binding pocket. Ascorbate oxidase shows a high degree of specificity for L-ascorbate and analogs, and ceruloplasmin shows a high specificity for Fe(II). Sulochrin oxidase and dihydrogeodin oxidase also have very high substrate specificities. In addition, the reactions these enzymes catalyze are stereospecific (Solomon *et al.*, 1996).

1.4.2. Multicopper Oxidases in Secondary Metabolite Biosynthesis

Sulochrin oxidase and dihydrogeodin oxidase are multicopper oxidases taking role in the biosynthesis of astrictic acid in *P. frequentans* and (+)-geodin in *A. terreus* (Figure 1.16). They catalyze the phenol oxidative coupling reactions, which is one of

the most important reactions in the biosynthesis of natural products. Typical model enzymes used in phenol oxidative reactions, such as laccase, tyrosinase and peroxidase lack both regio- and stereospecificity (Huang *et al.*, 1996).

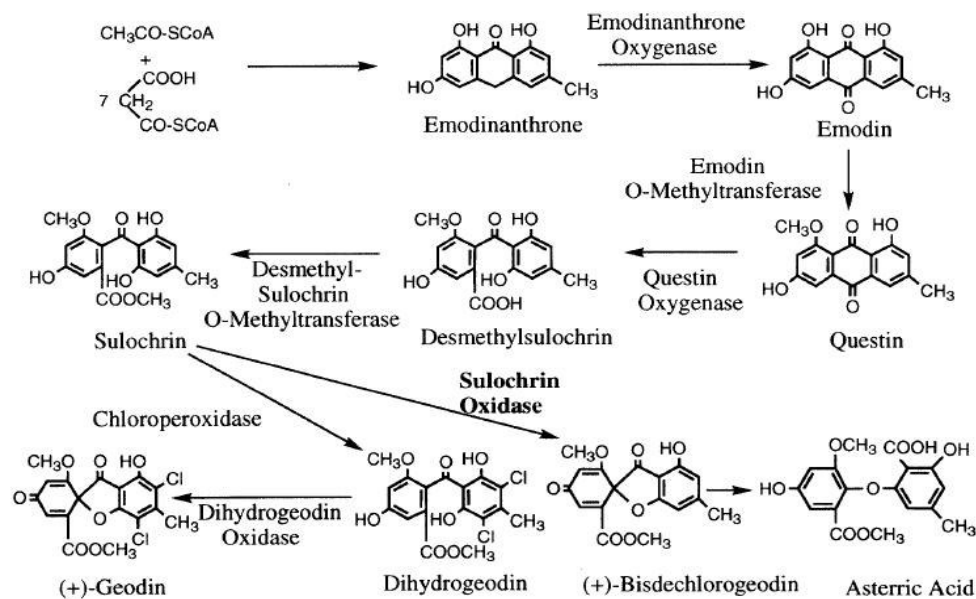


Figure 1.16. Biosynthesis of (+)-geodin in *A. terreus* and asterric acid in *P. frequentans* (Huang *et al.*, 1996).

Dihydrogeodin oxidase from *A. terreus* catalyzes the stereospecific phenol oxidative coupling reaction converting dihydrogeodin to (+)-geodin. Fujii *et al.* (1987) purified the enzyme and showed the presence of type 1 and type 2 copper atoms by EPR suggesting that the enzyme is a multicopper blue protein. Huang *et al.* (1995) cloned and heterologously expressed the gene encoding dihydrogeodin oxidase. They identified four potential copper binding domains in the amino acid sequence, which also showed significant homology to multicopper oxidases such as laccase and ascorbate oxidase.

P. frequentans possesses a similar biosynthetic pathway to that of (+)-geodin in *A. terreus* as shown in Figure 1.16. The end product of the pathway is asteric acid, which is reported to be a new binding inhibitor of endothelin (Ohashi *et al.*, 1992). Sulochrin is not subjected to chlorination and is directly converted to (+)-bisdechlorogeodin by sulochrin oxidase in *P. frequentans* (Huang *et al.*, 1996). Nordlov and Gatenbeck (1982) also purified sulochrin oxidase from *Oospora sulphurea-ochracea*, which catalyzes (-)-bisdechlorogeodin formation from sulochrin.

Substrate specificity studies by Huang *et al.* (1996) and Fujii *et al.* (1987) showed that neither dihydrogeodin oxidase from *A. terreus* nor sulochrin oxidase from *P. frequentans* oxidized diphenols and both were specific for benzophenone substrates like dihydrogeodin, sulochrin and griseophenone B, a possible biosynthetic precursor of griseofulvin, although the limited availability of possible benzophenone substrates hindered further study of their substrate specificity.

Multicopper oxidases also take role in melanin synthesis. Tsai *et al.* (1999) identified a gene cluster involved in pigment biosynthesis in *A. fumigatus*. They found that the *abr1* gene (for “*Aspergillus brown 1*”) encodes a putative protein possessing two signatures of multicopper oxidases. The *abr2* gene product showed homology to the laccase encoded by the *yA* gene of *Aspergillus nidulans*, which was shown to be necessary to convert the yellow pigment intermediate to the mature green form (Clutterbuck, 1972). The involvement of the two genes in the formation of the bluishgreen conidial colour was shown by disruption of each gene which led to altered conidial colour phenotypes (brown conidia). Since *abr1* and *abr2* have signature characteristics of oxidases, their existence indicates the presence of oxidation steps in the biosynthetic pathway. The laccase may involved in polymerization and oxidation of DHN into melanin. However, the gene encoding the putative multicopper oxidase has not yet been identified in brown and black fungi (Tsai *et al.*, 1999). Thus, at which point of the melanin biosynthetic pathway these enzymes are involved remains to be elucidated.

1.5. Aim of the Study

This study was aimed at the characterization and functional analysis of a novel polyketide gene cluster of *A. fumigatus* by deleting the polyketide synthase gene and a multi-copper oxidase gene within the cluster identified for the first time in this study.

The fact that fungal laccases have important biological roles such as pigment biosynthesis, detoxification and lignin degradation and have industrial application areas in food and textile industry, the newly sequenced *Aspergillus fumigatus* genome was analysed for putative laccases. This analysis using previously cloned *Aspergillus fumigatus* multi-copper oxidase gene (*abr1*), laccase gene, *abr2* (Tsai *et al.*, 1999), *Aspergillus nidulans* laccase genes, *yA* (O'Hara and Timberlake, 1989) and *tilA* (Scherer and Fischer, 2001), and laccase signature sequences (Suresh Kumar *et al.*, 2003) resulted in several laccase and multi-copper oxidase gene sequences. One of these genes, Afu4g14490, which had all four copper binding domains, characteristic of multi-copper oxidases, was selected for further characterization. After sequence alignment and characterization studies, the protein coded by Afu4g14490 was predicted to be 2128 bp long containing six introns, which makes the protein 606 amino acids long. The predicted amino acid sequence showed 63% identity with the dihydrogeodin oxidase of *Aspergillus terreus*.

Afu4g14490 was later found to be part of an uncharacterized gene cluster containing 13 genes including a polyketide synthase. In this study, it is shown that this gene cluster is involved in the biosynthesis of the *A. fumigatus* metabolites, trypacidin and monomethylsulochrin. By a comparative genomics approach, a putative geodin biosynthesis gene cluster containing 13 genes, including dihydrogeodin oxidase, in *A. terreus* and a putative trypacidin biosynthesis gene cluster containing 13 genes in *N. fischeri* were also established. Considering the nature of the reactions involving the conversion of dihydrogeodin to geodin in *A. terreus* and sulochrin to bisdechlorogeodin in *P. frequentans*, it was hypothesized in this study that a similar reaction, monomethylsulochrin to trypacidin conversion, takes place in *A. fumigatus* catalyzed by the Afu4g14490 gene product multi-copper oxidase and was named as monomethylsulochrin oxidase. In order to prove the

hypothesized functions of the polyketide synthase and multicopper oxidase genes, targeted gene deletion studies were performed. Identification of the absence of tryptacidin and monomethylsulochrin in polyketide synthase deletion strain by LC-MS analysis confirmed the hypothesis that the polyketide synthase gene product is involved in tryptacidin and monomethylsulochrin biosynthesis in *A. fumigatus*. Moreover, LC-MS analysis showed the absence of tryptacidin and the presence of a higher amount of monomethylsulochrin in the multicopper oxidase deletion strain confirming the hypothesized monomethylsulochrin oxidase function of the enzyme.

Further, Afu4g14490, monomethylsulochrin oxidase gene was cloned onto pAN52-1 and pAN52-4 vectors for heterologous expression in *Aspergillus sojae*. However, although integration into the genome was confirmed by Southern Blot analysis and transcription was detected by RT-PCR; activity assays using dihydrogeodin and sulochrin as the substrates failed to show an oxidation product.

CHAPTER 2

MATERIALS and METHODS

2.1. Materials

2.1.1. Fungal Strains

A. sojae ATCC11906 Δ *pyrGalpA* was kindly provided by Prof. Peter Punt from TNO Nutrition and Food Research, Netherlands. *A. fumigatus* IMI 385708 was kindly supplied by Prof. Peter Biely from Slovak Academy of Sciences, Slovakia. *A. fumigatus* Af293 (FGSC A1100) and *A. fumigatus* AfS28 (FGSC A1157) (genotype: Δ *akuA::ptrA*) were purchased from Fungal Genetics Stock Center (FGSC), USA.

2.1.2. Bacterial Strains

Escherichia coli XL1 Blue MRF' (Stratagene) was used for the maintenance of plasmids.

2.1.3. Plasmids

pAMDSPYRG, pAN52-1 and pAN52-4 were kindly provided by Prof. Peter Punt from TNO Nutrition and Food Research, Netherlands. pUCATPH was kindly supplied by Prof. Gillian Turgeon from Cornell University, Department of Plant Pathology, USA.

2.1.4. Chemicals and Enzymes

The list of chemicals and enzymes used and their suppliers are given in Appendix A. Dihydrogeodin was kindly provided by Prof. Yutaka Ebizuka from the Department of Molecular Pharmaceutics, University of Tokyo.

2.1.5. Growth Media, Buffers and Solutions

The preparation of the growth media, buffers and solutions are given in Appendix B.

2.2. Methods

2.2.1. Maintenance and Cultivation of Strains

A. sojae ATCC11906 Δ *pyrGalpA* strain was inoculated onto Minimal Medium agar plates (Appendix B) containing 10 mM uridine and 10 mM uracil and incubated at 30°C for 7 days. Resulting spores were suspended in Saline/Tween solution (Appendix B) containing 25% glycerol for long term storage.

A. fumigatus strains were inoculated onto PDA agar plates (Appendix B) and incubated at 37°C for 7 days. Glycerol stocks were prepared as explained.

E. coli XL1 Blue MRF' was grown on LB tetracycline agar plates (Appendix B) at 37°C and maintained at 4°C. Cultures were refreshed every two weeks.

For DNA isolation, *A. sojae* ATCC11906 Δ *pyrGalpA* was cultivated in 100 ml Complete Medium (Appendix B) containing 10 mM uridine and 10 mM uracil at 30°C and 150 rpm for 24 hours. For DNA isolation from *A. sojae* transformants, the same medium was used without uridine and uracil. *A. fumigatus* strains were again inoculated in Complete Medium, but were grown at 37°C.

For RNA isolation, *A. sojae* strains were cultivated in 250 ml Complete Medium (Appendix B) supplemented with 0.2 mM CuSO₄ at 30°C and 150 rpm for 3 days. For RNA isolation from *A. fumigatus*, the fungus was grown in 250 ml Czapek-

Dox medium (Appendix B) supplemented with 0.2 mM CuSO₄ at 37°C and 150 rpm for 5 days.

For detection of metabolites, *A. fumigatus* was grown on YES, CYA and MEA agar plates (Appendix B) at 25°C for two weeks.

For phenotypic assays, *A. fumigatus* Af293, *A. fumigatus* AfS28 and *A. fumigatus* knock-out strains, were grown on Minimal Medium agar plates with different compositions. To examine the effect of different agents on growth, the medium was supplemented with cell wall inhibitor agents, congo red (80 µg/ml) and SDS (0.01%); to examine osmotic stress, NaCl (1.5 M) was added; for oxidative stress, H₂O₂ (2 mM) was used; and to examine the effect of antifungals, amphotericin B (0.2 µg/ml) and voriconazole (0.2 µg/ml) were used. To analyze the effect of carbon sources, the strains were grown in Minimal Medium agar plates containing ethanol, fructose, galactose, glycerol, lactose, maltose or sorbitol at a concentration of 100 mM instead of glucose. To examine the effect of nitrogen sources, the strains were grown in Minimal Medium agar plates containing glutamine, alanine, proline, ammonium chloride or sodium glutamate at a concentration of 10 mM instead of sodium nitrate. The strains were inoculated on agar plates by placing a total of 10⁶ conidia in 5 µl on the plate. The plates were incubated at 37°C for 3 days. When examining the effect of temperature, Minimal Medium agar plates inoculated with fungal strains were incubated at 25°C, 37°C and 45°C for 3 days.

2.2.2. Nucleic Acid Isolation Techniques

2.2.2.1. Genomic DNA Isolation

Genomic DNA isolation was performed using Plant Genomic DNA Purification kit (Genemark) according to the manufacturer's instructions. The process is based on a spin column format, the procedures involve cell lysis at 65°C, precipitation of proteins, polysaccharides and secondary metabolites, removal of cell debris by SpinFilter, and DNA binding and elution by spin column.

First, fungal mycelium was collected by filtering through Whatman 3MM filter paper. The collected mycelium was frozen in liquid nitrogen and ground using

Micro-Dismembrator (Sartorius) without letting the sample to thaw. The powder (100 mg per isolation) was transferred to a 1.5 ml microcentrifuge tube, 360 µl Extraction Solution A, 40µl Extraction Solution B and 4 µl RNaseA solution were added. The mixture was vortexed vigorously for 5-10 sec and incubated at 65⁰C in water-bath inverting the tube from time to time. After that, 130µl Precipitation Solution was added, the contents of the tube were mixed by inverting the tube several times and the tube was incubated on ice for 5 min. After centrifugation at maximum speed for 5 min at room temperature, the supernatant was transferred into spin filter that was placed into a clean 2 ml collection tube. The collection tube with the spin filter was spinned at maximum speed for 2 min. The flow-through solution in the collection tube was transferred into a new 1.5 ml microcentrifuge tube without disturbing the pellet. 1.5 volume of Binding Solution was added and mixed thoroughly by pipeting. 650 µl of the mixture including any precipitate was transferred into a spin column with a collection tube, spinned for 1 min and the flow-through was discarded. This step was repeated with the remaining mixture and the flow-through was again discarded. The column was washed twice with 700 µl of Wash Solution. After discarding the flow-through, the column with the collection tube was centrifuged for 10 min at maximum speed to remove ethanol. Then, the column was placed in a new 1.5 ml microcentrifuge tube and 100 µl preheated Elution Solution (60-70°C) was added. After waiting for 2 min, the DNA was eluted by centrifugation for 1 min. This elution step was repeated to increase DNA yield. The resulting DNA was stored at -20°C.

DNA concentration was determined by comparing the intensity of the band with that of the bands of known concentration on agarose gel.

2.2.2.2. Plasmid DNA Isolation

Plasmid DNA isolation was performed using Plasmid Miniprep Purification kit (Genemark) according to the manufacturer's instructions. Solutions were provided in the kit. The procedure is based on alkaline lysis of the cells and DNA binding and elution by spin column.

First, 5 ml of cells grown overnight in 2TY medium (Appendix B) was pelleted by centrifugation for 3 min at maximum speed in a 1.5 microcentrifuge tube. The supernatant was poured off and excess media was removed. The cell pellet was completely resuspended in 200 μ l of Solution I. Then, 200 μ l of Solution II was added and the contents were mixed by inverting the tube 8 times. After that, 200 μ l of Solution III was added and the contents were mixed by inverting the tube 8 times. The lysate was centrifuged at maximum speed in a microcentrifuge for 5 min. A compact white pellet was formed at the bottom of the tube. All of the cleared lysate was carefully removed into a spin column inserted in a collection tube. The filtrate in the collection tube was discarded, 700 μ l of Washing Solution was added and the tube was centrifuged at top speed for 1 min. This washing step was repeated one more time. The filtrate was discarded and the tube was centrifuged for 10 min to remove the residual ethanol. The column was placed in a new 1.5 ml microcentrifuge tube and 30-50 μ l preheated Elution Solution (60-70°C) was added. After waiting for 2 min, the DNA was eluted by centrifugation for 1 min. The resulting plasmid DNA was stored at -20°C.

2.2.2.3. Total RNA Isolation

Total RNA isolation was performed using TriSolution Reagent Plus (Genemark) according to the manufacturer's instructions. TriSolution is a mixture of phenol, guanidium thiocyanate, buffers and stabilizers developed for the isolation of total RNA free from protein and DNA contamination. The reagent also includes a bottle of PS&PG Removal Solution, which eliminates polysaccharides and proteoglycans contamination, so that the RNA can dissolve easier and be purer.

First, fungal mycelium was collected by filtering through Whatman 3MM filter paper. The collected mycelium was frozen in liquid nitrogen and ground using Micro-Dismembrator (Sartorius) without letting the sample to thaw. The powder (100 mg per isolation) was transferred to a 1.5 ml microcentrifuge tube, 1 ml of TriSolution was added and the tube was incubated at room temperature for 5 min. After centrifugation at 12,000 g for 15 min at 4°C, the supernatant was transferred to a new tube. Then, 200 μ l of chloroform was added, the tube was shaken vigorously

for 15 seconds and incubated at room temperature for 2 min. The sample was then centrifuged at 12,000 g for 15 min at 4°C. After centrifugation, the mixture separated into a phenol chloroform phase, an interphase and a colorless upper aqueous phase. The aqueous phase was transferred to a new microcentrifuge tube without disturbing or touching the interphase. After that, 250 µl of isopropanol and 250 µl of PS&PG Removal Solution were added and the tube was mixed gently. After keeping at room temperature for 10 min, the sample was centrifuged at 12,000 g for 10 min at 4°C. The supernatant was carefully removed and the RNA pellet was washed with 1 ml of 75% ethanol. After centrifuging at 12,000 g for 5 min at room temperature, the ethanol was removed and the RNA pellet was dried briefly. RNA was dissolved in 20 µl of water by incubating for 5 min at 60°C and stored at -20°C.

The yield of RNA was determined spectrophotometrically at 260 nm, where 1 absorbance unit (A_{260}) = 40 µg of RNA. The purity was also estimated spectrophotometrically, where A_{260}/A_{280} ratio between 1.7 and 2.0 indicating sufficiently pure RNA. The integrity of the purified RNA was determined by agarose gel electrophoresis where the existence of ribosomal RNA bands was accepted as the proof of undegraded RNA.

2.2.2.4. Recovery of DNA from Agarose Gel

Elution of DNA from agarose gel was performed using Gel Elution kit (Genemark) according to the manufacturer's instructions. Solutions used were provided in the kit. The procedure is based on a spin column format.

The desired DNA band (not more than 350 mg per purification) was cut out from the gel and transferred into a 1.5 ml microcentrifuge tube. 2 volumes of Binding Solution were added and the tube was incubated at 60°C for 5-10 min until complete melting of agarose. The DNA/agarose solution was transferred to a spin column sitting in a collection tube, the tube was spinned for 1 min at top speed and the filtrate was discarded. 500 µl of Binding Solution was added to the column to remove residual agarose, the tube was spinned for 1 min at top speed and the filtrate was discarded. After that, 700µl of Wash Solution was added, the tube was spinned for 1 min at top speed and the filtrate was discarded. This washing step was repeated

one more time. Then, the tube was centrifuged for 10 min at top speed to remove residual trace of ethanol. The spin column was transferred into a new microcentrifuge tube and 30-50 μ l preheated Elution Solution (60-70°C) was added. After waiting for 2 min, the DNA was eluted by centrifugation for 1 min. The resulting plasmid DNA was stored at -20°C.

2.2.2.5. Recovery of DNA from PCR reaction

When purifying DNA from a PCR reaction, the same method explained in Section 2.2.2.4 was used with minor differences. 1.5 volume of Binding Solution was added to the PCR reaction, the resulting solution was transferred to a spin column sitting in a collection tube and the same procedure explained in Section 2.2.2.4 was applied.

2.2.3. The Polymerase Chain Reaction (PCR) and Reverse Transcriptase Polymerase Chain Reaction (RT-PCR)

When using Taq polymerase (Fermentas and Genemark) and Pfu polymerase (Genemark) in PCR, a 50 μ l reaction contained 10X reaction buffer with $MgCl_2$ to give a final concentration of 1X, 0.2 mM dNTP mix, 2 units of Taq polymerase, 25 pmols of each primer, 0.1 μ g of DNA and sterile double distilled water to give a final volume of 50 μ l. Amplifications were performed according to the following cycle:

Initial denaturation: 95°C for 5 min	} 35 cycles
Denaturation: 95°C for 15 seconds	
Annealing: T_a for 30 seconds	
Extension: 72°C for 1 min/kb	
Final extension: 72°C for 5 min	

where T_a is the annealing temperature, ranging from 50-58°C according to the melting temperature of the primers.

When using Long PCR Kit (Fermentas and Qiagen), PCR was performed according to the manufacturer's instructions. A 50 μ l reaction contained 10X reaction buffer with $MgCl_2$ to give a final concentration of 1X, 0.5 mM dNTP mix while using Qiagen kit and 0.2 mM dNTP mix while using Fermentas kit, 2 units of

enzyme mix, 20 pmols of each primer, 0.1 µg of DNA and sterile double distilled water to give a final volume of 50 µl. Amplifications were performed according to the following cycle:

Initial denaturation: 93°C for 3 min	
Denaturation: 93°C for 15 seconds	} 35 cycles
Annealing: 50°C for 30 seconds	
Extension: 68°C for 1 min/kb	

When doing RT-PCR, Superscript First-Strand Synthesis System for RT-PCR kit (Invitrogen) was used according to the manufacturer's instructions. This system is optimized to synthesize first-strand cDNA from poly(A) or total RNA. The first-strand synthesis reaction is catalyzed by Superscript II Reverse Transcriptase (RT). Oligo(dT) is used as a primer to hybridize to 3' poly(A) tails, which are found in the vast majority of eukaryotic mRNAs. The sensitivity of PCR from cDNA is increased by removal of the RNA template from the cDNA:RNA hybrid molecule by digestion with RNase H after first-strand synthesis. The following procedure was followed for first-strand cDNA reaction:

To 5 µg of RNA, 1µl of 10 mM dNTP mix, 1 µl of 0.5 µg/µl oligo(dT) and DEPC-treated water up to 10 µl were added. The sample was incubated at 65°C for 5 min and placed on ice for at least 1 min. To this sample, 2 µl of 10X RT buffer, 4 µl of 25 mM MgCl₂, 2 µl of 0.1 M DTT and 1 µl of RNase OUT were added. The tube was incubated at 42°C for 2 min, and then 1 µl of Superscript RT was added and mixed. The reaction was incubated at 42°C for 50 min and then at 70°C for 15 min. After that, the sample was chilled on ice and 1 µl of RNase H was added. The reaction was incubated at 37°C for 20 min. 1 to 5 µl of the resulting first strand cDNA was used in PCR.

2.2.4. Agarose Gel Electrophoresis and Visualization of DNA and RNA

To analyze genomic DNA, plasmid DNA, total RNA and PCR products, 0.8% (w/v) agarose gel (Appendix B) was used.

The gel was melted and cooled to 50-60°C. After adding ethidium bromide at a concentration of 0.5 µg/ml, the gel was poured into mould and allowed to solidify for about 15 min. Then it was placed in the electrophoresis tank filled with 1X TAE buffer (Appendix B). Electrophoresis was carried out at 100-140 V for approximately 30 min. After that, the gel was visualized on Gel Doc XR system (BioRad).

2.2.5. Restriction Enzyme Digestion of DNA

For digestion of plasmids and PCR products, to 0.1-50 µg DNA, appropriate 10X restriction enzyme buffer to give a final concentration of 1X, 10-50 U of restriction enzyme, and sterile double distilled water to give a final volume of 20 µl were added. The reaction was incubated at 37°C for 1 h.

For digestion of genomic DNA to be used in southern blot, to 2.5-3 µg of DNA, appropriate 10X restriction enzyme buffer to give a final concentration of 1X, 50-60 U of restriction enzyme, and sterile double distilled water to give a final volume of 30-40 µl changing according to the DNA volume were added. The reaction was incubated at 37°C for overnight.

The restriction enzymes and buffers were from Fermentas.

2.2.6. Ligation

For ligation, first plasmid DNA and purified PCR fragment were digested with the appropriate restriction enzyme as explained in section 2.2.5. Then, plasmid DNA was dephosphorylated with calf intestine alkaline phosphatase (Fermentas).

Dephosphorylation reaction contained 33 µl restriction reaction, 5 µl of 10X alkaline phosphatase reaction buffer, 1 µl of calf intestine alkaline phosphatase (1U/µl) and 11 µl water making the final volume 50 µl. The reaction was incubated at 37°C for 1 hour.

Digested and dephosphorylated plasmid DNA and digested PCR fragment were then purified as explained in Section 2.2.2.5. The concentrations of the purified

fragments were determined by comparing the intensity of the bands with that of the bands of known concentration on agarose gel.

Ligation reaction was performed with a vector-insert molar ratio of 1:3 using 100 ng vector and 110 ng insert using ligation kit from Sigma. The reaction consisted of 10X ligation buffer to give a final concentration of 1X, 0.5 U of ligase, 1 mM ATP and sterile double distilled water making the final volume 5 μ l. The reaction was incubated at 22°C overnight. 1 μ l aliquots of the ligation reaction were used to transform *E. coli* XL1 Blue MRF' as explained in Section 2.2.7.

2.2.7. Transformation of *E. coli* XL1 Blue MRF'

Preparation of competent cells and transformation of *E. coli* was performed using Transformation and storage solution, SSCS (Genemark) according to the manufacturer's instructions.

50 ml of 2TY medium (Appendix B) was inoculated with a 1 ml overnight culture of *E. coli* XL1 Blue MRF' and the cells were grown at 37°C with shaking until absorbance at 600 nm reached 0.5-0.7. Cells were centrifuged at 4000 rpm for 5 min and the supernatant was removed. After that, cells were resuspended in 1 ml of pre-cooled SSCS solution. Competent cells were dispensed in 100 μ l aliquots and stored at -80°C.

For transformation, 100 pg-10 ng DNA or 1-5 μ l of a ligation reaction was mixed with an aliquot of competent cells and the sample was placed on ice for 10 min, then 37°C for 5 min and then again on ice for 10 min. 1 ml of LB medium (Appendix B) was added and the sample was incubated at 37°C for 1 hour. 100 μ l aliquots of cells were plated on 2TY (Appendix B) supplemented with 100 μ g/ml ampicillin and incubated overnight at 37°C. When a blue-white colony selection was performed, 10 μ l 100 mM IPTG (Appendix B) and 49 μ l 2% X-Gal (Appendix B) were spread on plates 30 min before inoculation of cells.

2.3.8. Sequencing

The plasmids were sequenced by Iontek (İstanbul).

2.2.9. Transformation of *Aspergillus sojae*

2.2.9.1. *A. sojae* Strain Used for Heterologous Expression

A. sojae ATCC11906 Δ *pyrGalpA* developed by Heerikhuisen *et al* (2001) was used for heterologous expression strain. Strain ATCC11906, which exhibited low proteolytic profile, was selected among *A. sojae* strains and its proteolytic activity was further reduced by disrupting the most abundant alkaline protease coding gene *alpA* by Heerikhuisen *et al* (2001). To establish an auxotrophic selection method, orotidine 5-monophosphate decarboxylase (*pyrG*), the gene encoding an enzyme that takes role in uridine monophosphate pathway, mutants, which require uridine/uracil for growth, were isolated by direct selection for resistance to fluoro-orotic acid (FOA).

2.2.9.2. Selection Plasmid

The selection plasmid used as a cotransformation vector in transformation was pAMDSPYRG that contains *amdS* and *pyrG* selection markers. *AmdS*, originated from *A. nidulans*, is a dominant nutritional marker encoding acetamidase, which is an enzyme that confers the ability to use acetamide and acrylamide as nitrogen and carbon sources. On the other hand, *pyrG*, originated from *A. niger*, is an auxotrophic marker coding for orotidine 5-monophosphate decarboxylase, which confers a *pyrG⁻* strain the ability to grow without uridine/uracil.

2.2.9.3. Expression vectors

The expression vectors used in transformation were pAN52-1 (sequence accession number Z32524) and pAN52-4 (sequence accession number Z32750), the

maps of which are shown in Appendix C. They both contain the constitutive promoter sequence of *A. nidulans gpdA* gene, encoding glyceraldehyde-3-phosphate dehydrogenase, and terminator sequence of *A. nidulans trpC* gene, which encodes an enzyme taking role in tryptophan biosynthesis; however, while pAN52-1 does not involve a secretion sequence, pAN52-4 contains 24 amino acid-long signal and propeptide sequence of *A. niger glaA* gene encoding glucoamylase.

2.2.9.4. *Aspergillus sojae* Transformation Protocol

For *A. sojae* transformation, a procedure adapted from different protocols (Punt *et al.*, 1987; <http://clone.concordia.ca/aspergillus/protocols/nigtransf.html>) was followed. The protocol is based on preparation of protoplasts and subsequent PEG/CaCl₂-mediated DNA uptake.

A. sojae ATCC11906 Δ *pyrGalpA* strain was grown on Minimal Medium Agar plates (Appendix B) supplemented with 10 mM uridine and 10 mM uracil for 7 days at 30°C. Spore suspension was prepared using Saline/Tween solution (Appendix B) and spores were counted using a Thoma haemocytometer, number of spores/ml was calculated as follows:

$$\text{Number of spores/ml} = \frac{\text{Number of cells counted} \times 1000 \text{ mm}^3}{\text{Number of squares counted} \times \text{width}^2 \times \text{depth}}$$

where width=0.05 mm², depth=0.02 mm² for Thoma haemocytometer. Therefore, the final equation is,

$$\text{Number of spores/ml} = \frac{\text{Number of cells counted}}{\text{Number of squares counted}} \times 2 \times 10^7$$

Four 500 ml flasks each containing 250 ml Complete Medium (Appendix B) supplemented with 10 mM uridine and 10 mM uracil were inoculated with 2x10⁶ spores/ml. After growing for 18 hours at 30°C at 200 rpm, mycelium was collected by filtration through nylon mesh and washed with Lytic Solution (Appendix B). The collected mycelium was resuspended in filter sterilized 20 ml Lytic Solution containing 40 mg/ml lysing enzyme (appendix A). Protoplasts were prepared by incubating the enzyme solution with mycelium at 30°C for 3-5 hours with slow agitation. Protoplast formation was checked under microscope at 30 min intervals.

Protoplasts were separated from mycelial debris by filtering through sterile glass wool. From this step on, protoplasts were kept on ice. Protoplast solution was then centrifuged at 2000 rpm for 5 min and the supernatant was carefully discarded. The pellet was resuspended in 5 ml STC solution (Appendix B) and pelleted by centrifugation as before. This washing step was performed twice after which the protoplasts were resuspended in STC solution such that the concentration is 1×10^8 /ml. 200 μ l of the protoplast suspension was added to a 50 ml centrifuge tube for each transformation reaction. Then, 20 μ g of recombinant plasmid and 2 μ g of pAMDSPYRG contransformation plasmid were added and mixed gently. To this suspension, 50 μ l of PEG solution (Appendix B) was added, mixed gently and incubated at room temperature for 20 min. After that, 2 ml of PEG solution was added, mixed gently and incubated at room temperature for 5 min. Then 4 ml STC solution was added to the tubes and mixed gently. Lastly, 25 ml of melted Stabilized Minimal Medium Top Agar (Appendix B) was added to the tubes, mixed by inverting several times and the mixture was poured onto two 9 mm Minimal Medium Agar plates. Plates were incubated for 3-4 days at 30°C.

Obtained transformants were transferred to Minimal Medium Agar plates and incubated at 30°C until sporulation. Spores were suspended in a small volume of Saline/Tween solution and streaked onto Minimal Medium Agar plates with a loop to obtain single spores. After growing at 30°C until formation of small colonies, single colonies were transferred to Minimal Medium Agar plates and incubated at 30°C for 7 days. Glycerol stocks were prepared from these purified colonies by adding 25% glycerol to Saline/Tween solution containing the purified spores.

2.2.10. Southern Blot

For Southern Blotting, labeling of probe DNA, blot assembly, hybridization and detection were performed using Digoxigenin (DIG) system (Roche) according to the manufacturer's instructions.

2.2.10.1. Labeling of Probe DNA

Labeling was performed using random primed labeling method according to the manufacturer's instructions. In this method, template DNA is first linearized and denatured. Then, Klenow polymerase incorporates DIG-dUTP into the template as multiple locations that are determined by the binding of a random hexamer primer mixture.

First, DNA to be used as probe was purified as explained in Section 2.2.2.4 and 2.2.2.5. Then 15 μ l of DNA fragment of known concentration was heat-denatured in a boiling water bath and immediately chilled on ice for 30 seconds. On ice, 2 μ l of hexanucleotide mix (10x), 2 μ l of dNTP labeling mixture (10X) and 1 μ l of Klenow enzyme were added. The reaction was incubated at 37°C overnight. When necessary, the reaction was scaled up by increasing the amounts of the components in proportion to the increased reaction volume.

Probe yield was estimated according to DIG User Manual by preparing serial dilutions from the labeled probe and DIG labeled control DNA; spotting 1 μ l from the dilutions on a piece of Positively Charged Nylon Membrane (Roche); carrying out the detection procedure, which was explained in Section 2.2.10.4 and comparing the intensities of the spots.

2.2.10.2. Blot Assembly

Blot assembly and hybridization was performed according to the DIG manual (Roche). Namely, 2.5-5 μ g of DNA together with a molecular weight marker were loaded on 0.8% agarose gel, which did not contain ethidium bromide. The gel was run at 20-45 V until loading dye reached the end of the gel. Then, the gel was stained briefly in 1X TAE buffer (Appendix B) containing 1 μ g/ml ethidium bromide for 15 min, and visualized under UV light using Gel Doc XR system (BioRad). The gel was cut through the middle of the wells, and the top portion was discarded. Sides of the gels that do not contain DNA were also cut and discarded. Then the gel was photographed with a ruler next to the marker side and the gel was destained in 1X TAE Buffer for 10 min. After that, the gel was submerged in Denaturation Solution

(Appendix B) for 2 x 15 min at room temperature, with gentle shaking. After rinsing with water, the gel was submerged in Neutralization Solution (Appendix B) for 2 x 15 min at room temperature and equilibrated for 10 min in 20xSSC (Appendix B). To set up the blot, a piece of Whatman 3MM paper that had been soaked with 20xSSC was placed atop a bridge that rests in a shallow reservoir of 20x SSC. The gel was placed upside down atop the soaked sheet of Whatman 3MM paper. Air bubbles were removed and a piece of Positively Charged Nylon Membrane (Roche) at the same size of the gel was placed on the gel eliminating air bubbles. The blot assembly was completed by adding a dry sheet of Whatman 3MM paper, a stack of paper towels, a glass plate, and a 200– 500 g weight. The blot was allowed to transfer overnight. Then the membrane was washed briefly in 2xSSC and baked at 100°C for 1 hour to fix the nucleic acids on the membrane.

2.2.10.3. Hybridization

Prehybridization and hybridization was performed using DIG Easy Hyb. The appropriate hybridization temperature (T_{hyb}) was calculated according to the following formula:

$$T_m = 49.82 + 0.41 (\% G + C) - 600/l$$

$$T_{\text{hyb}} = T_m - (20^\circ \text{ to } 25^\circ\text{C})$$

Where:

T_m = melting point of probe-target hybrid

T_{hyb} = Optimal temperature for hybridization of probe to target in DIG Easy Hyb

l = length of hybrid in base pairs

For prehybridization, the membrane was put in a roller bottler with 20 ml of prewarmed DIG Easy Hyb. The roller bottle was placed in the rotator in the hybridization oven (Stuart Scientific) at the hybridization temperature for 30 min-3 hours. For hybridization, 25 ng/ml probe, which had been denatured in a boiling water bath for 5 min and chilled on ice, was added to at least 6 ml of prewarmed DIG Easy Hyb. Hybridization solution containing labeled probe was added to the roller

bottle immediately after pouring out the prehybridization buffer. The roller bottle was placed in the rotator in the hybridization oven at the hybridization temperature overnight. When hybridization was over, the hybridization solution was saved in a tube at -20°C. When reusing, the solution was kept at 68°C for 10 min to denature the probe. After pouring off the hybridization solution, the membrane was immediately placed in a plastic tray containing 100 ml Low Stringency Buffer (Appendix B). The tray was incubated at room temperature for 5 min with shaking. The used buffer was poured off and 100 ml fresh Low Stringency Buffer was immediately added. The tray was incubated an additional 5 min at room temperature with shaking. The used Low Stringency Buffer was poured off and 100 ml preheated High Stringency Buffer (Appendix B) was added to the tray containing the blot. The blot was incubated twice (2 x 15 min) with preheated High Stringency Buffer at 65°C. The blot was shaken gently during the washes.

2.2.10.4. Detection

The membrane was transferred to a plastic tray containing 100 ml Washing Buffer (Appendix B) and incubated for 2 min at room temperature, with shaking. After discarding Washing Buffer, 100 ml Blocking solution (Appendix B) was added to the tray and the membrane was incubated for 30 min to 3 hours with shaking. Then, Blocking Solution was discarded and 30 ml Antibody Solution (Appendix B) was added to the tray. The membrane was incubated for 30 min with shaking. After discarding the Antibody Solution, the membrane was washed twice with 100 ml portions of Washing Buffer for 2 x 15 min. Then the membrane was equilibrated 3 min in Detection Buffer (Appendix B) and placed on a plastic sheet, DNA side facing up. For every 100 cm² of membrane, 1 ml CSPD, 1:100 diluted in Detection Buffer was applied dropwise. The membrane was immediately covered with a second plastic sheet without letting any air bubbles between the membrane and plastic sheets. After that, the membrane was incubated for 5 min at room temperature. Excess liquid was squeezed out and the sides of the plastic sheet were heat-sealed close to the membrane. The sealed bag containing the membrane was exposed to X-ray film (XBM blue sensitive, Kodak) for 20 min-1 hour in the

Hyperscassette (Amersham) at 37°C. Then the film was developed in Medical Center, Radiology Department and photographed on a light box.

2.2.11. Enzyme Assays

Activity of the multi-copper oxidase heterologously expressed in *A. sojae* was first analyzed by growing the fungi in Minimal Medium Plates (Appendix B) containing 200 µM ABTS as explained by Record *et al.*, 2002. Plates were incubated 10 days at 30°C and checked for development of a green color.

Activity assays were also performed in liquid culture. *A. sojae* strains were cultivated in 250 ml Complete Medium (Appendix B) supplemented with 0.2 mM CuSO₄ at 30°C and 150 rpm for 5 days. *A. fumigatus* was cultivated in 250 ml Modified Czapek-Dox Medium (Appendix B) at 37°C for 5 days. The culture supernatants or cell extracts from day 3 and 5 were used in enzyme assays. The assay medium consisted of 50 µl of supernatant, 100 µl of 0.5 M Phosphate Buffer (Appendix B) and 10 µg dihydrogeodin or 10 µg of sulochrin as the substrate. The samples were incubated at 37°C for 24 hours, then extracted with ethyl acetate and examined by thin layer chromatography (TLC) for product formation.

2.2.12. SDS-PAGE

SDS-PAGE was performed using Blue Vertical 102 electrophoresis system and Blue Power 500 power supply (SERVA Elektrophoresis GmbH) following the instruction manual of Blue Vertical and BioRad.

2.2.12.1. Gel Plate Assembly

First, the comb, two spacers, small and large gel plates were cleaned with ethanol and dried. Then the spacers were placed on edges of the large gel plate and the small gel plate was overlaid to create a sandwich. The glass plate sandwich was placed into the electrophoresis running unit, with the small plate innermost and affixed to the inner core running unit by inserting the wedges and pressing down.

When running one gel, a dummy plate was placed on the other side of the unit and wedges were placed to affix the plate to the running unit. After that, the running unit was placed onto the silicon pads of the gel casting stand. The cams were used to tighten the assembly down onto the silicon pads by turning simultaneously with both hands the set of the two front cams gradually. Then the back two cams were turned in the same way to tighten the assembly down. The comb was placed in glass plates and 1 cm beneath well base was marked to indicate the height of the separating gel. Then the comb was removed.

2.2.12.2. Gel Pouring

After assembling the plates, a suitable separating gel was prepared by combining the components in Table 2.1 in a small centrifuge tube. TEMED and freshly made APS (Appendix B) were added just before the gel was ready to pour to prevent polymerization in the tube. Using a Pasteur pipette, the gel mixture was poured between the plates up to the level indicated. After overlaying with water, the gel was left for polymerization for 30 min-1 hour. Then, the stacking gel was prepared by combining the components indicated in Table 2.2 in a small centrifuge tube without TEMED and APS. The water overlay was poured off and the area above the gel was dried using 3MM filter paper. Then TEMED and APS were added to the stacking gel mixture and the gel was poured with a Pasteur pipette above the separating gel. The comb was inserted and the gel was left for polymerization for 30 min.

2.2.12.3. Sample Preparation and Electrophoresis

After the gel was polymerized, the running unit was separated from the gel casting stand by loosening the cams and placed in the electrophoresis tank. The top buffer chamber was filled with 1X running buffer (Appendix B) to halfway between small and large gel plates (about 200 ml). Then the lower buffer chamber was filled with 1X running buffer up to the maximum level sign indicated (about 700 ml). The comb was removed and wells were washed out with running buffer.

Table 2.1. Separating Gel Preparation

Separating gel components	Volume (ml)			
	8%	10%	12.5%	15%
Gel Buffer (Appendix B)	1.2	1.2	1.2	1.2
30% acrylamide stock	1.3	1.7	2.1	2.6
Water	2.5	2.1	1.7	1.2
APS	0.03	0.03	0.03	0.03
TEMED	0.003	0.003	0.003	0.003
Total	5	5	5	5

Table 2.2. Stacking Gel Preparation

Stacking Gel (7.5%) components	Volume (ml)
Stacking Gel Buffer (Appendix B)	0.6
30% acrylamide stock	0.4
Water	1.4
APS	0.02
TEMED	0.002
Total	2.4

Afterwards, sample denaturing mix was prepared by adding 1 volume of β -mercaptoethanol to 5 volumes of sample buffer (Appendix B). Sample denaturing mix (5 μ l) was added to 15 μ l of each sample. The samples were boiled for 5 min in a boiling water bath and allowed to cool on bench. Then the samples were centrifuged for 5 min at maximum speed and the supernatants were delivered to the base of the wells using a fine pointed tip. Unused wells were also filled with the equivalent volume of sample buffer to maintain uniform electrical resistance across the gel. After placing the lid of the tank, constant voltage of 150 V was applied and

the gel was run for about 2 hours until the blue dye was migrated at the base of the gel. Then the power supply was disconnected, lid was removed and running unit was pulled out from the buffer chamber. Buffer was poured off and wedges were removed. To release the gel from the glass plates, one spacer was pushed ½ way out of sandwich and gently twisted. One corner of the gel was cut to indicate orientation.

2.2.12.4. Silver Staining

The gel was placed in a plastic container with 100 ml fixer solution (Appendix B) for 1 hour to overnight. After that, the Fixer Solution was discarded and the gel was washed with 100 ml 50% ethanol for 3 x 20 min. After discarding ethanol, 100 ml Pretreatment Solution (Appendix B) was added to the container. After exactly 1 min, Pretreatment Solution was discarded and the gel was washed with water for 3 x 20 seconds exactly. Then, the gel was placed in 100 ml Silver Nitrate Solution (Appendix B) for 20 min. After discarding solution, the gel was rinsed with water for 2 x 20 seconds exactly. Then, 100 ml Developing Solution (Appendix B) was added to the container. When bands started to appear, reaction was slowed down by adding water. When desired band intensity was reached, Developing Solution was discarded, the gel was rinsed with water and photographed on a light box.

2.2.13. Split Marker Method for Targeted Gene Deletion

For targeted deletion of *A. fumigatus* genes, a method developed by Catlett *et al* (2002) was used. In this method, two constructs are required per transformation, each containing a flank of the target gene and roughly two thirds of a selectable marker cassette. Homologous recombination between the overlapping regions of the selectable marker gene and between the flank regions and their genome counterparts results in a targeted gene deletion and replacement with a marker gene (Figure 2.1).

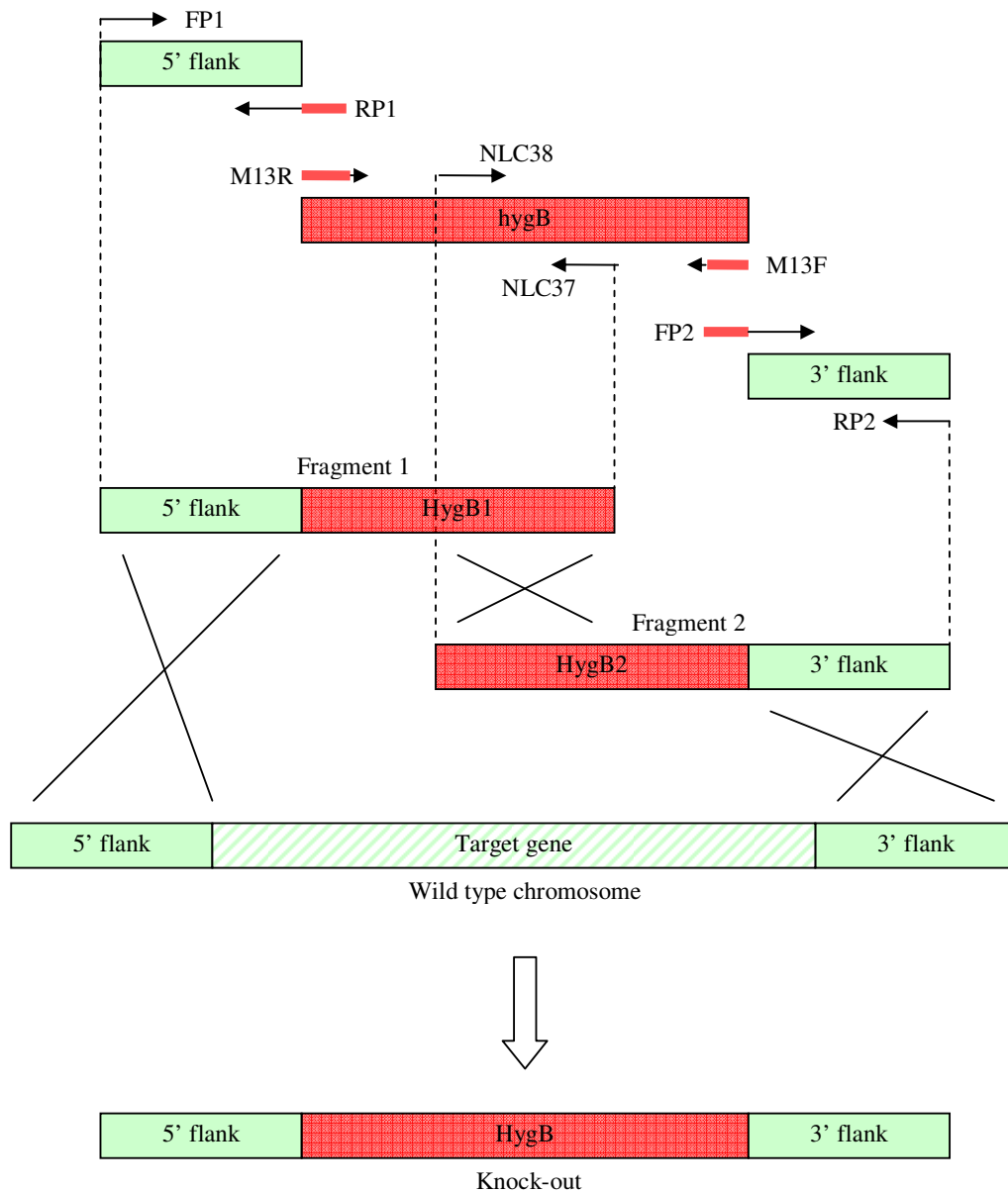


Figure 2.1. Split marker strategy for gene deletion. Primers FP1-RP1 and FP2-RP2 amplify the target gene flanking sequences. Primers M13R-NLC37 and NLC38-M13F amplify HygB1 and HygB2 marker fragments, respectively. 5' ends of the primers RP1 and FP2 are complementary to M13R and M13F sequences respectively, and 3' ends are gene specific. The two fusion PCR fragments (FP1-NLC37 and NLC38-RP2) are used directly for transformation. Homologous recombination between the overlapping regions of the selectable marker (HygB), and between the flank regions and chromosomal DNA results in a directed deletion.

The method is based on a PCR-based strategy eliminating subcloning of the target sequences, and requires only two rounds of PCR reactions. Four marker primers and four gene-specific primers are required for each deletion. In PCR round 1, the flanks and the selectable marker are amplified. The marker gene (*hygB*) codes for a hygromycin B phosphotransferase that inactivates the antibiotic hygromycin B, which disturbs protein synthesis in prokaryotes and eukaryotes, by phosphorylation (Punt *et al.*, 1987). The overlapping marker fragments of the hygromycin phosphotransferase cassette are amplified from pUCATPH (Appendix C). The 5' extensions for primers RP1 and FP2 facilitating fusion of the flanks and the marker sequences are complementary to the M13R and M13F primer sequences, respectively. In PCR round 2, each flank from round 1 is fused to the marker through overlap extension PCR. For the 5' construct, fragment 1, the templates are FP1-RP1 flank from round 1 and M13R-NLC37 marker fragment (HygB1); primers are FP1 and NLC37. For the 3' construct, fragment 2, the templates are NLC38-M13F marker fragment (HygB2) and FP2-RP2 flank from round 1; primers are NLC38 and RP2.

Long PCR kit was used for both rounds of PCR amplifications as explained in Section 2.2.3. Round 1 PCR products were purified as explained in Section 2.2.2.5 and used as templates for round 2 PCR. Since multiple bands were obtained in round 2 PCR, the fragments of interest were recovered from agarose gel as explained in Section 2.2.2.4 and used in transformation of *Aspergillus fumigatus* Δ *akuA*.

2.2.14. Transformation of *Aspergillus fumigatus* AfS28

For transformation, a procedure adapted from different protocols (Punt *et al.*, 1987; Wirsal *et al.*, 1996) (<http://clone.concordia.ca/aspergillus/protocols/nigtransf.html>) was followed. The protocol is based on preparation of protoplasts and subsequent PEG/CaCl₂-mediated DNA uptake.

A. fumigatus AfS28 was grown on Potato Dextrose Agar (PDA) (Appendix B) at 37°C for 7 days. Then, spore suspension was prepared as explained in Section 2.2.8.4.

One 500 ml flask containing 250 ml Complete Medium (Appendix B) was inoculated with 2×10^6 spores/ml. After growing for 16 hours at 37°C at 200 rpm, mycelium was collected by filtration through nylon mesh and washed with Lytic Solution (Appendix B). The collected mycelium was resuspended in filter sterilized 20 ml Lytic Solution containing 40 mg/ml lysing enzyme (appendix A). Protoplasts were prepared by incubating the enzyme solution with mycelium at 30°C for 1.5-2 hours with slow agitation. Protoplast formation was checked under microscope at 30 min intervals. Protoplasts were separated from mycelial debris by filtering through nylon mesh. From this step on, protoplasts were kept on ice. Protoplast solution was then centrifuged at 6000 rpm for 6 min and the supernatant was carefully discarded. The pellet was resuspended in 5 ml STC solution (Appendix B) and pelleted by centrifugation as before. This washing step was performed twice after which the protoplasts were resuspended in STC solution such that the concentration is 1×10^8 /ml. 100 μ l of the protoplast suspension was added to a 50 ml centrifuge tube for each transformation reaction. Then, 1-2 μ g split marker fragments in a total volume of 20 μ l were added, mixed gently and incubated on ice for 2-10 min. To this suspension, 3 aliquots of PEG solution (Appendix B), 200 μ l, 200 μ l, 800 μ l were added. The solution was mixed gently after each addition and incubated for 2-10 min. After that, 1 ml STC solution (Appendix B) was added. Then, 15 ml molten regeneration medium (Appendix B) was added to the tube, mixed by swirling and poured into 9 mm Petri plate. The plates were incubated at 37°C for 12 hours. Lastly, 15 ml freshly prepared Hygromycin Top Agar (Appendix B) were added to the plates so that the final hygromycin concentration is 266 μ g/ml. Plates were incubated for 3-4 days at 37°C.

Obtained transformants were transferred to Hygromycin Agar (Appendix B) plates and incubated at 37°C for 1-2 days. The growing colonies were then transferred to PDA (Appendix B) plates and incubated at 37°C until sporulation. Spores were suspended in a small volume of Saline/Tween Solution (Appendix B) and streaked onto Hygromycin Agar plates with a loop to obtain single spores. After growing at 37°C until formation of small colonies, single colonies were transferred to PDA and incubated at 37°C for 7 days. Glycerol stocks were prepared from these

purified colonies by adding 25% glycerol to Saline/Tween Solution containing the purified spores.

2.2.15. Detection of Monomethylsulochrin and Trypacidin from *Aspergillus fumigatus*

For detection of metabolites, *A. fumigatus* strains were grown on yeast extract sucrose agar (YES), Czapek yeast autolysate agar (CYA) and malt extract agar (MEA) plates (Appendix B) at 25°C in the dark for two weeks. The cultures were extracted by the plug extraction method (Larsen *et al*, 2007), where three plugs cut from the cultures were extracted ultrasonically first with ethyl acetate with 0.5% (v/v) formic acid (final volume: 1 ml) in the first step and re-extracted with isopropanol (final volume: 1 ml) in the second step. The combined extracts were evaporated to dryness using a vacuum concentrator (Eppendorf), re-dissolved in 500 µl methanol.

The extracts were then examined in liquid chromatography mass spectrometry (LC-MS) in TÜBİTAK ATAL laboratory. Analyses were done on an Agilent 1100 series LC MSD instrument. Samples were separated on a Zorbax Elipse XDB C18 column (100 mm x 4.6 mm with 3 µm particles). A gradient of 2 mM ammonium acetate in 0.1% formic acid and acetonitrile was used as the mobile phase with 0.4 ml/min flow rate going from 15% acetonitrile to 100% acetonitrile in 50 min and maintained for 5 min before returning to the starting conditions in 5 min. The source was operated in positive electrospray mode: drying gas flow 10 l/min, nebulizer pressure 40 psig, drying gas temperature 350°C, capillary voltage 3 kV and fragmentor 60 eV. Mass spectra were collected in a scan range of 100-1000 m/z.

CHAPTER 3

RESULTS and DISCUSSION

3.1. Experimental Strategy

For characterization and functional analysis of a novel polyketide gene cluster of *A. fumigatus*, the strategy shown in Figure 3.1 was followed.

First, *A. fumigatus* genome was analyzed for laccases, which resulted in several laccase and multicopper oxidase gene sequences. A multicopper oxidase gene, Afu4g14490, was selected for further characterization. When the genome region of Afu4g14490 was investigated, the presence of a polyketide biosynthesis gene cluster was realized. For functional analysis of this gene cluster, the polyketide synthase and multicopper oxidase genes were selected for targeted deletions.

For targeted deletions, split-marker methodology was applied, which requires two rounds of PCR. The resulting PCR fragments were used to transform *A. fumigatus*. The resulting transformant strains were analyzed by PCR and Southern Blotting, which confirmed the presence of one multicopper oxidase and three polyketide synthase knock-out strains.

LC-MS analysis of the knock-out strains confirmed the hypothesis that the polyketide synthase and multicopper oxidase genes are involved in tryptacidin and monomethylsulochrin biosynthesis. Knock-out strains were also analyzed by phenotypic assays; however, neither deletion a lead to a different phenotype.

Further, Afu4g14490 was cloned onto pAN52-1 and pAN52-4 vectors for heterologous expression in *Aspergillus sojiae*. However, although integration into the genome was confirmed by Southern Blot analysis and transcription was detected by RT-PCR; activity assays using dihydrogeodin and sulochrin as the substrates failed to show an oxidation product.

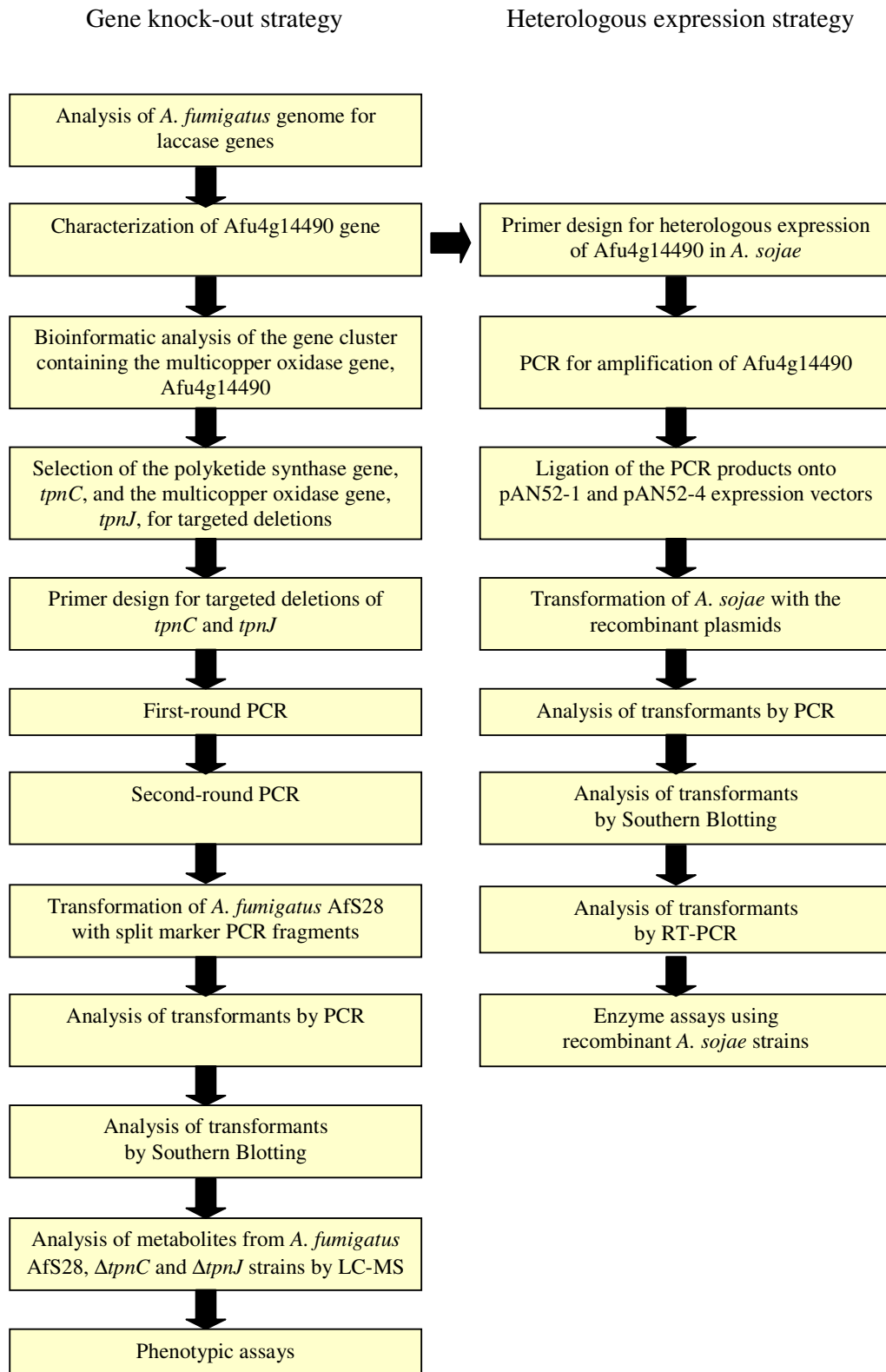


Figure 3.1. Experimental strategy flow chart

3.2. Analysis of *A. fumigatus* Genome for Laccase Genes

The fact that fungal laccases have important biological roles such as pigment biosynthesis, detoxification and lignin degradation and have industrial application areas in food and textile industry, the newly sequenced *Aspergillus fumigatus* genome was analysed for putative laccases. Previously cloned *Aspergillus fumigatus* multi-copper oxidase gene (*abr1*), laccase gene, *abr2* (Tsai *et al.*, 1999), *Aspergillus nidulans* laccase genes, *yA* (O'Hara and Timberlake, 1989) and *tilA* (Scherer and Fischer, 2001), and laccase signature sequence (Suresh Kumar *et al.*, 2003) were used to analyze *A. fumigatus* genome in the TIGR *Aspergillus fumigatus* genome database for homologous regions using “protein query vs. translated sequence database” (tblastn). This analysis resulted in some *A. fumigatus* sequences, which were then analyzed using “translated query vs. protein database BLAST” (blastx) among fungi. At the end of this search, sequences that showed homology to multi-copper oxidase and laccase genes were found in four contigs:

- Contig 72 \Rightarrow *abr1* and *abr2*
- Contig 53 \Rightarrow a putative multicopper oxidase gene
- Contig 58 \Rightarrow a putative multicopper oxidase / laccase (named as Afu4g14490 after annotation of *A. fumigatus* genome) and a putative laccase gene
- Contig 70 \Rightarrow a putative laccase gene

In this study, one of these genes (Afu4g14490) was selected for further characterization.

3.2.1. Characterization of Afu4g14490 Gene

When the translated Afu4g14490 sequence was compared to the fungal protein database using BLAST the sequence showing the highest homology was found to be dihydrogeodin oxidase from *Aspergillus terreus*.

Comparison of dihydrogeodin oxidase (DHGO) gene and Afu4g14490 both at the amino acid and DNA level using ClustalW multiple sequence alignment program resulted in the following probable outcomes:

- Afu4g14490 protein consists of 606 amino acids showing 62% identity to dihydrogeodin oxidase of *A. terreus* and 38% identity to the laccase 2 of *Botryotinia fuckeliana*.
- Afu4g14490 gene was predicted to have 7 exons separated by 6 short introns which are located at the same positions as the introns of DHGO gene.
- Afu4g14490 protein has a signal peptide of 21 amino acids long making the mature protein 585 amino acid

Figure 3.2 shows the alignment of the predicted amino acid sequence of Afu4g14490 and dihydrogeodin oxidase. Predicted Afu4g14490 sequence both at the DNA and amino acid level is shown in Figure 3.3.

When the laccase signature sequence developed by Suresh Kumar *et al.* (2003) was compared to the corresponding residues in the predicted gene product of Afu4g14490 and DHGO, few amino acids were shown to be different (Figure 3.4). Huang *et al.* (1996) showed that DHGO did not oxidize common laccase substrates, but very specific for benzophenone substrates. The laccase signature sequences developed by Suresh Kumar *et al.* (2003) are based on copper binding regions. Therefore, it may not differentiate laccases from all other multicopper oxidases.

M	I	T	V	I	K	W	L	V	S	G	C	C	A	L	A	A	V	T	T	20	
ATG	ATC	ACT	GTC	ATC	AAG	TGG	CTC	GTC	TCT	GGC	TGC	TGT	GCT	CTC	GCA	GCC	GTG	ACA	ACC	60	
R	A	P	L	P	K	D	C	R	N	T	P	N	S	R	G	C	W	K	D	40	
AGA	GCC	CCT	TTG	CCA	AAA	GAT	TGC	CGG	AAT	ACT	CCA	AAC	AGT	CGA	GGC	TGC	TGG	AAA	GAC	120	
G	F	D	I	L	T	D	Y	T	D	P	K	R	A	P	P	G	K	L	V	60	
GGG	TTT	GAT	ATT	CTG	ACA	GAC	TAC	ACC	GAT	CCC	AAA	CGC	GCC	CGG	CCT	GGA	AAG	CTG	GTC	180	
E																	V	Q	S	64	
GAG	gtcagtggtcttccggtgttgctcgtcctcctggttgaatggatcagataccaacgtgataata	GTA	CAA	TCT																254	
Y	R	Q	S	T	S	H	R	S	R	W	I	R	E	T	R	N	G	G	Q	84	
TAC	CGT	CAG	TCA	ACA	AGT	CAT	CGC	TCC	CGA	TGG	ATA	CGA	GAA	ACT	AGG	AAT	GGT	GGC	CAA	314	
																					91
TG	gttcgtagtggtcgcatacgtgggaggacgtgggaataatgagactctaca	G	GGC	AGT	TTC	CCG	GTC	CTA												385	
R	S	K	Q	I	G	G	T	Q	S											101	
CGA	TCG	AAG	CAG	ATT	GGG	GGG	ACA	CAA	TCC	gtacgactctacttgcatcacatgtaactactgacag										454	
G	I	S	V	Y	N	N	F	T	D	N	N	N	G	S	A	I	H	W	120		
gtaca	GGC	ATT	AGC	GTA	TAC	AAC	AAT	TTC	ACC	GAC	AAC	AAC	AAC	GGT	AGC	GCT	ATC	CAC	TGG	516	
H	G	L	R	Q	F	E	N	N	V	Q	D	G	V	P	G	V	T	Q	C	140	
CAT	GGG	CTT	CGT	CAG	TTC	GAG	AAC	AAT	GTC	CAG	GAC	GGA	GTC	CCC	GGA	GTC	ACA	CAG	TGT	576	
P	S	K																		147	
CCG	AGC	AAG	gtaacaattagcccagcgggagatcgagagaagcgcactgacctgtcattata	GCC	TGG	AGA	AAC													648	
A	G	I	R	V	S	G	D	A	I	W	N	V	L	V	S	F	A	F	Q	167	
GCA	GGT	ATA	CGA	GTT	TCG	GGC	GAC	GCA	ATA	TGG	AAC	GTC	CTG	GTA	TCA	TTC	GCA	TTT	CAG	708	
L	A																			175	
CTT	GCA	GT	gtgagtgctcctctgttcagttcaaagtatggctagtaatggatctca	G	ACA	GCA	ATG	GAC	TCT											779	
L																				183	
TTG	gtacgtaatcatcctacgacaatgtggctatactgaagacgtcgcca	GGA	CCG	ATC	GTC	ATT	CAT	GGC												850	
P	S	S	M	D	W	D	E	D	L	G	P	W	L	L	H	D	W	Y	H	203	
CCG	TCA	AGC	ATG	GAC	TGG	GAT	GAG	GAC	CTG	GGG	CCC	TGG	CTC	CTG	CAC	GAC	TGG	TAC	CAC	910	
D	D	V	F	S	L	L	W	V	G	E	T	K	N	R	G	A	I	P	E	223	
GAC	GAT	GTG	TTT	TCC	TTG	CTT	TGG	GTA	GGC	GAG	ACG	AAA	AAT	CGA	GGA	GCT	ATT	CCC	GAG	970	
S	T	I	L	N	G	K	G	K	F	D	C	N	H	H	N	D	T	R	C	243	
TCC	ACC	ATC	CTC	AAT	GGC	AAG	GGG	AAG	TTC	GAC	TGT	AAT	CAC	CAC	AAC	GAC	ACG	CGC	TGC	1030	
T	G	T	G	G	E	Y	F	E	V	N	F	R	K	G	V	R	Y	K	F	263	
ACC	GGA	ACG	GGT	GGA	GAG	TAT	TTT	GAG	GTC	AAC	TTC	CGA	AAG	GGC	GTC	AGG	TAC	AAG	TTC	1090	
T	I	A	N	T	G	T	L	L	E	Y	M	F	W	I	D	G	H	N	L	283	
ACC	ATC	GCC	AAT	ACG	GGG	ACC	CTG	CTA	GAA	TAT	ATG	TTC	TGG	ATT	GAT	GGG	CAT	AAC	CTG	1150	
T	V	I	A	A	D	F	V	P	I	E	P	Y	V	T	D	V	V	N	V	303	
ACC	GTC	ATT	GCG	GCC	GAC	TTC	GTC	CCC	ATC	GAA	CCC	TAT	GTC	ACC	GAC	GTG	GTC	AAT	GTG	1210	
A	M	G	Q	R	Y	E	I	I	V	E	A	N	A	D	F	T	H	G	S	323	
GCG	ATG	GGC	CAG	CGG	TAT	GAA	ATC	ATC	GTC	GAG	GCA	AAC	GCC	GAC	TTC	ACG	CAC	GGT	TCT	1270	
N	F	W	I	Y	A	Q	Y	C	D	E	V	D	L	L	P	H	K	A	V	343	
AAC	TTC	TGG	ATT	TAC	GCC	CAA	TAC	TGT	GAC	GAG	GTC	GAT	CTG	CTG	CCC	CAC	AAG	GCA	GTG	1330	
G	I	V	R	Y	D	E	Q	D	R	Q	D	P	R	T	P	P	L	S	D	363	
GGA	ATT	GTG	CGC	TAC	GAC	GAA	CAG	GAC	CGT	CAG	GAC	CCC	CGG	ACG	CCA	CCT	CTC	AGC	GAC	1390	
Q	H	R	D	F	G	C	E	D	P	D	L	D	N	L	V	P	V	V	Q	383	
CAG	CAT	CGA	GAC	TTT	GGC	TGC	GAG	GAC	CCC	GAT	CTA	GAC	AAC	CTC	GTT	CCT	GTC	GTC	CAG	1450	
Q	S	V	G	R	R	V	N	R	M	E	M	K	D	Y	L	R	M	G	Q	403	
CAG	TCG	GTC	GGC	AGG	CGA	GTG	AAC	CGC	ATG	GAG	ATG	AAG	GAC	TAC	CTG	AGA	ATG	GGC	CAA	1510	
E	G	Y	P	D	P	M	N	F	D	G	D	L	H	K	W	V	L	G	D	423	
GAG	GGC	TAC	CCC	GAC	CCG	ATG	AAC	TTC	GAC	GGT	GAC	CTC	CAC	AAA	TGG	GTC	CTG	GGG	GAT	1570	

```

V P M F V D W K N P S L K K L A V D E H 443
GTC CCG ATG TTT GTG GAT TGG AAG AAT CCC AGC CTC AAG AAA TTG GCC GTA GAT GAG CAT 1630

P D F P P E T V P I L L D F D T G D W V 463
CCG GAC TTT CCA CCG GAG ACC GTT CCC ATC CTG CTG GAC TTC GAT ACA GGC GAC TGG GTT 1690

H F V I T N N Y T F E K V H F P R N L T 483
CAC TTC GTC ATT ACC AAC AAC TAT ACC TTC GAA AAG GTG CAT TTC CCG CGC AAT CTG ACC 1750

P V M H P M H L H G H D F A I L A Q G R 503
CCG GTC ATG CAT CCG ATG CAC TTG CAC GGG CAT GAC TTT GCC ATT CTC GCT CAG GGC AGA 1810

G E F D P S I V P K L D N P P R R D V V 523
GGC GAG TTT GAC CCG AGC ATA GTC CCG AAG CTG GAT AAT CCT CCC CGC CGC GAC GTG GTG 1870

N V D T G S Y V W I A F Q V N N P G A W 543
AAC GTC GAT ACT GGC AGC TAT GTC TGG ATT GCC TTC CAG GTC AAC AAC CCG GGG GCA TGG 1930

L L H C H I A F H V S S G L S L Q F I E 563
CTG CTG CAT TGC CAC ATC GCC TTC CAT GTC AGT AGT GGG CTC TCC TTG CAG TTC ATC GAG 1990

Q P K K V K P L M E A A G V L G E F H D 583
CAG CCC AAG AAG GTC AAG CCG CTC ATG GAG GCG GCC GGT GTG TTG GGG GAG TTT CAC GAT 2050

R C A K W T E Y Y D S V N I P D N H T I 603
CGA TGC GCG AAA TGG ACA GAA TAT TAC GAC AGC GTG AAC ATC CCT GAT AAC CAT ACC ATC 2110

D D S G I * 609
GAC GAC TCG GGC ATC TAG 2128

```

Figure 3.3. Predicted Afu4g14490 sequence both at the DNA and amino acid level. The highlighted region is the predicted signal peptide, non-coding sequences are introns.

```

Signature 1 H-W-H-G-X9-D-G-X5-Q-C-P-I
Afu4g14490 H-W-H-G-X9-D-G-X5-Q-C-P-S
DHGO H-W-H-G-X9-D-G-X5-Q-C-P-I

Signature 2 G-T-X-W-Y-H-S-H-X3-Q-X-C-D-G-L-X-G-X- (F/L/I/M)
Afu4g14490 G-T-X-W-Y-H-S-H-X3-Q-X-S-N-G-L-X-G-X- I
DHGO G-T-X-W-Y-H-S-H-X3-Q-X-S-N-G-L-X-G-X- L

Signature 3 H-P-X-H-L-H-G-H
Afu4g14490 H-P-X-H-L-H-G-H
DHGO H-P-X-H-L-H-G-H

Signature 4 G-(P/A)-W-X-(L/F/V)-H-C-H-I-(D/A/E)-X-H-X3-G-(L/M/F)-X3-(L/F/M)
Afu4g14490 G- A -W-X- L -H-C-H-I- A -X-H-X3-G- L -X3- F
DHGO G- A -W-X- L -H-C-H-L- C -X-H-X3-G- M -X3- Y

```

Figure 3.4. Comparison the laccase signature sequences developed by Suresh Kumar *et al.* (2003) to the corresponding residues in DHGO and the predicted amino acid sequence of Afu4g14490.

3.2.2. Bioinformatic Analysis of the Gene Cluster Containing Afu4g14490

When the genome region of Afu4g14490 was investigated by blastx (translated query vs. protein database BLAST), the presence of a gene cluster was realized (Figure 3.5). This uncharacterized gene cluster contains 13 genes including a polyketide synthase gene, two genes that show homology to aflatoxin regulatory genes, *AflR* and *AflJ*, a lactamase-like gene, a glutathione-S-transferase gene, methyl transferases and oxidoreductases and two hypothetical genes (Figure 3.5).

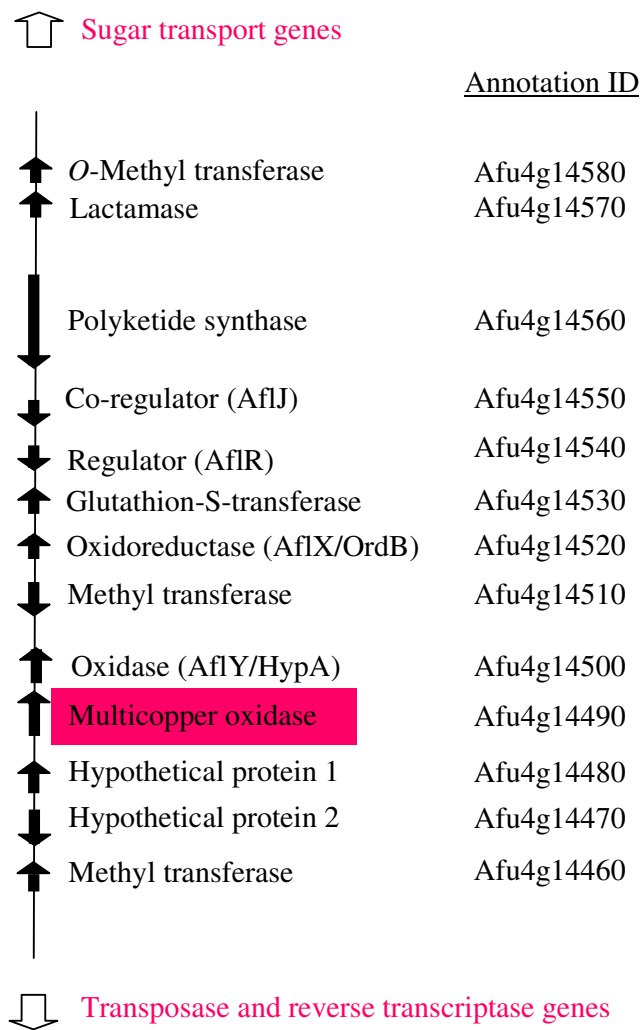


Figure 3.5. The 21.8 kb-gene cluster containing Afu4g14490

Table 3.1. Bioinformatic analysis of the putative proteins encoded by genes in the cluster containing Afu4g14490

PROTEIN	SIZE (AA)	DEDUCED FUNCTION	CLOSEST HOMOLOGUES			IDENTITIES/ POSITIVES (%)	PROTEIN ACCESSION #
			Organism	Locus tag	Putative product		
Afu4g14460	319	Methyl transferase	<i>Neosartorya fischeri</i> <i>Aspergillus terreus</i> <i>Neosartorya fischeri</i>	NFIA_101910 ATEG_08456 NFIA_101610	hypothetical protein predicted protein hypothetical protein	91/94 60/74 55/69	EAL89349
Afu4g14470	142	Hypothetical protein	<i>Neosartorya fischeri</i> <i>Neosartorya fischeri</i> <i>Aspergillus terreus</i>	NFIA_101890 NFIA_101630 ATEG_08457	conserved hypothetical protein conserved hypothetical protein conserved hypothetical protein	95/97 74/87 75/88	EAL89347
Afu4g14480	161	Hypothetical protein	<i>Neosartorya fischeri</i> <i>Neosartorya fischeri</i> <i>Mycosphaerella pini</i>	NFIA_101900 NFIA_101640 DUF1772	conserved hypothetical protein conserved hypothetical protein hypothetical protein	91/95 52/67 41/58	EAL89348
Afu4g14490	606	Multicopper oxidase	<i>Neosartorya fischeri</i> <i>Aspergillus terreus</i> <i>Gibberella zeae</i>	NFIA_101880 ATEG_08458 FG00142.1	multicopper oxidase dihydrogeodin oxidase hypothetical protein	92/94 62/77 43/61	EAL89346
Afu4g14500	445	Oxidase (AfiY/HypA)	<i>Neosartorya fischeri</i> <i>Aspergillus terreus</i> <i>Neosartorya fischeri</i>	NFIA_101870 ATEG_08459 NFIA_101620	conserved hypothetical protein predicted protein conserved hypothetical protein	92/94 59/74 50/68	EAL89345
Afu4g14510	282	Methyl transferase	<i>Neosartorya fischeri</i> <i>Aspergillus clavatus</i> <i>Neosartorya fischeri</i>	NFIA_101860 ACLA_070080 NFIA_086410	conserved hypothetical protein UbiE/COQ5 family methyltransferase, putative UbiE/COQ5 family methyltransferase, putative	85/86 52/71 53/71	EAL89344
Afu4g14520	263	Oxidoreductase (AfiX/ordB/stcQ)	<i>Neosartorya fischeri</i> <i>Neosartorya fischeri</i> <i>Cochliobolus lunatus</i>	NFIA_101850 NFIA_101500 AAR04487	conserved hypothetical protein conserved hypothetical protein StcQ-like protein	94/97 59/76 52/73	EAL89343
Afu4g14530	225	Glutathione-S-transferase	<i>Neosartorya fischeri</i> <i>Aspergillus terreus</i> <i>Aspergillus terreus</i>	NFIA_101840 ATEG_08454 ATEG_05524	glutathione S-transferase, putative hypothetical protein hypothetical protein	93/98 67/82 63/78	EAL89342
Afu4g14540	396	Regulator (AfiR)	<i>Neosartorya fischeri</i> <i>Aspergillus nidulans</i> <i>Aspergillus flavus</i>	NFIA_101830 AN0148.2 AFLR	C6 zinc finger domain protein hypothetical protein aflatoxin biosynthesis regulatory protein	87/91 27/43 29/40	EAL89341
Afu4g14550	437	Co-regulator (AfiJ)	<i>Neosartorya fischeri</i> <i>Aspergillus nidulans</i> <i>Aspergillus terreus</i>	NFIA_101820 AN0145.2 ATEG_08452	conserved hypothetical protein hypothetical protein predicted protein	89/93 41/55 42/58	EAL89340
Afu4g14560	1765	Polyketide synthase	<i>Neosartorya fischeri</i> <i>Aspergillus terreus</i> <i>Aspergillus nidulans</i>	NFIA_101810 ATEG_08451 AN0150.2	polyketide synthase, putative hypothetical protein hypothetical protein	93/96 66/80 66/80	EAL89339
Afu4g14570	320	Lactamase	<i>Neosartorya fischeri</i> <i>Aspergillus terreus</i> <i>Neosartorya fischeri</i>	NFIA_101800 ATEG_08450 NFIA_101650	metallo-beta-lactamase superfamily protein conserved hypothetical protein metallo-beta-lactamase superfamily protein	94/96 75/84 65/77	EAL89338
Afu4g14580	482	O-Methyl transferase	<i>Neosartorya fischeri</i> <i>Aspergillus terreus</i> <i>Aspergillus terreus</i>	NFIA_101790 ATEG_05526 ATEG_08449	O-methyltransferase, putative conserved hypothetical protein conserved hypothetical protein	95/98 74/84 72/83	EAL89337

When the predicted protein sequence of the polyketide synthase (Afu4g14560) found in the gene cluster was compared to the fungal protein database using blastp (before the completion and public release of *N. fischerii* and *A. terreus* genomes), the most similar proteins were found to be *Cochliobolus heterostrophus* ChPKS19 (identities/positives: 55/71%), *Aspergillus terreus* at5 (46/64%) and *Botryotinia fuckeliana* BfPKS14 (45/62%), whose functions are not known. The conserved domain analysis of the polyketide synthase using NCBI tools “Conserved Domain Search” and CDART (Conserved Domain Architecture) showed a minimal polyketide synthase domain structure consisting of a ketoacyl synthase (KS), an acyltransferase (AT) and an acyl carrier protein (ACP) (Figure 3.6). In the study by Kroken *et al.* (2003) where fungal polyketide synthases were classified according to KS sequence similarities and domain structures, KS-AT-ACP domain structure enters into an uncharacterized group with the nearest relatives toxins and pigments (Figure 3.7).

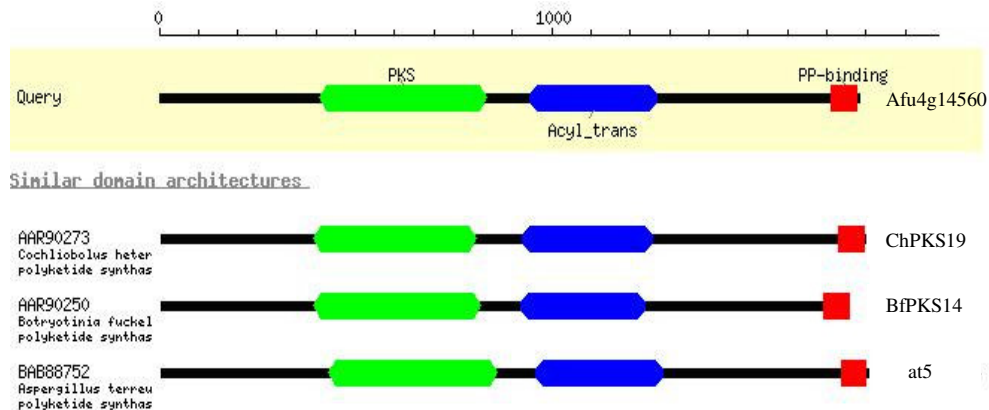


Figure 3.6. Conserved domain architecture analysis of the polyketide synthase of *A. fumigatus*, Afu4g14560. Similar domain architectures show the domains of ChPKS19, BfPKS14 and at5. Ketoacyl synthase (KS), acyltransferase (AT) and acyl carrier protein (ACP) domains were designated as pks (green bar), acyl-trans (blue bar) and PP-binding (red square) in the analysis tool.

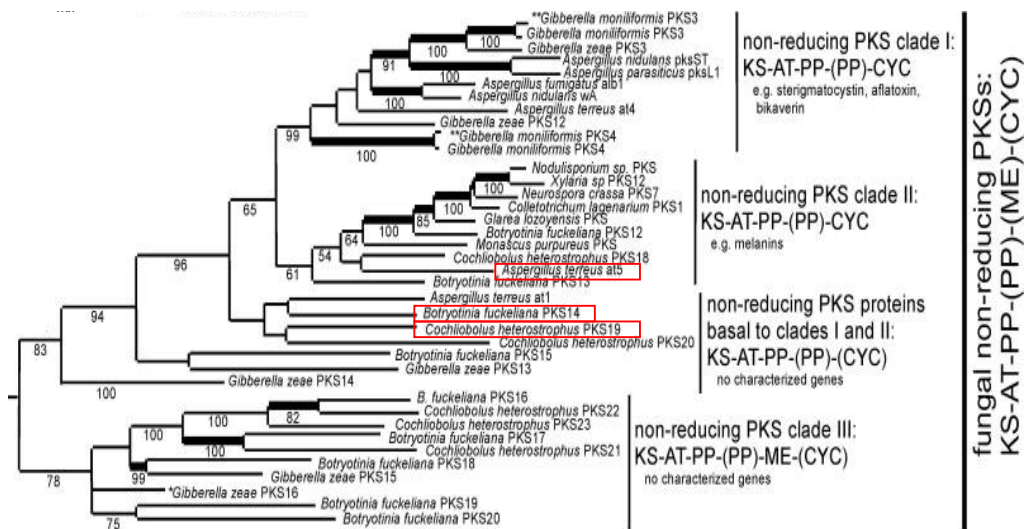


Figure 3.7. Genealogy of fungal type I PKSs (Kroken *et al.*, 2003). Acyl carrier protein (ACP) was designated as PP (phosphopantetheine attachment site). The most similar proteins to the polyketide synthase of *A. fumigatus* are shown in red boxes. *Aspergillus terreus* at5 is actually uncharacterized and its domain structure is KS-AT-ACP, but in this figure, it was shown to be in KS-AT-ACP-(ACP)-CYC domain group comprising melanin producing polyketide synthases mistakenly.

The fact that Afu4g14490 shows the highest similarity to DHGO of *A. terreus*, which is involved in the biosynthesis of the antifungal agent geodin (Figure 3.8) (Huang *et al.*, 1995), indicates a possible involvement of the gene cluster in the biosynthesis of a substance similar to geodin in terms of its chemistry. Since *A. fumigatus* is known to produce a metabolite, trypacidin, whose chemical structure is similar to geodin, it was hypothesized that the cluster may be involved in the biosynthesis of trypacidin (Figure 3.9).

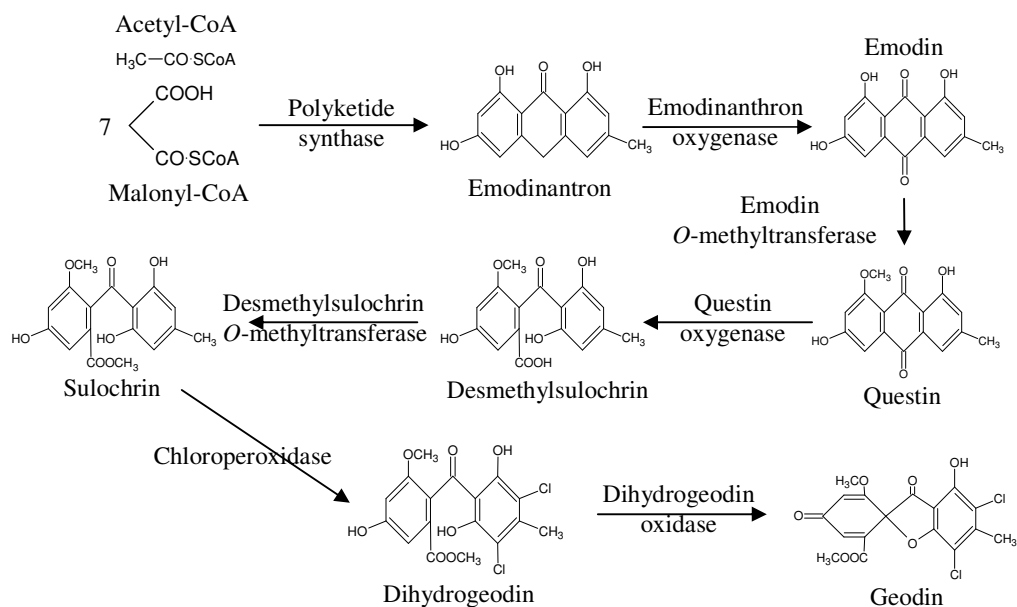


Figure 3.8. Biosynthesis of geodin (Huang *et al.*, 1995)

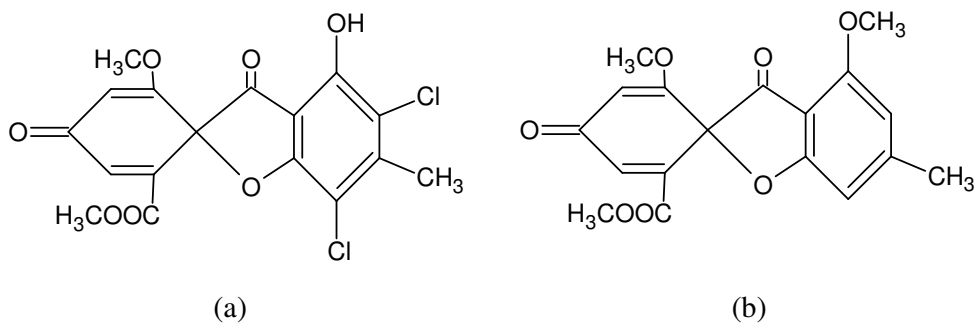


Figure 3.9. Chemical structures of geodin (a) and trypacidin (b).

In this study, by a comparative genomics approach, a putative cluster of 13 genes including dihydrogeodin oxidase was identified in *A. terreus* genome responsible for geodin biosynthesis (Figure 3.10(b)). The two clusters are very similar including the gene directions; however, the last region of the *A. fumigatus*

cluster is reversely oriented in the *A. terreus* cluster. The only difference in the two clusters is that there is an extra methyl transferase in the *A. fumigatus* cluster while *A. terreus* cluster involves a halogenase. This finding is in accordance with the existence of an extra methyl group in tryptacidin and a chlorine group in geodin. The genes in the clusters were denoted with the prefix *tpn* for tryptacidin and *geo* for geodin followed by a single letter.

After sequencing and public release of the genome sequence of *N. fischeri*, which is closely related to *A. fumigatus*, a putative tryptacidin gene cluster was also identified in *N. fischeri* genome (Figure 3.11). The physical arrangement of the putative tryptacidin gene clusters from *A. fumigatus* and *N. fischeri* are very similar in terms of orientation and order of genes. Homology among the corresponding genes are also very high (>90%, Table 3.1). This is also in accordance with the studies by Larsen *et al* (2007), where they detected tryptacidin as a secondary metabolite of *N. fischeri*.

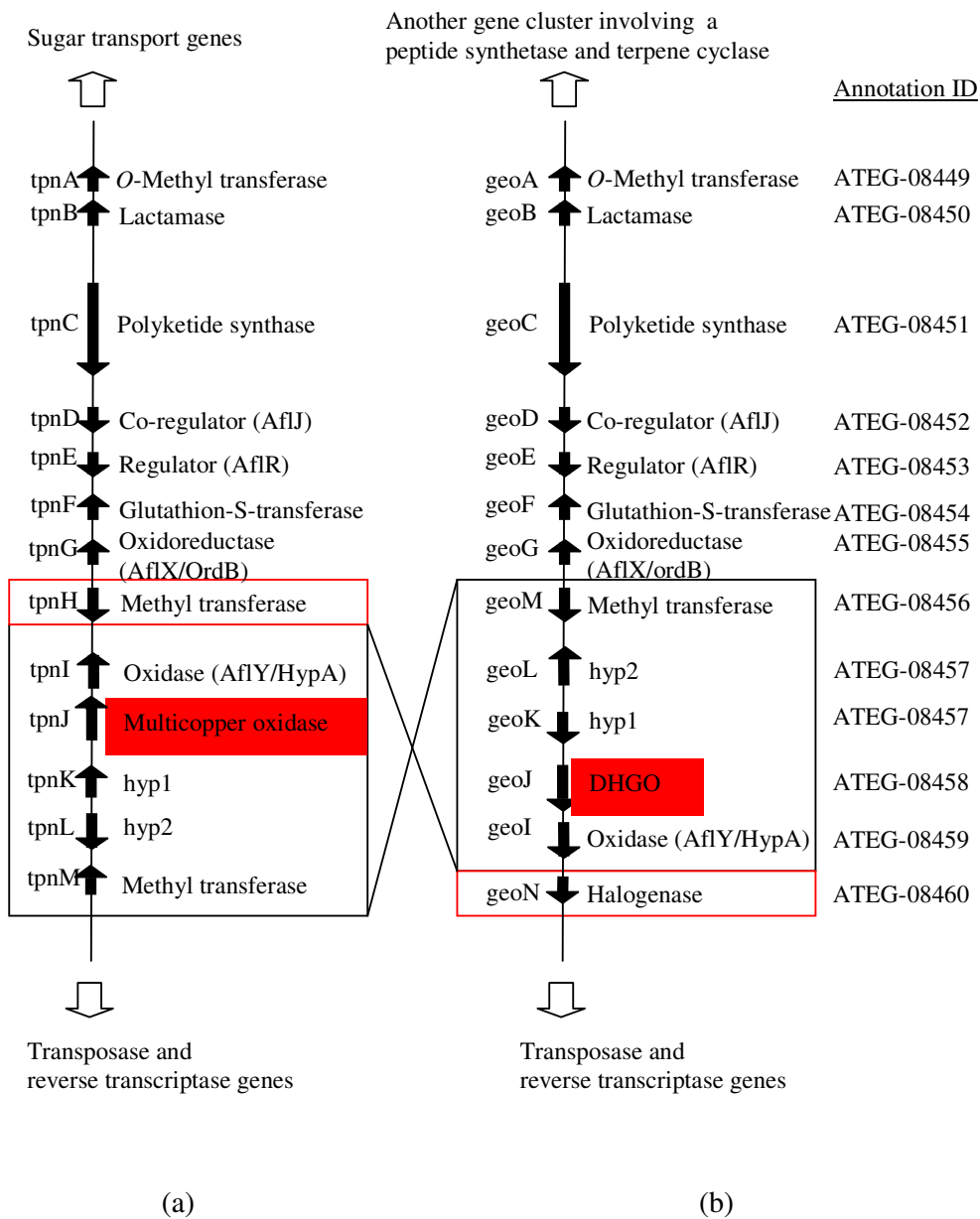


Figure 3.10. Comparison of the putative trypacidin (a) and geodin (b) gene clusters from *A. fumigatus* and *A. terreus*, respectively, identified by a comparative genomics approach in this study.

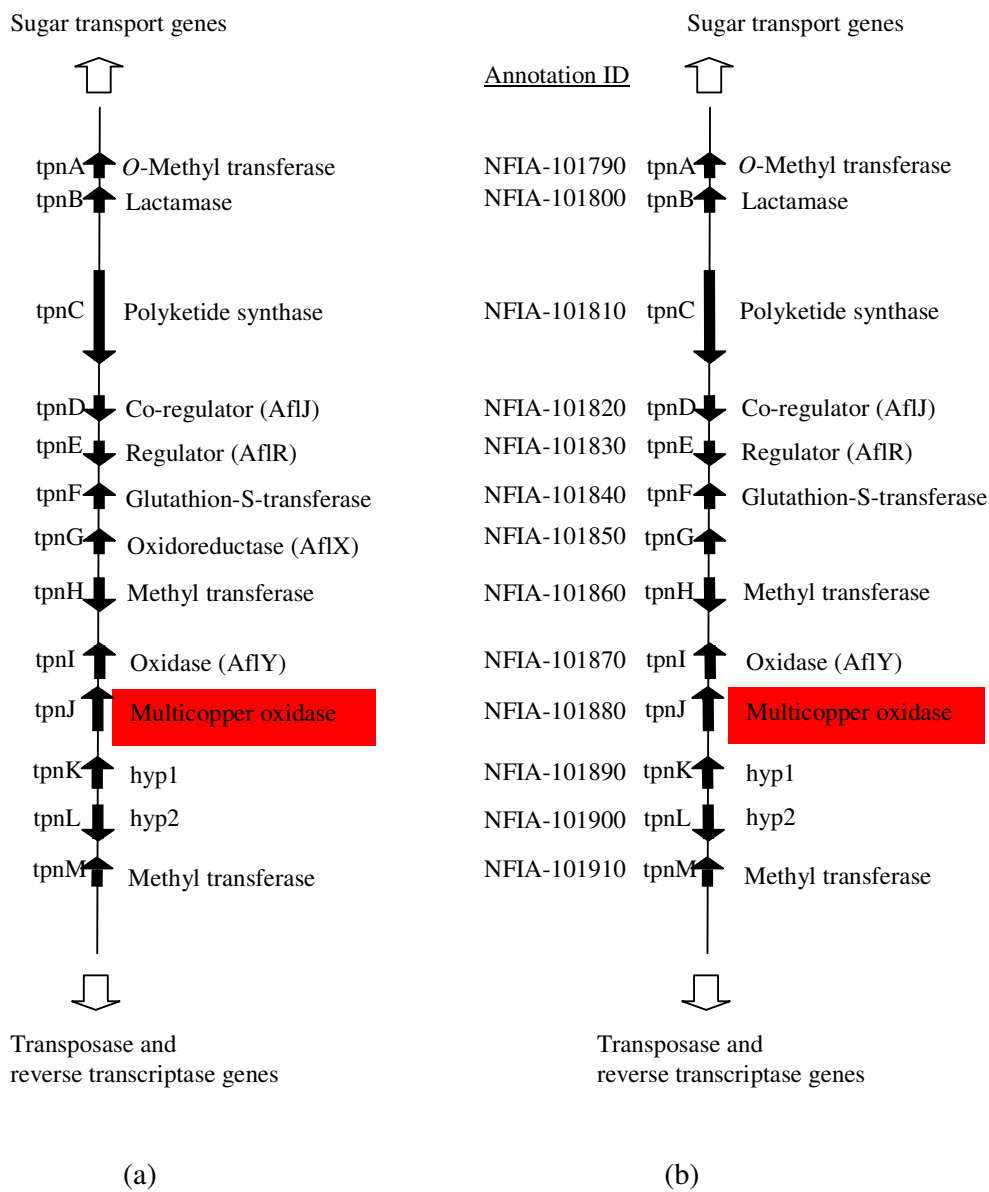


Figure 3.11. Comparison of the putative trypacidin gene clusters from *A. fumigatus* (a) and *N. fischeri* (b) identified by a comparative genomics approach in this study.

In all three gene clusters, there are genes (*tpnE* and *tpnD*, *geoE* and *geoD*) that show high similarity to *AflR* and *AflJ* aflatoxin regulatory genes, which function probably as the regulatory elements in the tryptacidin and geodin gene clusters. In addition, *tpnG* and *tpnI* (*geoG* and *geoI*) show high homology to aflatoxin biosynthesis genes *aflX* (*ordB*) and *aflY* (*hypA*), which were shown by targeted deletions to be involved in the conversion of anthraquinone versicolorin A (VA) to xanthone demethylsterigmatocystin (DMST) in the aflatoxin biosynthetic pathway (Ehrlich *et al.*, 2005; Cary *et al.*, 2006). Although this conversion step is not fully understood, Henry and Townsend (2005) proposed a reaction scheme which involves Baeyer-Villiger oxidation of a dienone intermediate formed by epoxidation of the anthraquinone ring of VA (shown in paranthesis in Figure 3.12). Ehrlich *et al.* (2005) proposed that *aflY* (*hypA*) may encode the Baeyer-Villiger oxidase necessary for formation of the xanthone ring of the aflatoxin precursor demethylsterigmatocystin. Additionally, Cary *et al.* (2006) hypothesized that AflX might be the enzyme responsible for catalysis of the epoxide ring-opening step shown in Figure 3.12 with a question mark.

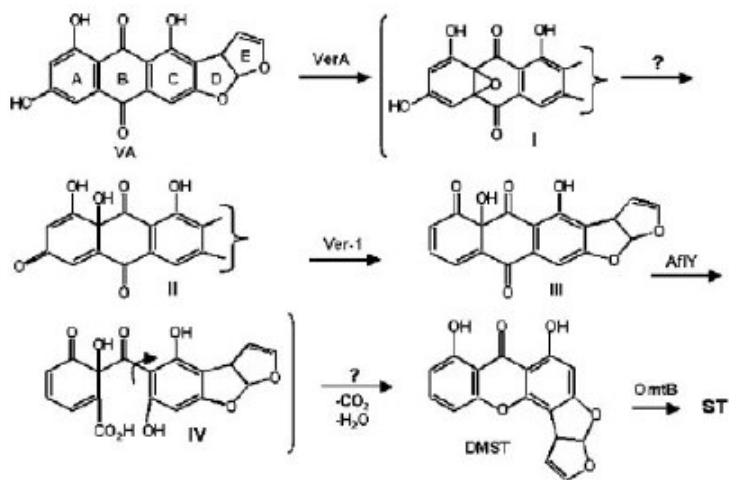


Figure 3.12. Putative enzymatic steps for conversion of VA to DMST. The suggested intermediates shown in brackets are hypothetical. Arrows shown with a question mark are steps that are expected to require enzymatic catalysis (Henry and Townsend, 2005; Ehrlich *et al.*, 2005; Cary *et al.*, 2006).

Henry and Townsend (2005) also proposed a reaction scheme for geodin biosynthesis (Figure 3.13). In this scheme, emodin is O-methylated to questin, which they proposed to be oxidized to an epoxide and, in turn, opens to a dienone. Baeyer-Villiger cleavage then takes place followed by dehydration, which rearomatizes the ring to form desmethylsulochrin.

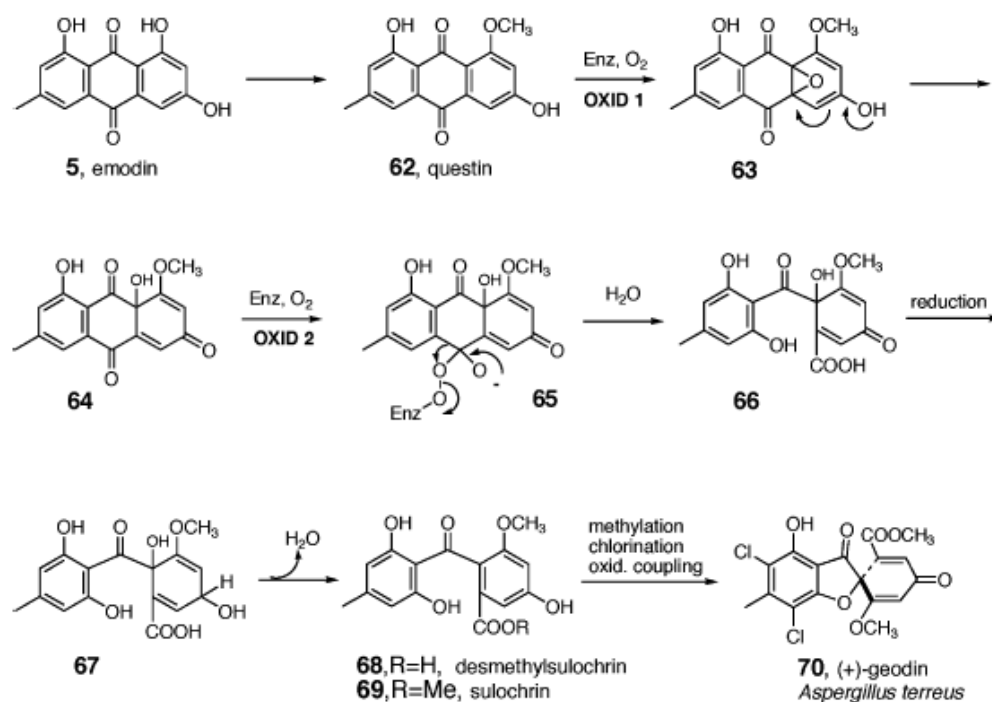


Figure 3.13. Reaction scheme for questin to desmethylsulochrin conversion proposed by Henry and Townsend (2005).

These studies show that questin to desmethylsulochrin conversion does not take place in a single oxidation step as proposed by Huang *et al.* (1995) (Figure 3.8) and requires more than one enzyme. Moreover, *aflX* (*ordB*) and *aflY* (*hypA*) homologues *,tpnG* and *tpnI*, (*geoG* and *geoI*), respectively, are involved in this conversion.

In the putative trypacidin and geodin biosynthesis gene clusters, there is a glutathione-S-transferase homologue (*tpnF*, *geoF*), which is also present in sirodesmin (Gardier *et al.*, 2004) and gliotoxin (Gardiner and Howlett, 2005) biosynthetic clusters. Since glutathione S-transferases (GST) are common detoxification enzymes (Hayes and Pulford, 1995; Hayes and Strange, 1995) and gliotoxin-glutathione conjugates form non-enzymatically (Bernardo *et al.*, 2001), trypacidin (or geodin)-glutathione conjugates could occur during the biosynthetic process and require degradation by the reverse reaction of a GST. Therefore, the *tpnF* (or *geoF*) product may be involved in auto-detoxification.

The reactions involving the conversion of dihydrogeodin to geodin in *A. terreus* and sulochrin to bisdechlorogeodin in *P. frequentans* can be seen in Figure 3.14. It can be predicted from the nature of these reactions that a similar reaction involving the conversion of monomethylsulochrin, which is also a metabolite of *A. fumigatus*, into trypacidin, takes place in *A. fumigatus* and is catalyzed by Afu4g14490 (*tpnJ*) gene product. In this respect, the novel multi-copper oxidase discovered in this study is likely to be a monomethylsulochrin oxidase. The stereochemistry of trypacidin has not been determined in previous studies; therefore, the stereospecificity of monomethylsulochrin oxidase is not known.

According to the studies involving aflatoxin and geodin biosynthesis pathways and genes found in geodin and trypacidin clusters in this study, possible gene products in the biosynthesis of geodin in *A. terreus* and proposed biosynthetic pathway of trypacidin and monomethylsulochrin in *A. fumigatus* and *N. fischeri* were determined as in Figures 3.15 and 3.16. The sequence of the reactions in trypacidin biosynthesis was based on geodin biosynthesis. The sequential reactions and intermediate products might be different in *A. fumigatus* and needs to be determined by further studies.

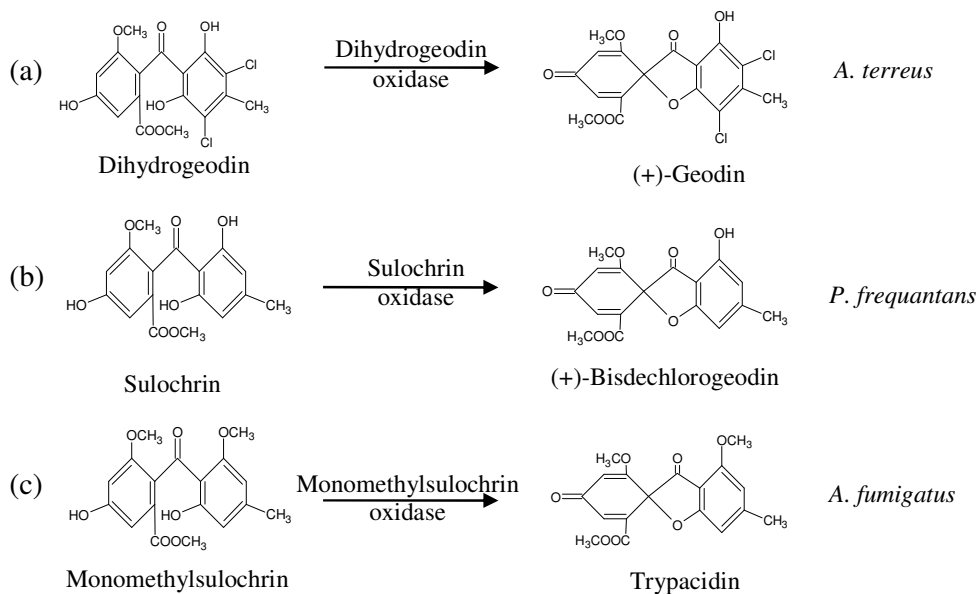


Figure 3.14. (a) Conversion dihydrogeodin to geodin in *A. terreus* (Fujii *et al.* (1987); (b) conversion of sulochrin to bisdechlorogeodin in *P. frequentans* (Huang *et al.*, 1996); (c) proposed conversion of monomethylsulochrin to trypacidin in *A. fumigatus*.

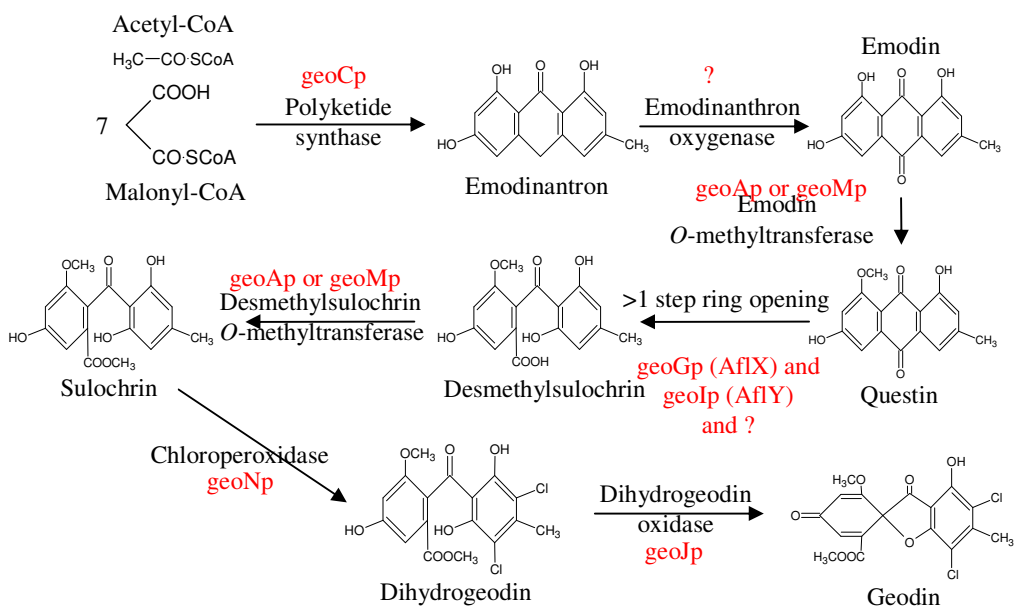


Figure 3.15. Possible gene products in the biosynthesis of geodin.

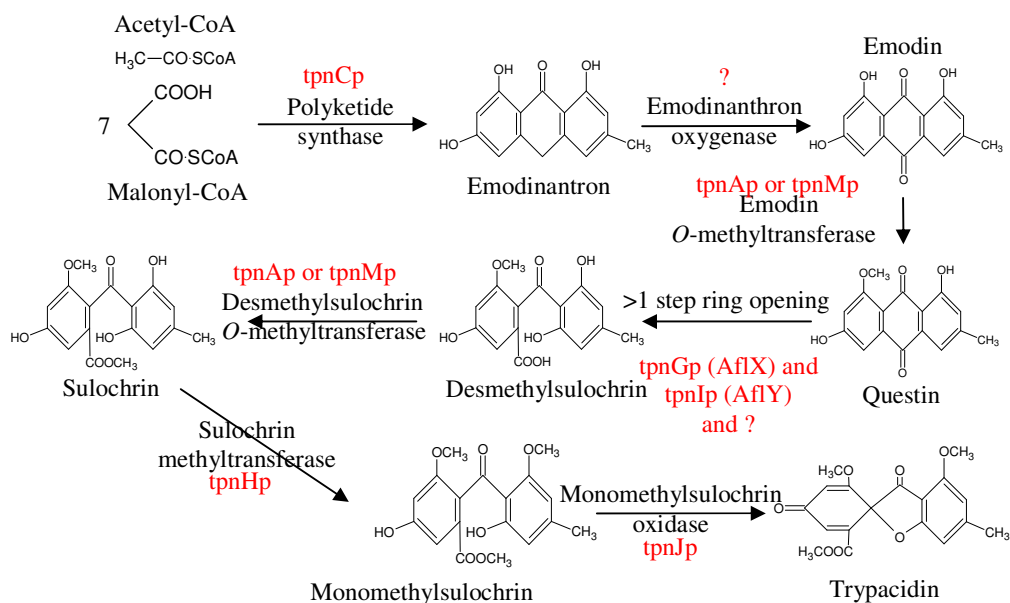


Figure 3.16. Proposed biosynthesis of trypticidin and monomethylsulochrin.

3.3. Heterologous Expression Studies of *tpnJ* in *Aspergillus sojae*

3.3.1. Primer Design

In expression studies, *Aspergillus sojae* expression vectors, pAN52-1 and pAN52-4 were used as explained in Section 2.2.8.3. Primers were designed according to vector features as shown in Table 3.2 and Figure 3.17 with P5-P6 primer pair amplifying the *tpnJ* gene with its own signal peptide sequence and P7-P8 primer pair amplifying the *tpnJ* gene without the signal peptide sequence. The latter primer pair was designed for cloning onto pAN52-4 that contains the signal sequence of *A. niger glaA* gene encoding glucoamylase, which works well in secretion, in case the signal peptide sequence of *tpnJ* is not recognized by the heterologous expression host *A. sojae*.

Table 3.2. Features of the primers designed for heterologous expression. Underlined sequences are *NcoI* and *BamHI* restriction sites.

Name	Direction	Restriction site	Sequence
P5	Forward	<i>NcoI</i>	5' -CTTGCAGTCACAC <u>CCATGGT</u> CACTGTCATC-3'
P6	Reverse	<i>NcoI</i>	5' -TTCCAGCTCACT <u>CCATGGT</u> CTAGATAGG-3'
P7	Forward	<i>BamHI</i>	5' -GTGACAACCAGAG <u>GATCCT</u> TGCCAAAAG-3'
P8	Reverse	<i>BamHI</i>	5' -TCCCTCTAGATAG <u>GATC</u> CGGACTTTCC-3'

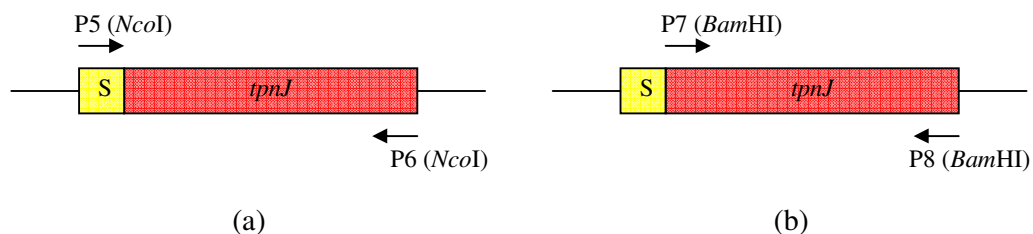


Figure 3.17. Annealing sites of the primers designed to amplify *tpnJ*. S denotes the signal peptide region. (a) Annealing sites of the primers P5 and P6 for cloning *tpnJ* in the presence of its signal peptide region, (b) annealing sites of primers P7 and P8 for cloning the mature protein coding region of *tpnJ*.

3.3.2. Amplification of *tpnJ* by Genomic PCR

Amplification of *tpnJ* with and without its signal sequence was achieved by PCR with the enzyme Pfu polymerase (Genemark) using the primer pairs P5-P6 and P7-P8 against *A. fumigatus* genomic DNA. The resulting PCR products, 2183 bp with P5-P6 and 2103 bp with P7-P8 are seen in Figure 3.18.

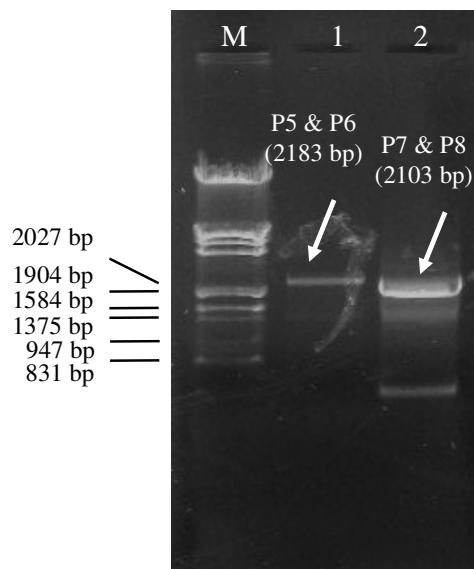


Figure 3.18. Amplification of *tpnJ* using the primer pairs P5-P6 (lane 1) and P7-P8 (lane 2). M: Lambda DNA/*EcoRI*+*HindIII* marker.

3.3.3. Ligation of the PCR Products onto pAN52-1 and pAN52-4 Expression Vectors

For ligation of PCR products, first, the expression vectors pAN52-1 and pAN52-4 were used to transform *E. coli* XL1Blue MRF⁺ as explained in Section 2.2.7 and plasmid isolation was carried out as explained in Section 2.2.2.2 to obtain the vectors in large quantities. Isolated vectors are shown in Figure 3.19.

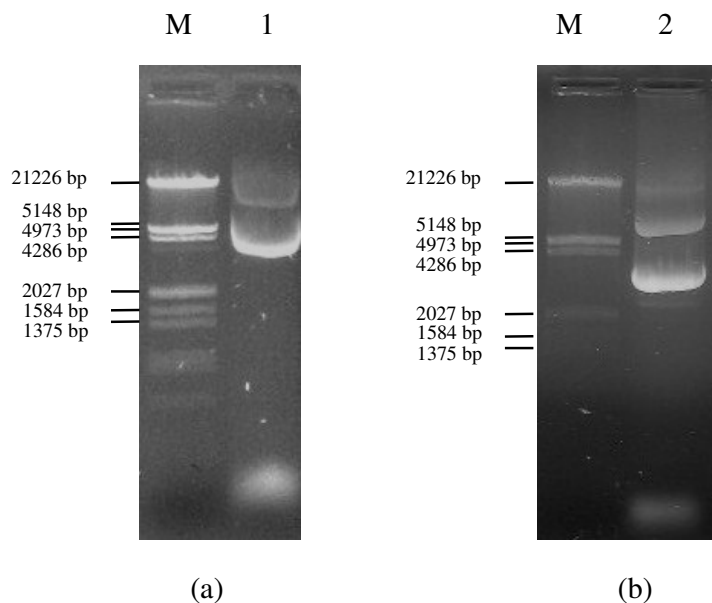


Figure 3.19. Isolation of (a) pAN52-1, lane 1, 5733 bp and (b) pAN52-4, lane 2, 5760 bp. M: Lambda DNA/*EcoRI*+*HindIII* marker.

For ligation, P5-P6 PCR product purified from agarose gel and pAN52-1 were digested with *NcoI*, as explained in Section 2.2.5 and ligation was performed (Section 2.2.6) with a vector:insert ratio of 1:3. Similarly, P7-P8 PCR product and pAN52-4 were digested with *BamHI* and used in ligation. Each ligation reaction product was used to transform *E. coli* XL1 Blue MRF^r. Plasmids from ampicillin-resistant colonies were isolated, screened for the presence of insert and correct insert orientation. At the end of this screening process, 1 recombinant plasmid (pTPNJ52-1) with pAN52-1 and the insert P5-P6 PCR fragment and 1 recombinant plasmid (pTPNJ52-4) with pAN52-4 and the insert P7-P8 PCR fragments were obtained (Figure 3.20 and 3.21, respectively). Maps of the recombinant plasmids are shown in Figure 3.22.

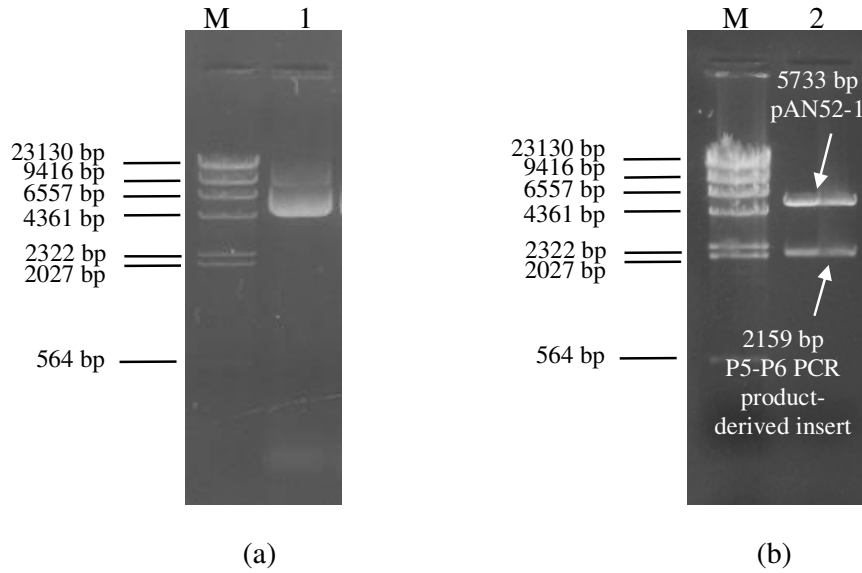


Figure 3.20. (a) Recombinant plasmid pTPNJ52-1, 7892 bp, lane 1; (b) Restriction digestion of pTPNJ52-1 with *Nco*I leading to 5733 bp vector and 2159 bp insert (lane 2). M: Lambda DNA/*Hind*III marker.

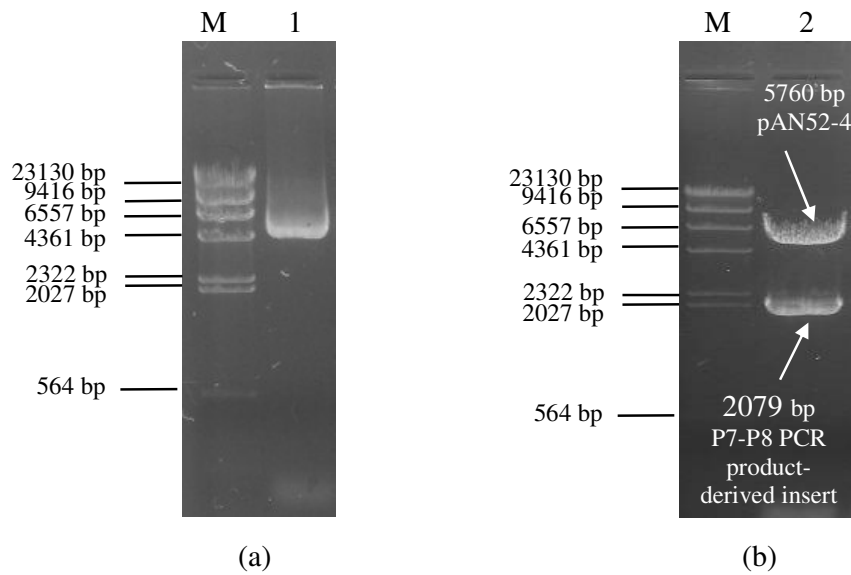


Figure 3.21. (a) Recombinant plasmid pTPNJ52-4, 7839 bp, lane 1; (b) Restriction digestion of pTPNJ52-4 with *Bam*HI leading to 5760 bp vector and 2079 bp insert (lane 2). M: Lambda DNA/*Hind*III marker.

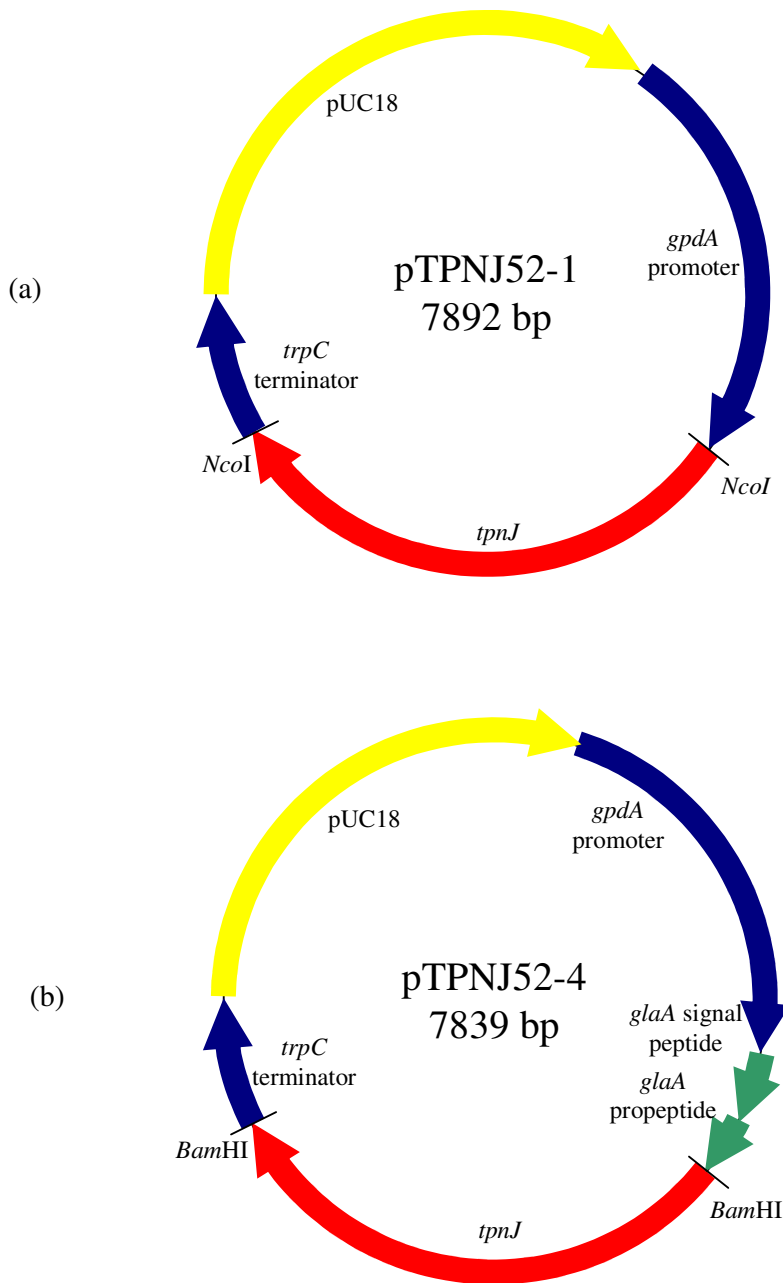


Figure 3.22. Maps of recombinant pTPNJ52-1 (a) and pTPNJ52-1 (b) plasmids.

3.3.5. Sequencing of Plasmids pTPNJ52-1 and pTPNJ52-4

Sequencing of pTPNJ52-1 and pTPNJ52-4 showed that A16P mutation occurred on pTPNJ52-1, which is within the signal peptide sequence and R364E mutation occurred on pTPNJ52-4. Amino acid sequences of both TpnJp and TpnJp with A16P mutation were analyzed by SOSUisignal program (Gomi *et al.*, 2004) and it was seen that the signal peptide cut site does not change with A16P mutation (Figure 3.23). In addition, since R364E mutation is not in the active site (copper binding regions), it was decided to use both recombinant plasmids in heterologous expression studies.

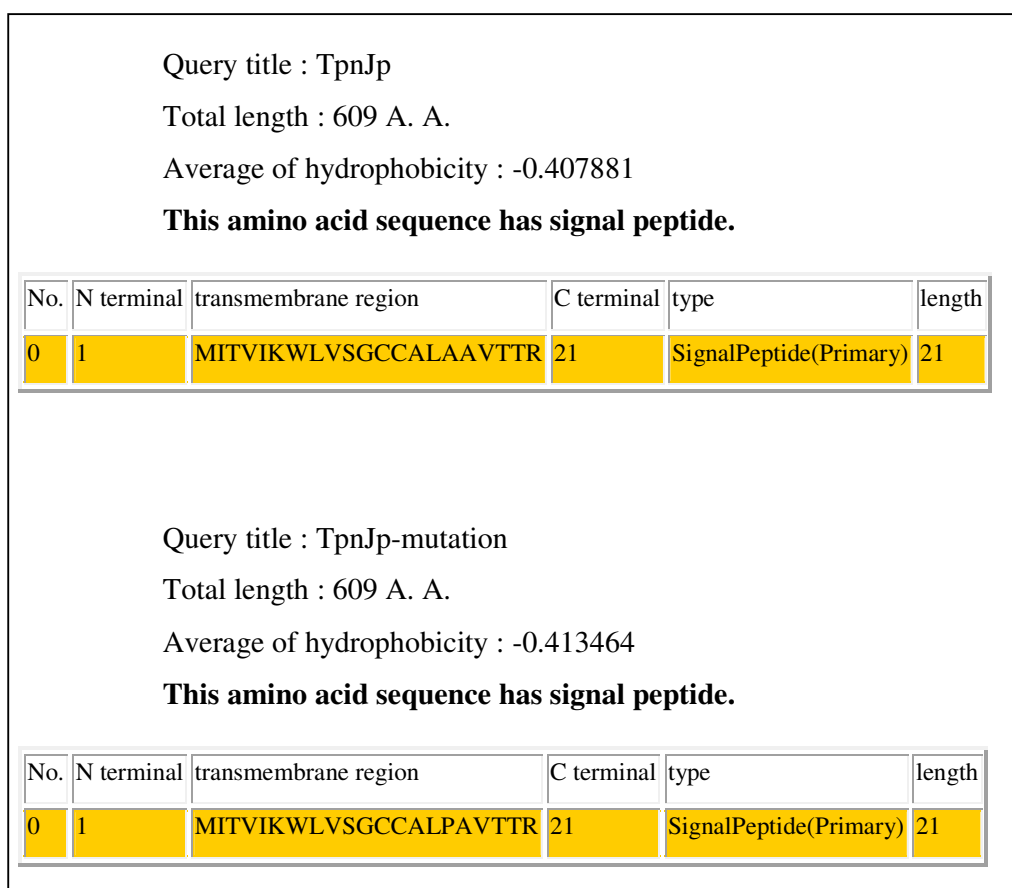


Figure 3.23. Analysis of amino acid sequences of TpnJp and TpnJp with A16P mutation by SOSUisignal program.

3.3.6. Transformation of *A. sojae* with pTPNJ52-1 and pTPNJ52-4

A. sojae ATCC11906*pyrGΔalpA* was transformed with pTPNJ52-1 and pTPNJ52-4 with the co-transformation vector pAMDSPYRG by protoplast formation and PEG/CaCl₂-mediated DNA uptake. Transformants were selected in the absence of uridine/uracil in the growth medium, which are required by the auxotrophic host strain *A. sojae* ATCC11906*pyrGΔalpA*. Transformation performed with pTPNJ52-1 resulted in 25 transformants, while transformation performed with pTPNJ52-4 resulted in 6 transformants.

3.3.7. Analysis of Transformant Strains

3.3.7.1. Analysis of Transformant Strains by PCR

3.3.7.1.1. Primer Design to Amplify *tpnJ* Gene

Two primers, TpnJinF and TpnJinR, were designed to amplify *tpnJ* gene. The features and annealing sites of the primers designed are shown in Table 3.3 and Figure 3.24, respectively.

Table 3.3. Features of the primers designed for amplification of *tpnJ*

Name	Direction	Sequence
TpnJinF	Forward	5'-TTACGCCCAATACTGTGACG-3'
TpnJinR	Reverse	5'-AGAGCCCCTACTGACATGG-3'

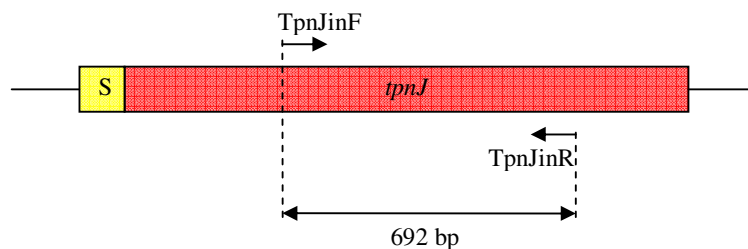


Figure 3.24. Annealing sites of the primers TpnJinF and TpnJinR.

3.3.7.1.2. PCR with TpnJinF and TpnJinR

Among each group of transformants, 5 strains were selected and DNA isolation was performed. PCR was performed with transformant DNAs together with *A. sojae* and *A. fumigatus* DNAs as a control (Figure 3.25). As can be seen from the figure, with *A. sojae* host strain DNA, no amplification occurs (lane 1). Whereas with *A. fumigatus* (lane 2), pTPNJ52-1 transformants #1-5 (lanes 3-7) and pTPNJ52-4 transformants #1, 3, 4, 5 (lanes 8, 10, 11, 12), amplification of 692 bp *tpnJ* PCR fragment was observed. PCR results showed that all of the 5 strains selected among pTPNJ52-1 transformants (#1-5) and 4 of 5 strains selected among pTPNJ52-4 transformants (#1, 3, 4, 5) contain *tpnJ* gene.

One strain from each transformant, pTPNJ52-1 transformant #3 (*A. sojae* TPNJ52-1#3) and pTPNJ52-4 transformant #1 (*A. sojae* TPNJ52-4#1) was selected for analysis of genomic integration by Southern Blot analysis.

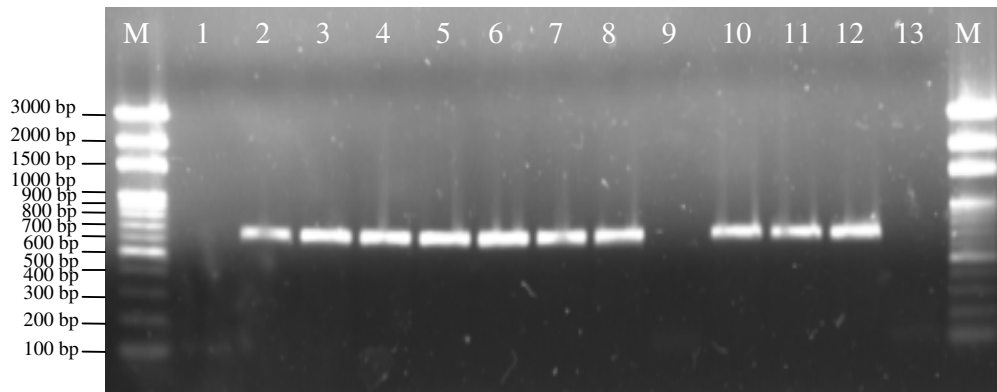


Figure 3.25. PCR with TpnJinF and TpnJinR using transformant, *A. sojae* and *A. fumigatus* DNAs. 1, *A. sojae*; 2, *A. fumigatus*; lanes 3-7, pTPNJ52-1 transformants #1-5; lanes 8-12, pTPNJ52-4 transformant #1-5; 13, no DNA control.

3.3.7.2. Analysis of Transformant Strains by Southern Blotting

A. sojae TPNJ52-1#3, *A. sojae* TPNJ52-4#1 together with *A. sojae* host strain and *A. fumigatus* DNAs were digested by *Bam*HI and analyzed by Southern Blotting using the 692 bp *tpnJ* PCR fragment as a probe (Figure 3.26). In Southern Blot, three bands in *A. fumigatus* (lane 1) and two bands in *A. sojae* host strain (lane 2) were observed. Seeing multiple bands due to insufficiently digested DNA is unlikely since the same *A. sojae* host strain bands are also observed in transformant strains. Therefore, observation of these signals might be due to annealing of *tpnJ* probe not only the *tpnJ* gene but also to other multi-copper oxidase/laccase genes in the genome unspecifically. At least two bands were observed in *A. sojae* TPNJ52-1#3 (lane 3) in addition to the bands observed also in *A. sojae* host strain, which may indicate multiple integration of *tpnJ* gene (at least on two sites) in the genome. Only one 2079 bp band was expected in *A. sojae* TPNJ52-4#1 because of digestion by *Bam*HI (*tpnJ* gene was inserted at *Bam*HI cut site in pTPNJ52-4). However, in addition to the bands observed also in *A. sojae* host strain and a band at the correct size (2079 bp), 2 different bands were observed. This result may be due to insufficient digestion of DNA, which would cause multiple signals.

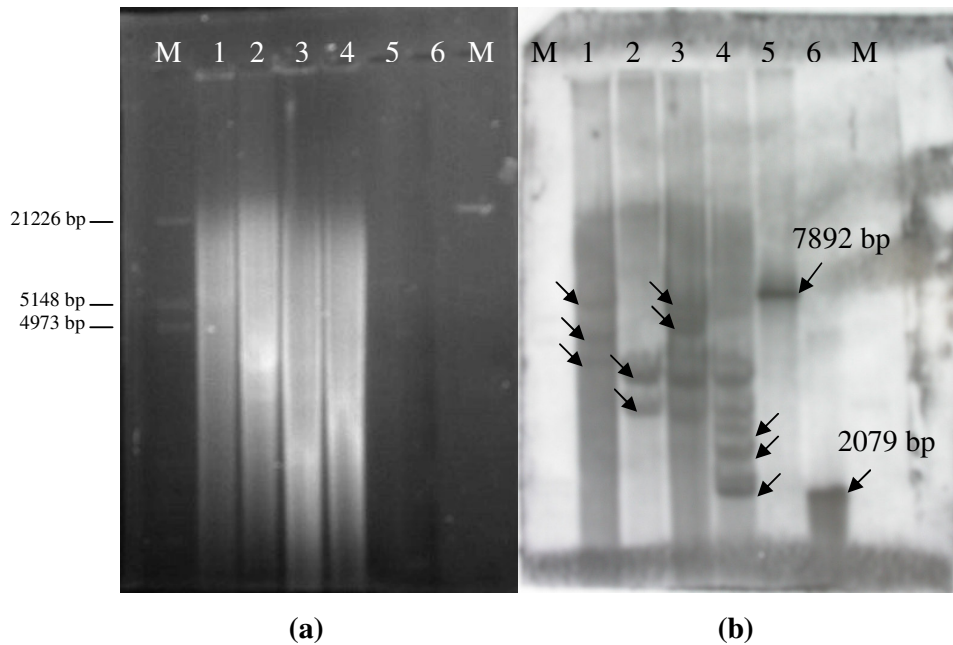


Figure 3.26. Analysis of *A. sojae* TPNJ52-1#3, *A. sojae* TPNJ52-4#1, *A. fumigatus* and *A. sojae* host strains by genomic Southern Blotting (a) Digestion of DNAs with *Bam*HI (b) Results of blotting, hybridization and chemiluminescent detection. M, Lambda DNA/*Eco*RI+*Hind*III marker; 1, *A. fumigatus*; 2, *A. sojae* host strain; 3, *A. sojae* TPNJ52-1#3; 4, *A. sojae* TPNJ52-4#1; 5, *Bam*HI digested pTPNJ52-1 (7892 bp); 6, *Bam*HI digested pTPNJ52-4 (2079 and 5760 bp).

3.3.7.3. Analysis of *tpnJ* Transcription by RT-PCR

3.3.7.3.1. Preparation of RNA Samples

Total RNA isolation was performed using the mycelia from *A. sojae* host strain, *A. sojae* TPNJ52-1#3 and *A. sojae* TPNJ52-4#1 that were grown in CuSO₄ supplemented Complete Medium (Appendix B) at 30°C for 3 days to use in RT-PCR. Additionally, *A. fumigatus* strain was grown in modified Czapek-Dox Medium (Appendix B) at 37°C for 5 days. Modified Czapek-Dox medium is CuSO₄ supplemented Czapek-Dox, which was described by Fujii *et al.* (1987) while they were purifying dihydrogeodin oxidase from *A. terreus*. While *A. fumigatus* was

grown for 5 days, *A. sojae* strains were grown for 3 days since the recombinant *A. sojae* strains carry *tpnJ* gene under the control of the constitutive *gpdA* promoter. Therefore, transcription of *tpnJ* from recombinant *A. sojae* strains is expected to start much earlier and at a higher level.

The integrity of the purified RNA was determined by agarose gel electrophoresis (Figure 3.27). The purity was estimated spectrophotometrically using A_{260}/A_{280} . The yield of RNA was also determined spectrophotometrically at 260 nm (Table 3.4). The results indicated sufficiently pure RNA for RT-PCR.

Table 3.4. Determination of RNA yield and purity by spectrophotometer

Strain	A_{260}	A_{280}	A_{260}/A_{280}	Amount ($\mu\text{g}/\mu\text{l}$)
<i>A. sojae</i> host	0.3192	0.1685	1.89	3.83
<i>A. sojae</i> TPNJ52-1#3	0.2999	0.1605	1.87	3.60
<i>A. sojae</i> TPNJ52-4#1	0.2065	0.1069	1.93	2.50
<i>A. fumigatus</i> -3 rd day	0.2045	0.1097	1.88	4.09
<i>A. fumigatus</i> -5 th day	0.1654	0.0875	1.91	3.31

3.3.7.3.2. RT-PCR

Isolated *A. sojae* RNAs were used in RT-PCR against TpnJinF and TpnJinR primers. For each different reaction, no reverse transcriptase (RT) control reaction was also included, which is a control for DNA contamination. The results showed that while expression is not observed in *A. sojae* host strain, both transformants, *A. sojae* TPNJ52-1#3 and *A. sojae* TPNJ52-4#1 transcribe *tpnJ* gene (Figure 3.28). *A. fumigatus* 3rd and 5th day RNAs were also used in RT-PCR against P5 and TpnJinR (Figure 3.29). P5 and TpnJinR primer pair amplifies 1586 bp PCR product while used against genomic DNA, but should amplify 1279 bp product against cDNA due to the lack of the introns. In Figure 3.29, although DNA contamination is seen in all

reactions, 1279 bp cDNA amplification product is also observed with the reaction performed using RNA from 5th cultivation day. The fact that this product is not observed at all with the reaction performed using RNA from 3rd cultivation day shows that *tpnJ* transcription starts in late stages of growth, which is a feature of secondary metabolite production. In addition, to obtain an RT-PCR product from *A. fumigatus* reaction, 4 times more cDNA was used compared to *A. sojae* reactions, which shows that transcription level of *tpnJ* is considerably higher in recombinant *A. sojae* strains compared to *A. fumigatus*.

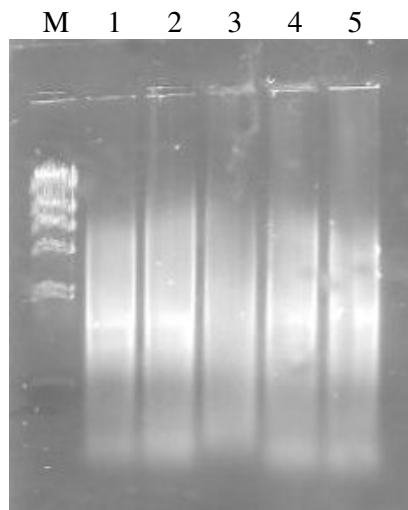


Figure 3.27. Total RNA isolation from the 3rd cultivation day of *A. sojae* strains and 3rd and 5th cultivation day of *A. fumigatus*. M, Lambda DNA/*Hind*III marker; 1, *A. sojae*; 2, *A. sojae* TPNJ52-1#3; 3, *A. sojae* TPNJ52-4#1; 4, *A. fumigatus* 3rd day; 5, *A. fumigatus* 5th day.

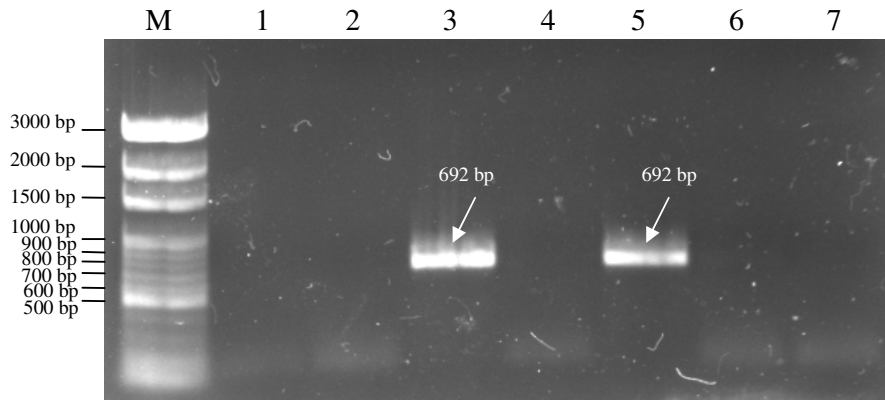


Figure 3.28. Analysis of transcription of *tpnJ* in *A. sojae* strains by RT-PCR using primers TpnJinF and TpnJinR. M, 100 bp DNA ladder; 1, *A. sojae* host strain; 2, *A. sojae* host strain no reverse transcriptase (RT) control; 3, *A. sojae* TPNJ52-1#3; 4, *A. sojae* TPNJ52-1#3 no RT control; 5, *A. sojae* TPNJ52-4#1; 6, *A. sojae* TPNJ52-4#1 no RT control; 7, no DNA control.

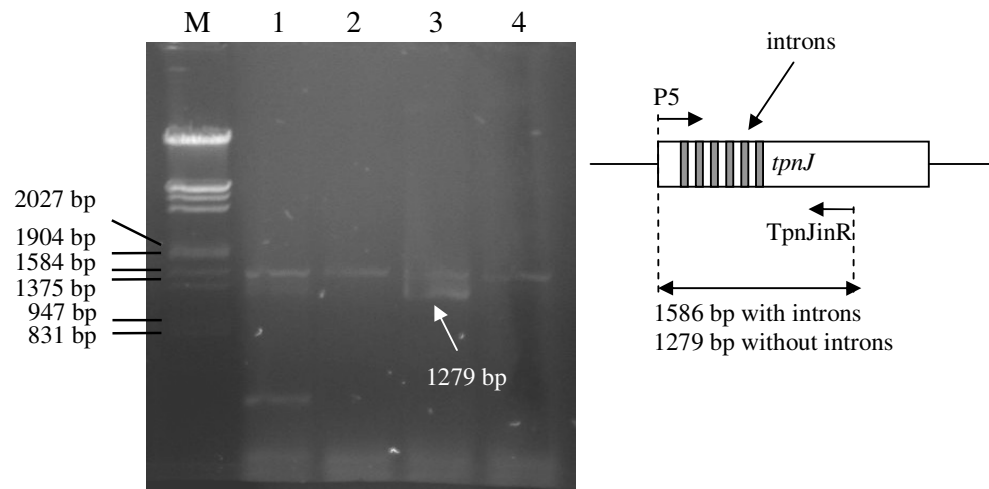


Figure 3.29. Analysis of transcription of *tpnJ* in *A. fumigatus* by RT-PCR using primers TpnJinF and TpnJinR. M, Lambda DNA/*EcoRI*+*HindIII*. 1, reaction performed using RNA from 3rd cultivation day; 2, no reverse transcriptase (RT) control with RNA from 3rd cultivation day; 3, reaction performed using RNA from 5th cultivation day; 4, no RT control with RNA from 5th cultivation day.

3.3.7.4. Enzyme Assays with *A. sojae* TPNJ52-1#3, *A. sojae* TPNJ52-4#1 and *A. fumigatus*

Activity of the multi-copper oxidase, shown to be a putative monomethylsulochrin oxidase in this study, in recombinant *A. sojae* strains was first analyzed by growing the fungus on Minimal Medium Plates with ABTS as explained in Section 2.2.9. However, neither *A. sojae* host strain nor transformants *A. sojae* TPNJ52-1#3 and *A. sojae* TPNJ52-4#1 showed activity.

Considering that similar enzymes such as sulochrin oxidase from *P. frequentans* (Huang *et al.*, 1996) and dihydrogeodin oxidase from *A. terreus* (Huang *et al.*, 1995) did not oxidize typical multicopper oxidase/laccase substrates like several *p*- and *o*-diphenols, phenylenediamines or ascorbic acid but oxidize benzophenone substrates like sulochrin, dihydrogeodin and griseophenone A, it was decided to use sulochrin (Sigma) and dihydrogeodin (kindly provided by Prof. Ebizuka, University of Tokyo) in enzyme assays. Although monomethylsulochrin is predicted to be the actual substrate of *A. fumigatus* TpnJp, since it is neither commercially available nor readily available from other laboratories, it could not be used in enzyme assays.

Enzyme assays were performed with sulochrin and dihydrogeodin as the substrate, and supernatant or cell extracts from 3 day-old *A. sojae* cultures or 5 day-old *A. fumigatus* cultures grown in media supplemented with CuSO₄ using the reaction conditions explained in Section 2.2.11.

Figure 3.30 shows the result of enzyme assays performed with sulochrin dissolved in ethanol (Figure 3.30a) and DMSO (Figure 3.30b) as the substrate and 3 day-old *A. sojae* and 5 day-old *A. fumigatus* supernatants. Reaction mixture was incubated for 24 hours and extracted with ethyl acetate before analysis by TLC. An oxidation product was not observed either in *A. sojae* or *A. fumigatus*.

To see if sulochrin is oxidized by a commercial laccase, assays were performed with *Trametes versicolor* laccase. TLC result showed that sulochrin is converted into an oxidation product both in ethanol and in DMSO by *T. versicolor* laccase (Figure 3.31).

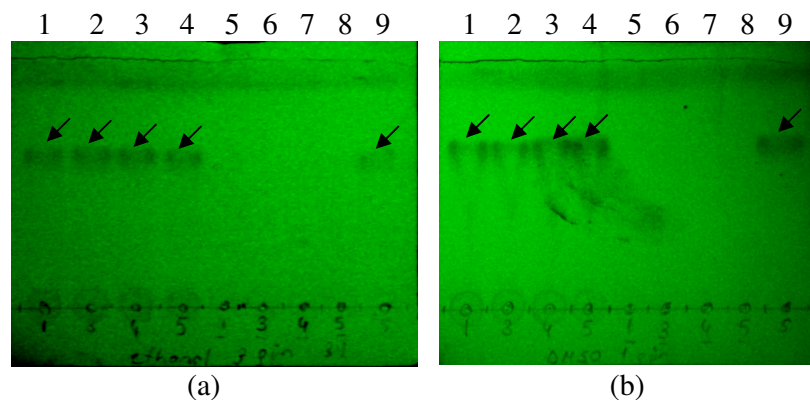


Figure 3.30. Thin layer chromatography (TLC) of sulochrin reactions. (a) Reactions performed with sulochrin in ethanol (b) in DMSO. 1, *A. fumigatus* 5th day supernatant + sulochrin; 2, *A. sojae* host strain + sulochrin; 3, *A. sojae* TPNJ52-1#3 + sulochrin; 4, *A. sojae* TPNJ52-4#1 + sulochrin; 5, *A. fumigatus* 5th day supernatant + ethanol/DMSO; 6, *A. sojae* host strain + ethanol/DMSO; 7, *A. sojae* TPNJ52-1#3 + ethanol/DMSO; 8, *A. sojae* TPNJ52-4#1 + ethanol/DMSO; 9, buffer + sulochrin. Elution buffer: ethyl acetate-hexane (3:1).

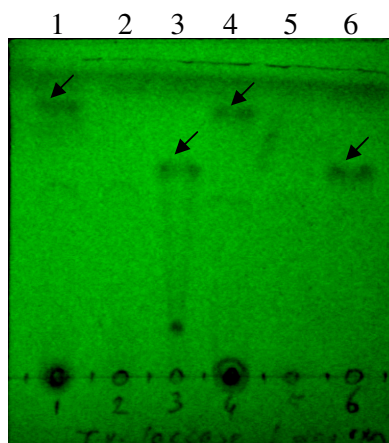


Figure 3.31. TLC of control reaction with commercial laccase (from *Trametes versicolor*) and sulochrin. 1, commercial laccase + sulochrin in ethanol; 2, commercial laccase + ethanol; 3, buffer + sulochrin in ethanol; 4, commercial laccase + sulochrin in DMSO; 5, commercial laccase + DMSO; 6, buffer + sulochrin in DMSO. Elution buffer: ethyl acetate-hexane (3:1).

Since a reaction product was not observed with sulochrin using culture supernatants, reaction was repeated with cell extracts considering the possibility that recombinant TpnJp cannot be secreted into the supernatant but stays in the cells in the heterologous expression host *A. sojae*. However, cell extracts did not lead to an oxidation product, either (Figure 3.32).

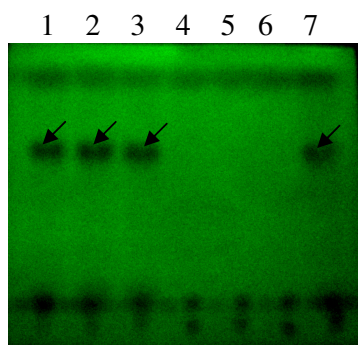


Figure 3.32. TLC of reactions performed with cell extracts and sulochrin. 1, *A. sojae* host strain + sulochrin; 2, *A. sojae* TPNJ52-1#3 + sulochrin; 3, *A. sojae* TPNJ52-4#1 + sulochrin; 4, *A. sojae* host strain + ethanol; 5, *A. sojae* TPNJ52-1#3 + ethanol; 6, *A. sojae* TPNJ52-4#1 + ethanol; 7, buffer + sulochrin. Elution buffer: ethyl acetate-hexane (3:1).

Enzyme assays were also performed with dihydrogeodin using both supernatants (Figure 3.33a) and cell extracts (Figure 3.33b). Neither case lead to an oxidation product.

The fact that an oxidation product was not seen either with sulochrin or dihydrogeodin might be due to the specificity of TpnJp only on its actual substrate monomethylsulochrin. However, since monomethylsulochrin is not commercially available and could not be obtained from other laboratories, it could not be used in enzyme assays. However, considering the fact that sulochrin oxidase and dihydrogeodin oxidase enzymes oxidize a narrow range of benzophenone substrates

such as sulochrin and dihydrogeodin, the problem with monomethylsulochrin oxidase (TpnJp) might also be at the level of protein synthesis. Therefore, transcription of *tpnJ* was analyzed and shown to occur in recombinant strains (Figure 3.28). To see if TpnJp is expressed at the protein level, SDS-PAGE was performed both with cell extracts and supernatants (Figure 3.34). However, in neither cell extracts nor supernatants an additional protein band was observed in recombinant TPNJ52-1#3 and TPNJ52-4#1 strains. Although this may be due to the presence of other protein bands that may hinder the appearance of TpnJp protein band, it may also be an indication of degradation of the foreign protein by proteases. An antibody against TpnJp would prove the presence or absence of TpnJp protein band by Western Blotting, however, this requires purification of the protein and raising an antibody against it. Another possibility of not seeing activity is the difference between post-translational modifications such as glycosylation of the native and heterologously expressed protein (if expressed). Also, the single mutations that have occurred during amplification of *tpnJ* (see Section 3.3.5) might have lead to the activity loss in recombinant proteins.

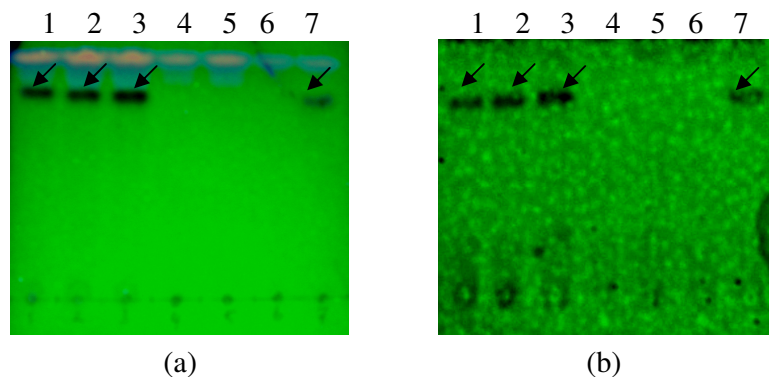


Figure 3.33. TLC of reactions performed with dihydrogeodin (DHG) using (a) supernatants (b) cell extracts. 1, *A. sojae* host strain + DHG; 2, *A. sojae* TPNJ52-1#3 + DHG; 3, *A. sojae* TPNJ52-4#1 + DHG; 4, *A. sojae* host strain + ethanol; 5, *A. sojae* TPNJ52-1#3 + ethanol; 6, *A. sojae* TPNJ52-4#1 + ethanol; 7, buffer + DHG. Elution buffer: ethyl acetate-hexane (3:1).

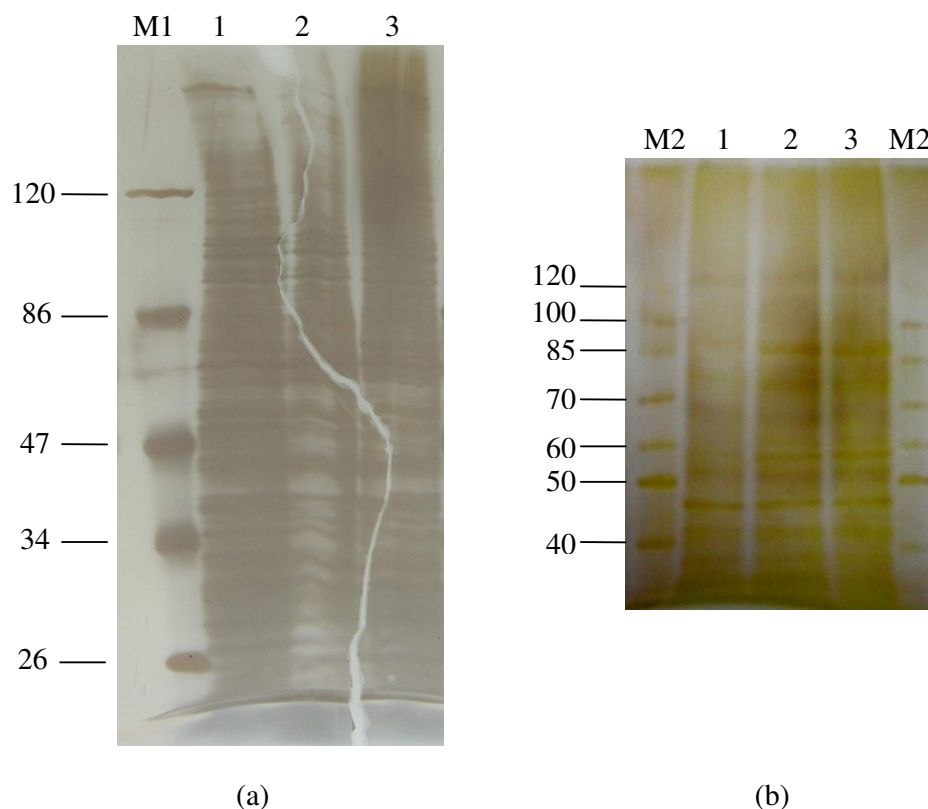


Figure 3.34. SDS-PAGE of proteins from pAMDSPYRG transformed *A. sojae* host strain, *A. sojae* TPNJ52-1#3 and *A. sojae* TPNJ52-4#1. (a) from cell extracts, (b) from supernatants. M, Molecular weight marker; 1, pAMDSPYRG transformed *A. sojae* host strain, 2, *A. sojae* TPNJ52-1#3; 3, *A. sojae* TPNJ52-4#1.

3.4. Characterization of the Putative Trypacidin Gene Cluster

3.4.1. Targeted Deletions of *tpnC* (Afu4g14550, Polyketide Synthase) and *tpnJ* (Afu4g14490, Multicopper Oxidase-Monomethylsulochrin Oxidase)

To prove the function of the gene cluster, the gene probably coding the key enzyme in the pathway, polyketide synthase, that is, *tpnC*, was selected for targeted deletion. Deletion of *tpnC* should prevent the production of the metabolites trypacidin and monomethylsulochrin according to our hypothesis. Furthermore, to

prove the function of the *tpnJ* gene product multicopper oxidase as a monomethylsulochrin oxidase, *tpnJ* gene was also decided to be deleted. This deletion should prevent the production of tryptacidin and lead to the accumulation of monomethylsulochrin if the pathway is blocked at monomethylsulochrin oxidation step.

For targeted deletions, split marker methodology explained in Section 2.2.13 was used (Catlett *et al.*, 2002). In this method, two constructs are required per transformation, each containing a flank of the target gene and roughly two thirds of a selectable marker cassette. Homologous recombination between the overlapping regions of the selectable marker gene and between the flank regions and their genome counterparts results in a targeted gene deletion and replacement with a marker gene.

3.4.1.1. The *A. fumigatus* Strain for Targeted Gene Deletion

In gene knock-out experiments, homologous recombination ratio decreases due to nonhomologous end-joining pathway in fungi. Integration events mediated by nonhomologous end joining do not rely on homologous sites and therefore attenuate homologous recombination, which results in decreased frequencies of the desired gene knock-out in a given transformation experiment with a suitable gene replacement cassette (Krappman *et al.*, 2006). To solve this problem, Krappman *et al.* (2006) developed an *Aspergillus fumigatus* strain, originated from the clinical isolate D141, that lacks the *akuA* locus (for *Aspergillus* Ku), which codes for a gene that is orthologous to the Ku70 subunit of the gene of *N. crassa*, previously shown to have an important role in nonhomologous end-joining pathway. In comparison to its wild-type progenitor, the *A. fumigatus* Δ *akuA* deletion strain (*A. fumigatus* AfS28) did not display any deviation with respect to vegetative growth, sporulation capacities, nutritional requirements, pigmentation, and sensitivity towards phleomycin. Also, conidia of the deletion strain did not display any virulence reduction in insect model compared to the wild-type isolate D141 (Krappman *et al.*, 2006). Relative frequencies of homologous recombination in wild-type and *akuA* genetic backgrounds of *A. fumigatus* was estimated from targeted replacement of the

abr2 locus, the result of which showed that 22% homologous recombination ratio is observed in wild type even when 2 kb flanking sequences are used, whereas, the ratio increased to 95% in \DeltaakuA strain. The strain was proved to be very successful even when 0.5 and 0.1 kb flanking sequences are used. In this case while the wild type showed 0-2% homologous recombination ratio, in \DeltaakuA strain, the ratio increased to 75-84%. The study by Krappman *et al.* (2006) validated the convenience of *A. fumigatus* AfS28 for targeted integration of replacement cassettes into the fungal genome. Therefore, in this study, *A. fumigatus* AfS28 strain was obtained from Fungal Genetics Stock Center and used for targeted deletion.

3.4.1.2. PCR to Amplify *hygB* (Hygromycin B Phosphotransferase) Split Marker Fragments

The sequence of the primers to amplify *hygB* from the template pUCATPH vector is according to Catlett *et al.* (2002) and are shown in Table 3.5. Annealing sites of the primers on pUCATPH are shown in Figure 3.35.

Table 3.5. Features of the primers amplifying *hygB* (Hygromycin B Phosphotransferase)

Name	Direction	Sequence
M13F	Forward	5'-CGCCAGGGTTTTCCCAGTCACGAC-3'
M13R	Reverse	5'-AGCGGATAACAATTTTCACAGGA-3'
NLC37	Forward	5'-GGATGCCTCCGCTCGAAGTA-3'
NLC38	Reverse	5'-CGTTGCAAGACCTGCCTGAA-3'

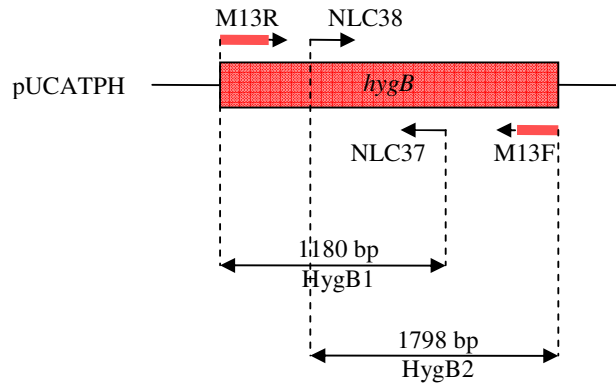


Figure 3.35. Annealing sites of the primers to amplify *hygB*.

The overlapping marker fragments HygB1 (1180 bp) and HygB2 (1798 bp) were amplified using M13R-NLC37 and NLC38-M13F primer pairs, respectively (Figure 3.36).

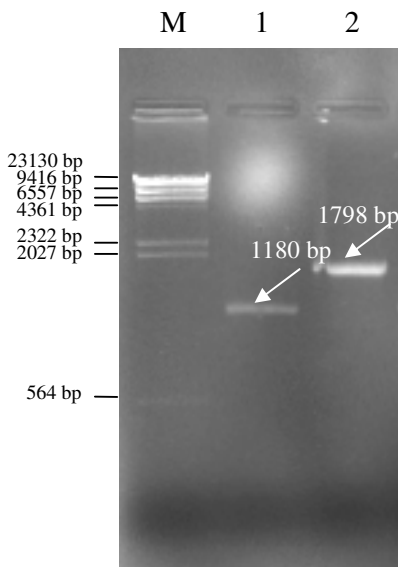


Figure 3.36. Amplification of the overlapping marker fragments. M, Lambda DNA/*Hind*III; 1, HygB1 fragment; 2, HygB2 fragment.

3.4.1.3. Targeted *tpnC* Deletion

3.4.1.3.1. Primer Design for *tpnC* Deletion

Split marker methodology requires 4 gene-specific primers for each deletion to amplify 5' and 3' flanking regions of the target gene. To amplify 5' flanking region of *tpnC*, FP12-RP1 primer pair was designed. Similarly, FP2-RP22 primer pair was designed to amplify 3' flanking region of *tpnC*. 5' ends of the primers RP1 and FP2 are complementary to M13R and M13F sequences, respectively, to allow fusion with the HygB fragments. The features of the primers and annealing sites are shown in Table 3.6 and Figure 3.37. The primers PKSInF and PKSInR amplify *tpnC* gene; PKSoutF and PKSoutR anneal to the upstream site of the 5' flanking region and downstream of the 3' flanking region, respectively. These primers were designed to verify gene deletions in the transformant strains.

Table 3.6. Features of the primers designed for *tpnC* deletion. Underlined sequences are complementary to *hygB* marker primers.

Name	Annealing site	Direction	Sequence
FP12	5' flanking region	Forward	5'-ATTCTGAAACTGCGTTGCT-3'
RP1	5' flanking region	Reverse	5'- <u>TCCTGTGTGAAATTGTTATCCGCTTCG</u> GAGAGGGATCTTTGCTA-3'
FP2	3' flanking region	Forward	5'- <u>GTCGTGACTGGGAAAACCCCTGGCGTG</u> CTGTCTTCGATTTTGTCG-3'
RP22	3' flanking region	Reverse	5'-CCAGCCCTACACAGTTCCAT-3'
PKSinF	Inside the gene	Forward	5'-CACCAAGGAAACACGTTCT-3'
PKSinR	Inside the gene	Reverse	5'-TTGATCACGTTTGCCATTT-3'
PKSoutF	Upstream of the 5' flanking region	Forward	5'-GACCTTGCTCGTAACCCTCA-3'
PKSoutR	Downstream of the 3' flanking region	Reverse	5'-CAAGGGAGTCTCACCGAGTC-3'

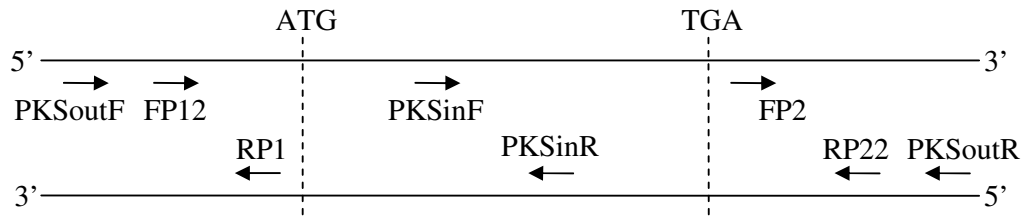


Figure 3.37. Annealing sites of the primers for *tpnC* deletion.

3.4.1.3.2. First Round PCR

First round PCR was performed with FP12-RP1 and FP2-RP22 primer pairs to obtain 5' and 3' flank of *tpnC*, respectively using *A. fumigatus* AfS28 genomic DNA as a template (Figure 3.38).

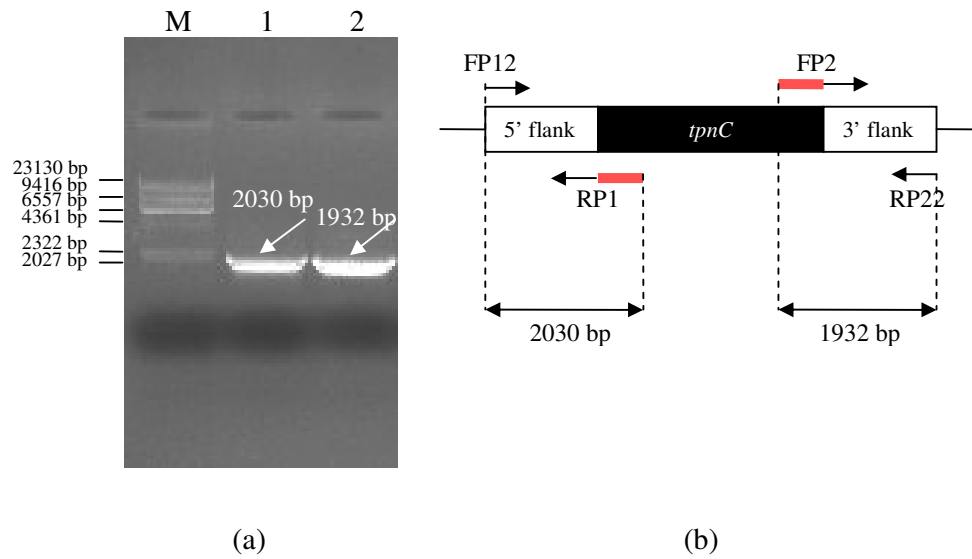


Figure 3.38. First round PCR for *tpnC* deletion (a) PCR showing 5' and 3' flank fragments, (b) Annealing sites of the primers used in first round PCR. M, Lambda DNA/*Hind*III; 1, 5' flank amplified by FP12-RP1; 2, 3' flank amplified by FP2-RP22.

3.4.1.3.3. Second Round PCR

In PCR round 2, each flank from round 1 was fused to the marker through overlap extension PCR. For the 5' construct, fragment 1, the templates are FP12-RP1 flank from round 1 and M13R-NLC37 marker fragment (HygB1); primers are FP12 and NLC37. For the 3' construct, fragment 2, the templates are NLC38-M13F marker fragment (HygB2) and FP2-RP22 flank from round 1; primers are NLC38 and RP22. Fragment 1 (3210 bp) and fragment 2 (3730 bp) are shown in Figure 3.39.

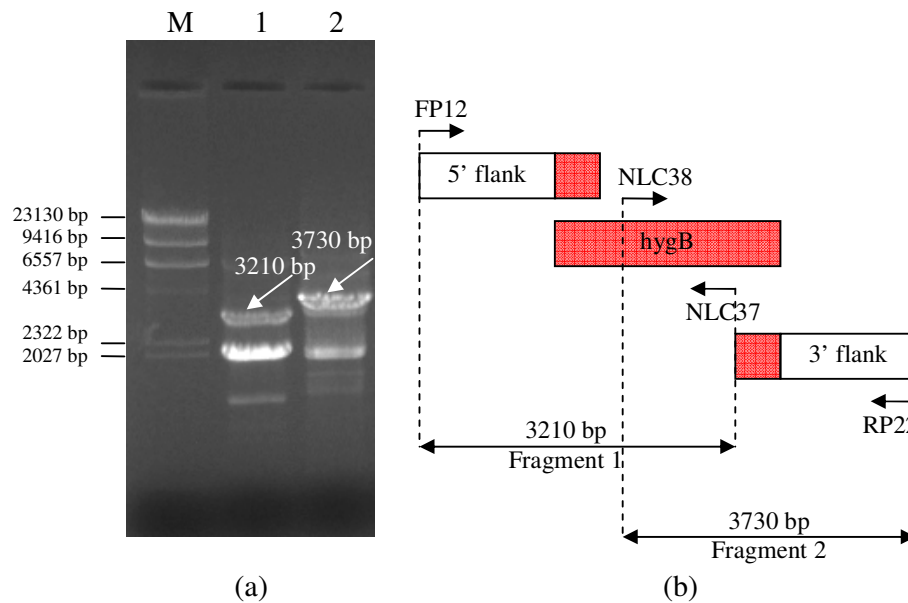


Figure 3.39. Second round PCR for *tpnC* deletion (a) PCR showing 5' and 3' flank fragments fused to HygB1 and HygB2, respectively; (b) Annealing sites of the primers used in second round PCR. M, Lambda DNA/*Hind*III; 1, 5' flank fused to HygB1 by the primers FP12 and NLC37; 2, 3' flank fused to HygB2 by the primers NLC38 and RP22.

3.4.1.3.4. Transformation of *A. fumigatus* AfS28 with *tpnC* Split Marker Fragments

The gel purified fragment 1 and fragment 2 obtained in second round PCR were used to transform *A. fumigatus* AfS28 as explained in the Section 2.2.14. At the end of transformation, three hygromycin-resistant colonies were obtained. These colonies were purified by single spore isolation as explained in the Section 2.2.14.

3.4.1.3.5. Analysis of $\Delta tpnC$ Transformants by PCR

To analyze the three hygromycin-resistant transformants by PCR, DNA isolation was performed as explained in Section 2.2.2.1. PCR was carried out with DNAs from the transformants and *A. sojiae* host AfS28. The annealing sites of the primers designed on *A. fumigatus* AfS28 DNA, on the DNA from a knock-out strain and on the DNA from a strain with ectopic integration (random, non-homologous integration) were determined (Figure 3.40) and PCR product sizes that can be obtained with these three possibilities were calculated (Table 3.7). When PCR was performed with the primers indicated in Table 3.7, it was seen that in all three transformants, homologous recombination took place and the *tpnC* gene was successfully replaced by *hygB* (Figure 3.41).

Table 3.7. PCR products that can be obtained with *A. fumigatus* AfS28, $\Delta tpnC$ knock-out strain and a strain with a possible ectopic integration.

	PKSoutF & NLC37 (bp)	NLC38 & PKSoutR (bp)	NLC37 & NLC38 (bp)	PKSinF & PKSinR (bp)
AfS28	-	-	-	478
Knock-out	3368	3794	465	-
Ectopic	-	-	465	478

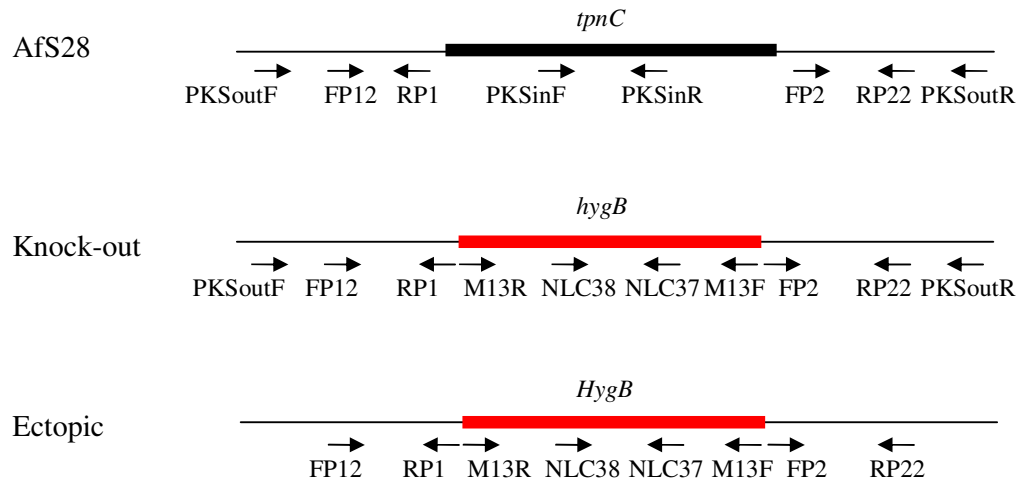


Figure 3.40. The annealing sites of the primers designed on DNA from *A. fumigatus* Afs28, from a knock-out strain and from a strain with ectopic integration.

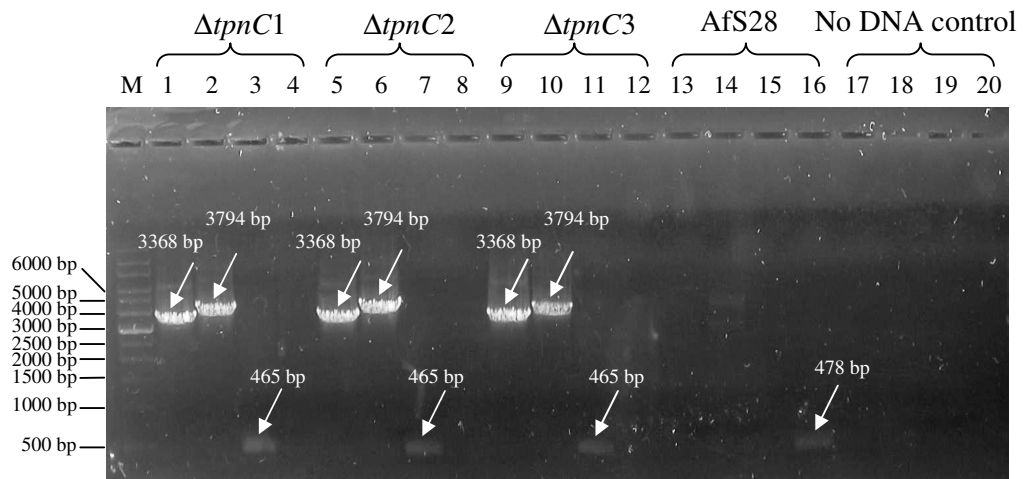


Figure 3.41. Analysis of *A. fumigatus* Afs28 and $\Delta tpnC$ transformants by PCR. M, DNA ladder, 1-4, transformant $\Delta tpnC1$; 5-8, transformant $\Delta tpnC2$; 9-12, transformant $\Delta tpnC3$; 13-16, *A. fumigatus* Afs28; 17-20, no DNA control. 1, 5, 9, 13, 17, primers PKSoutF & NLC37; 2, 6, 10, 14, 18, primers NLC38 & PKSoutR; 3, 7, 11, 15, 19, primers NLC37 & NLC38; 4, 8, 12, 16, 20, primers PKSinF & PKSinR.

3.4.1.3.6. Analysis of $\Delta tpnC$ Transformants by Southern Blot

Transformants $\Delta tpnC1$, $\Delta tpnC2$ and $\Delta tpnC3$ were also analyzed by Southern Blotting. To verify that double cross-over took place, two probes, 5' and 3' flanks of *tpnC*, were used. The restriction sites on the *tpnC* region of *A. fumigatus* AfS28 and on a possible knock-out strain are shown in Figure 3.42. To perform Southern Blotting, *A. fumigatus* AfS28 DNA was digested with *Xho*I that should lead to 4340, 3030 and 1581 bp fragments, while transformant DNAs were digested with *Xho*I and *Xba*I that will result in 2613, 1581 and 986 bp fragments. The expected signals were obtained as a result of Southern Blotting and hybridization proving conclusively that in all three transformants double cross-over took place and *tpnC* gene was replaced by *hygB* by a single insertion into the genome (Figure 3.43).

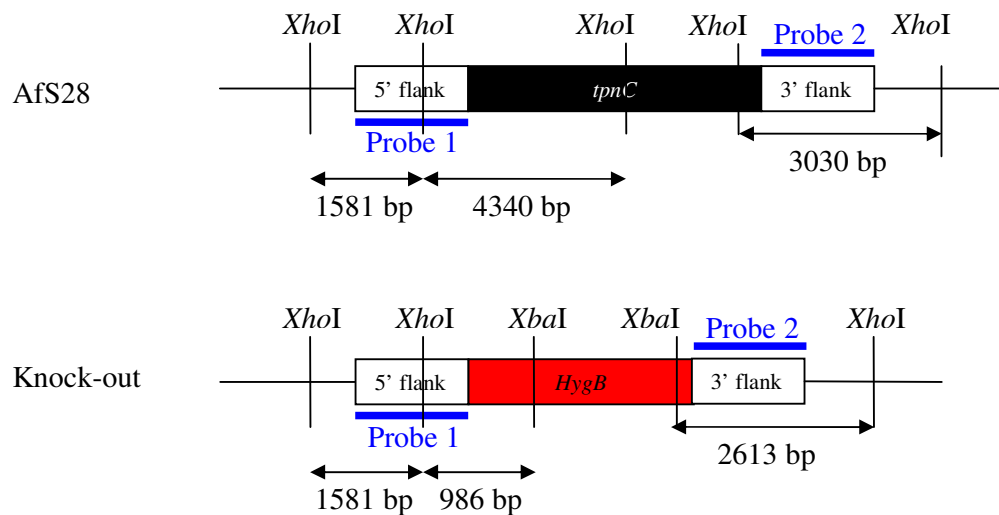


Figure 3.42. The restriction sites on the *tpnC* locus of *A. fumigatus* AfS28 and on a possible knock-out strain.

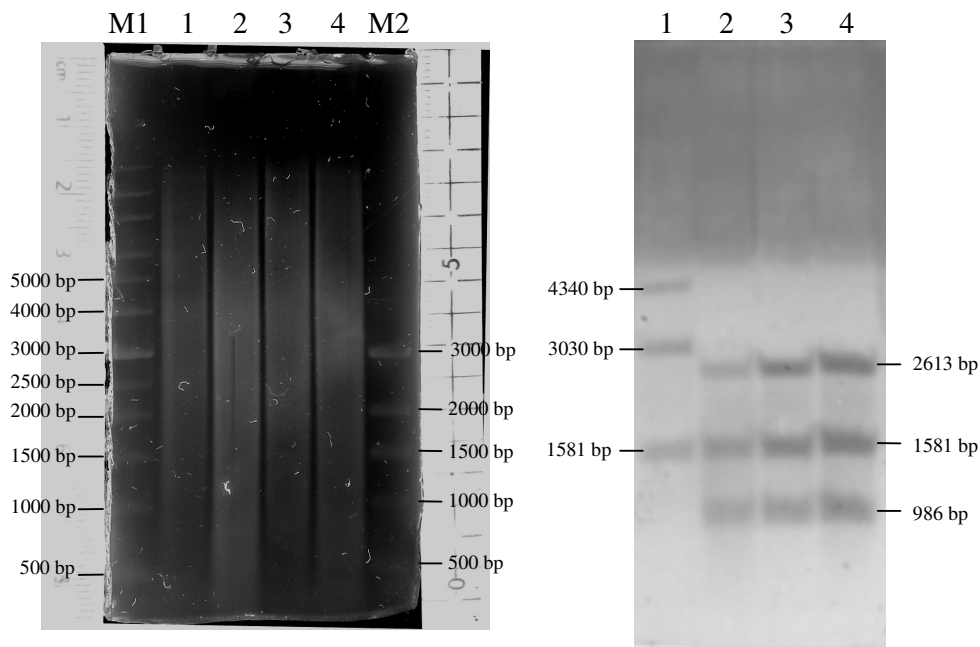


Figure 3.43. Analysis of *A. fumigatus* AfS28 and transformants $\Delta tpnC1$, $\Delta tpnC2$ and $\Delta tpnC3$ by Southern Blot. M1 and M2 DNA ladders; 1, *A. fumigatus* AfS28; 2, $\Delta tpnC1$; 3, $\Delta tpnC2$; 4, $\Delta tpnC3$.

3.4.1.4. Targeted *tpnJ* Deletion

3.4.1.4.1. Primer Design for *tpnJ* Deletion

To amplify the 5' flanking region of *tpnJ*, McoFP1-McoRP1 primer pair was designed. Likewise, McoFP2-McoRP2 primer pair was designed to amplify 3' flanking region of *tpnJ*. Similar to *tpnC* deletion, 5' ends of the primers McoRP1 and McoFP2 are complementary to M13R and M13F sequences, respectively, to allow fusion with the HygB fragments. The features of the primers and annealing sites are shown in Table 3.8 and Figure 3.44. The primers TPNJinF and TPNJinR amplify the *tpnJ* gene; McoFP12 and McoRP22 anneal to the upstream of the 5' flanking region and downstream of the 3' flanking region, respectively.

Table 3.8. Features of the primers designed for *tpnJ* deletion. Underlined sequences are complementary to *hygB* marker primers.

Name	Annealing site	Direction	Sequence
McoFP1	5' flanking region	Forward	5'-AATGACCAACGTCGTGGACT-3'
McoRP1	5' flanking region	Reverse	5'- <u>TCCTGTGTGAAAATGTTATCCGCTAAT</u> CGAGCCCGACCTATTCT-3'
McoFP2	3' flanking region	Forward	5'- <u>GTCGTGACTGGGAAAACCC</u> TGGCGGG ATTGAGTGAGCTGGAAGC-3'
McoRP2	3' flanking region	Reverse	5'-GGGGTCTTTGTTGGAGTTCA-3'
TPNJinF	Inside the gene	Forward	5'-TTACGCCCAATACTGTGACG-3'
TPNJinR	Inside the gene	Reverse	5'-AGAGCCCACTACTGACATGG-3'
McoFP12	Upstream of the 5' flanking region	Forward	5'-TGGTAGCGATAGATGCGTTG-3'
McoRP22	Downstream of the 3' flanking region	Reverse	5'-ACCCGACGTCAATCAGTTTC-3'

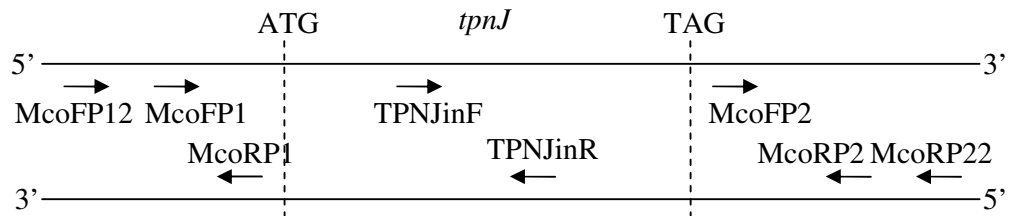


Figure 3.44. Annealing sites of the primers for *tpnJ* deletion.

3.4.1.4.2. First Round PCR

First round PCR was performed with McoFP1-McoRP1 and McoFP2-McoRP2 primer pairs to obtain 5' and 3' flank of *tpnJ*, respectively using *A. fumigatus* AfS28 genomic DNA as a template (Figure 3.45).

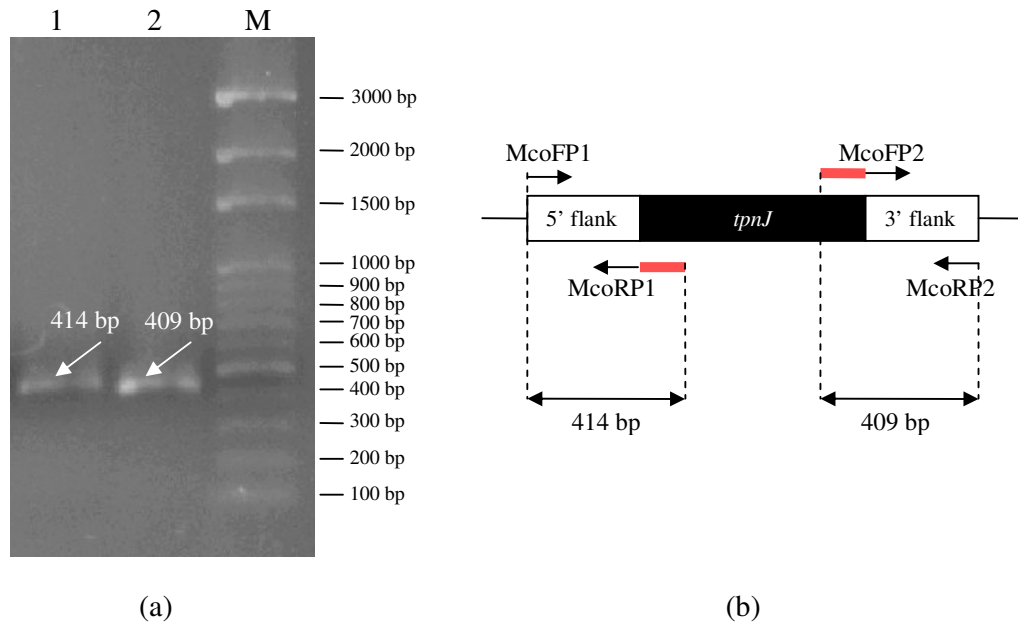


Figure 3.45. First round PCR for *tpnJ* deletion (a) PCR showing 5' and 3' flank fragments, (b) Annealing sites of the primers used in first round PCR. M, 100 bp DNA ladder; 1, 5' flank amplified by McoFP1-McoRP1; 2, 3' flank amplified by McoFP2-McoRP2.

3.4.1.4.3. Second Round PCR

In PCR round 2, each flank from round 1 was fused to the marker through overlap extension PCR. For the 5' construct, fragment 1, the templates are McoFP1-McoRP1 flank from round 1 and M13R-NLC37 marker fragment (HygB1); primers are McoFP1 and NLC37. For the 3' construct, fragment 2, the templates are NLC38-M13F marker fragment (HygB2) and McoFP2-McoRP2 flank from round 1; primers are NLC38 and McoRP2. Fragment 1 (1594 bp) and fragment 2 (2207 bp) obtained are shown in Figure 3.46.

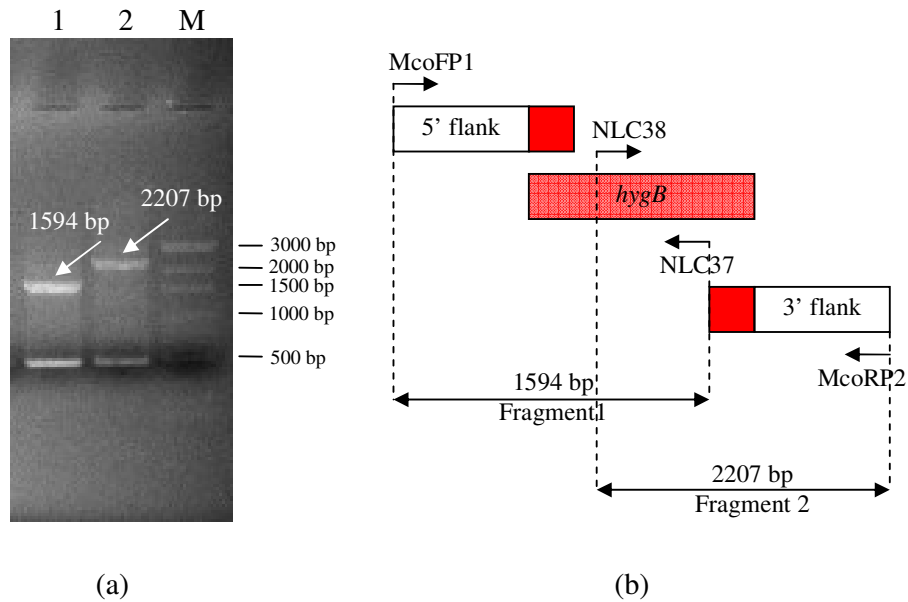


Figure 3.46. Second round PCR for *tpnJ* deletion (a) PCR showing 5' and 3' flank fragments fused to HygB1 and HygB2, respectively; (b) Annealing sites of the primers used in second round PCR. M, DNA ladder; 1, 5' flank fused to HygB1 by the primers McoFP1 and NLC37; 2, 3' flank fused to HygB2 by the primers NLC38 and McoRP2.

3.4.1.4.4. Transformation of *A. fumigatus* AfS28 with *tpnJ* Split Marker Fragments

The gel purified fragments obtained in second round PCR were used to transform *A. fumigatus* AfS28 as explained in Section 2.2.14. At the end of transformation, three hygromycin-resistant colonies were obtained. These colonies were purified by single spore isolation.

3.4.1.4.5. Analysis of $\Delta tpnJ$ Transformants by PCR

To analyze the three hygromycin-resistant transformants by PCR, DNA isolation was performed as explained in Section 2.2.2.1. PCR was carried out with DNAs from the transformants and *A. fumigatus* host AfS28. The annealing sites of the primers designed on *A. fumigatus* AfS28 DNA, on the DNA from a knock-out strain and on the DNA from a strain with ectopic integration were determined (Figure 3.47) and PCR product sizes that can be obtained with these three possibilities were calculated (Table 3.9). When PCR was performed with the primers indicated in Table 3.9, it was seen that in transformants $\Delta tpnJ2$ and $\Delta tpnJ3$, expected McoFP12-NLC37 and NLC38-McoRP22 bands were observed indicating *tpnJ* gene was successfully replaced by *hygB* (Figure 3.48); however, in transformant $\Delta tpnJ1$, only McoFP12-NLC37 PCR product was observed, which shows the insertion of only fragment 1 into the *tpnJ* locus.

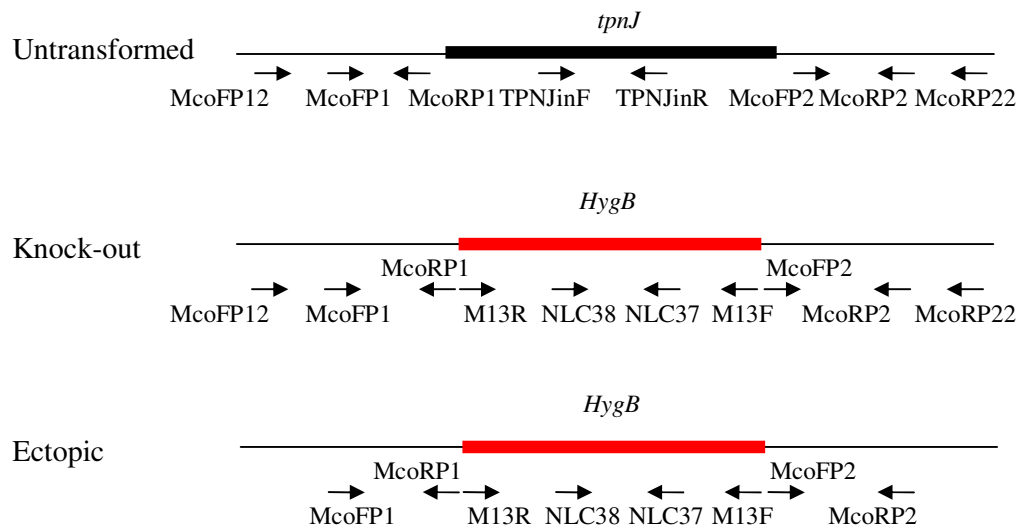


Figure 3.47. The annealing sites of the designed primers on *A. fumigatus* AfS28 DNA, on the DNA from a knock-out strain and on the DNA from a strain with ectopic integration.

Table 3.9. PCR products that can be obtained with *A. fumigatus* AfS28, $\Delta tpnJ$ knock-out strain and a strain with a possible ectopic integration.

	McoFP12 & NLC37 (bp)	NLC38 & McoRP22 (bp)	NLC37 & NLC38 (bp)	TPNJinF & TPNJinR (bp)
AfS28	-	-	-	692
Knock-out	3174	3620	465	-
Ectopic	-	-	465	692

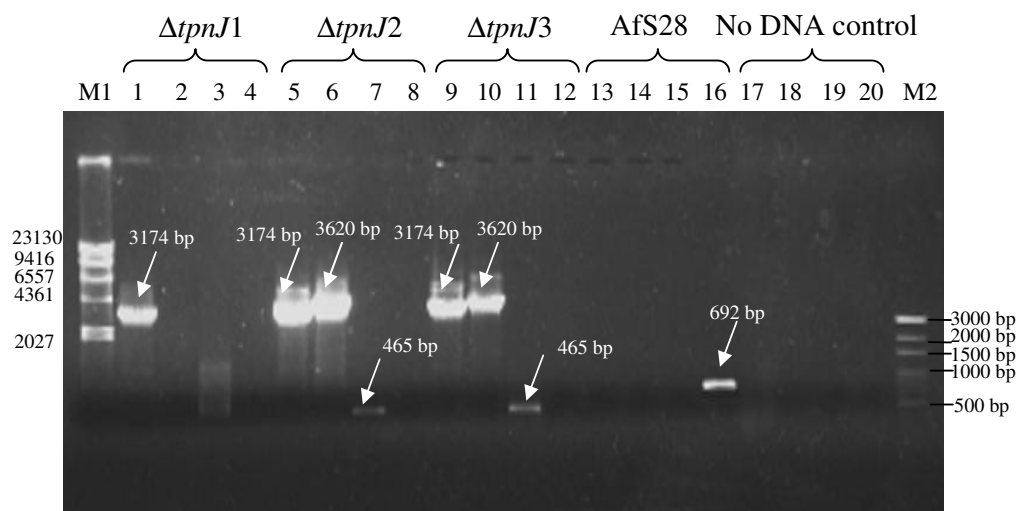


Figure 3.48. Analysis of *A. fumigatus* AfS28 $\Delta tpnJ$ transformants by PCR. M, DNA ladder, 1-4, transformant $\Delta tpnJ1$; 5-8, transformant $\Delta tpnJ2$; 9-12, transformant $\Delta tpnJ3$; 13-16, *A. fumigatus* AfS28; 17-20, no DNA control. 1, 5, 9, 13, 17, primers McoFP12 & NLC37; 2, 6, 10, 14, 18, primers NLC38 & McoRP22; 3, 7, 11, 15, 19, primers NLC37 & NLC38; 4, 8, 12, 16, 20, primers TPNJinF & TPNJinR.

3.4.1.4.6. Analysis of *ΔtpnJ* Transformants by Southern Blotting

In Southern blotting, transformants *ΔtpnJ2* and *ΔtpnJ3*, which were shown to be knock-out strains by PCR were used. To verify that both fragment 1 and fragment 2 were inserted at *tpnJ* locus, two probes, 5' and 3' flanks of *tpnJ*, were used. The restriction sites on the *tpnC* region of *A. fumigatus* AfS28 and on a possible knock-out strain are shown in Figure 3.49. To perform Southern Blot, DNAs from *A. fumigatus* AfS28, *ΔtpnJ2* and *ΔtpnJ3* were digested with *Pst*I that will lead to a single 3684 bp band in AfS28; and two bands, 1772 bp and 512 bp in size, in transformants where a correct gene replacement event takes place. The expected signals were observed in AfS28, *ΔtpnJ2* and *ΔtpnJ3*; however, ectopic integrations were also seen in *ΔtpnJ3* (Figure 3.50). Therefore, a single insertion at the correct locus was observed only in transformant *ΔtpnJ2*. Observation of ectopic integrations in *ΔtpnJ3* and only fragment 1 insertion in *ΔtpnJ1* indicates that small-sized flanks (414 bp and 409 bp) are not suitable for gene deletion studies in *A. fumigatus* although using a *ΔakuA* genetic background. The correct single insertion in all three *ΔtpnC* mutants, where longer flanks, 2030 bp and 1932 bp, were used confirms this hypothesis.

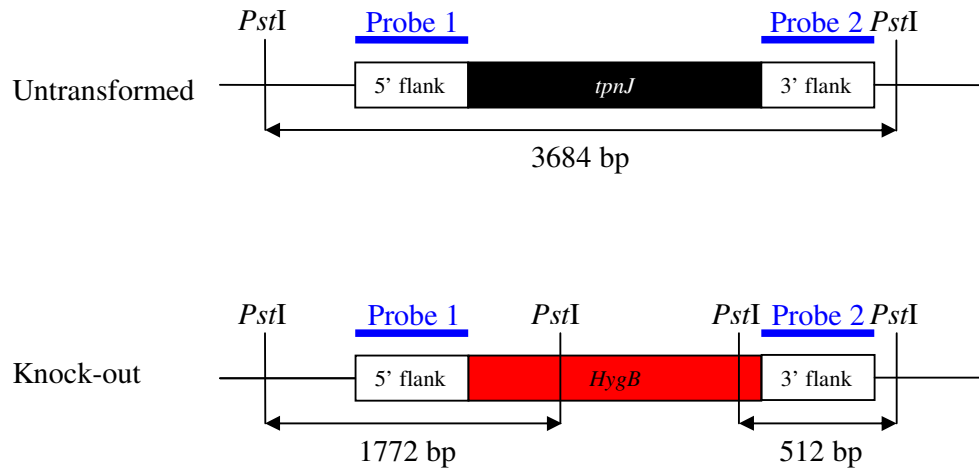


Figure 3.49. The restriction sites on the *tpnJ* locus of *A. fumigatus* AfS28 and on a possible knock-out strain.

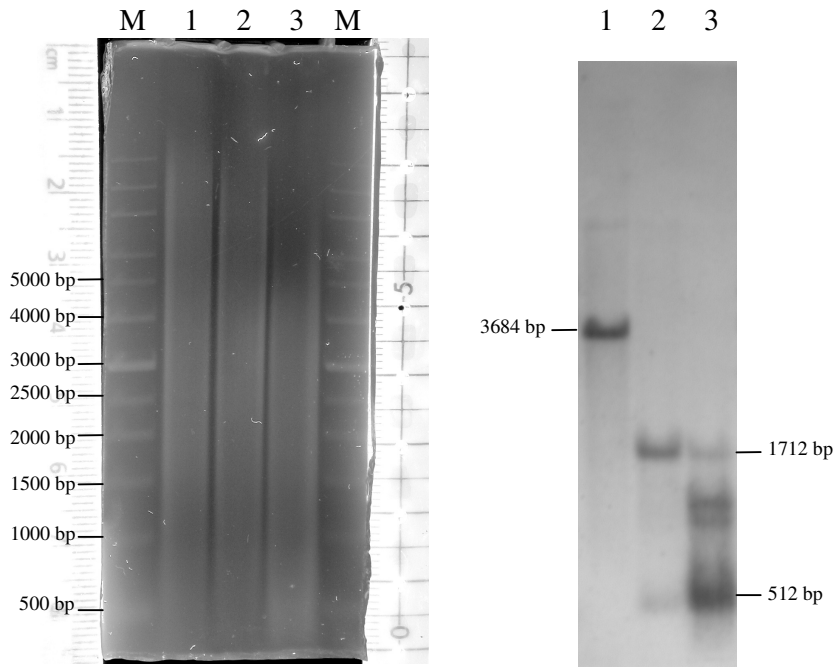


Figure 3.50. Analysis of *A. fumigatus* AfS28 and transformants $\Delta tpnJ2$ and $\Delta tpnJ3$ by Southern Blotting and hybridization. M, DNA ladder; 1, *A. fumigatus* AfS28; 2, $\Delta tpnJ2$; 3, $\Delta tpnJ3$.

3.4.2. Detection of Metabolites from *A. fumigatus* AfS28, Δ *tpnC1*, and Δ *tpnJ2* by Liquid Chromatography Mass Spectrometry

Metabolites from *A. fumigatus* AfS28, Δ *tpnC1*, and Δ *tpnJ2* were determined by LC-MS as explained in Section 2.2.15. The chromatograms of *A. fumigatus* AfS28, Δ *tpnC1*, and Δ *tpnJ2* extracts, when searched for the presence of tryptacidin having a molecular weight of 344, revealed a single compound eluted from the column at 23.422 min in AfS28 extracts, which is absent in Δ *tpnC1*, and Δ *tpnJ2* extracts (Figure 3.51). The mass spectrum showed a 345 M+H⁺ peak (Figure 3.52), clearly indicating the compound as tryptacidin. This result strongly supports the hypothesis that the *tpnJ* and *tpnC* are involved in the biosynthesis of tryptacidin.

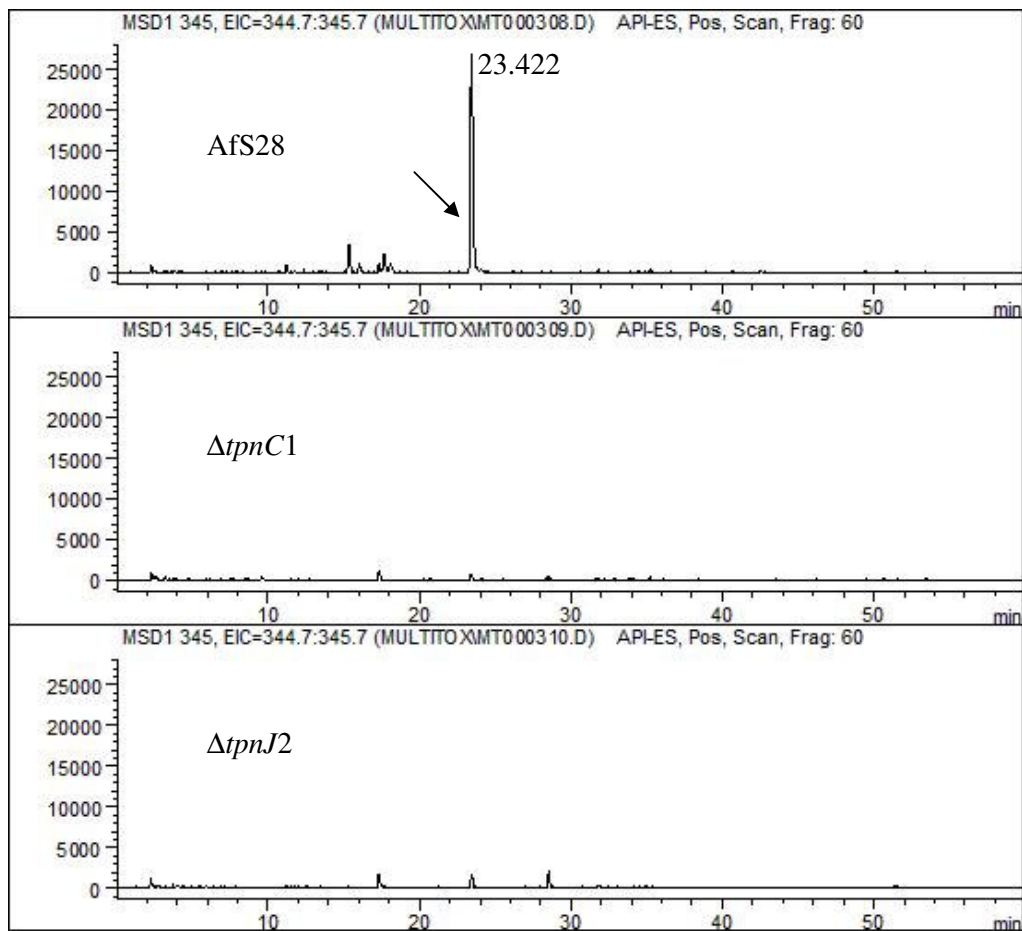


Figure 3.51. Chromatograms of *A. fumigatus* AfS28, $\Delta tpnC1$, and $\Delta tpnJ2$ extracts when searched for the presence of trypacidin having a molecular weight of 344.

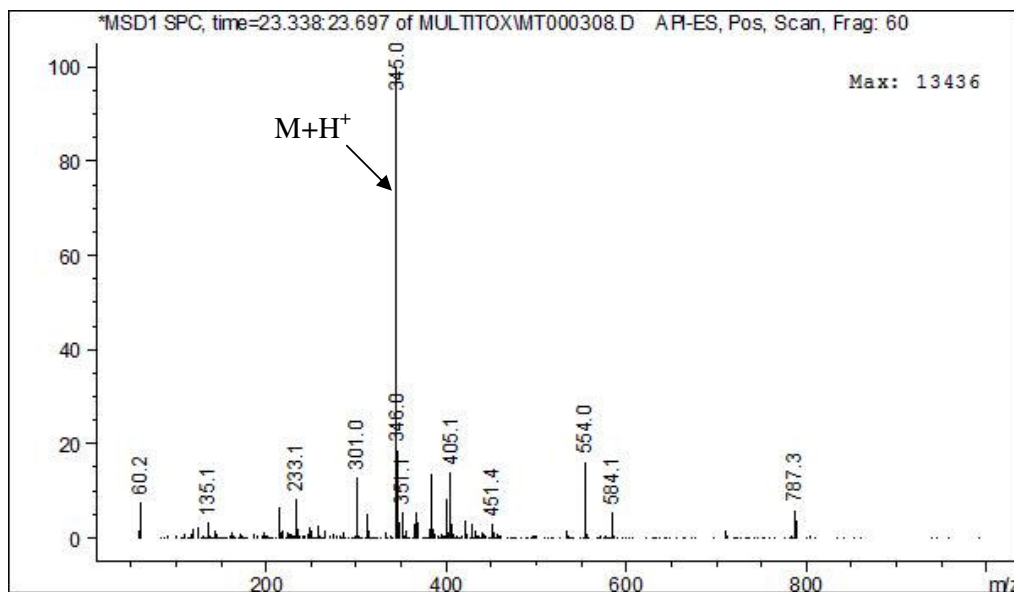


Figure 3.52. Mass spectrum of the compound eluted at 23.4 min.

The chromatograms of *A. fumigatus* AfS28, $\Delta tpnC1$, and $\Delta tpnJ2$ extracts when searched for the presence of monomethylsulochrin having a molecular weight of 346 revealed several compounds (Figure 3.53). However, only the compound eluted at 24.7 min showed typical $M+H^+$, $M+Na^+$, and a peak of 209 mass fragment, which is a characteristic of benzophenone compounds including sulochrin and dihydrogeodin, which results from the separation of the second ring from the first ring (Figure 3.54). This result indicates strongly that the compound eluted at 24.7 min is monomethylsulochrin. Absence of the monomethylsulochrin peak in $\Delta tpnC1$ and the increase of peak height in $\Delta tpnJ2$, strongly suggests that indeed *tpnC* is involved in the biosynthesis of monomethylsulochrin and *tpnJ* is thus responsible for the oxidation of monomethylsulochrin into trypacidin.

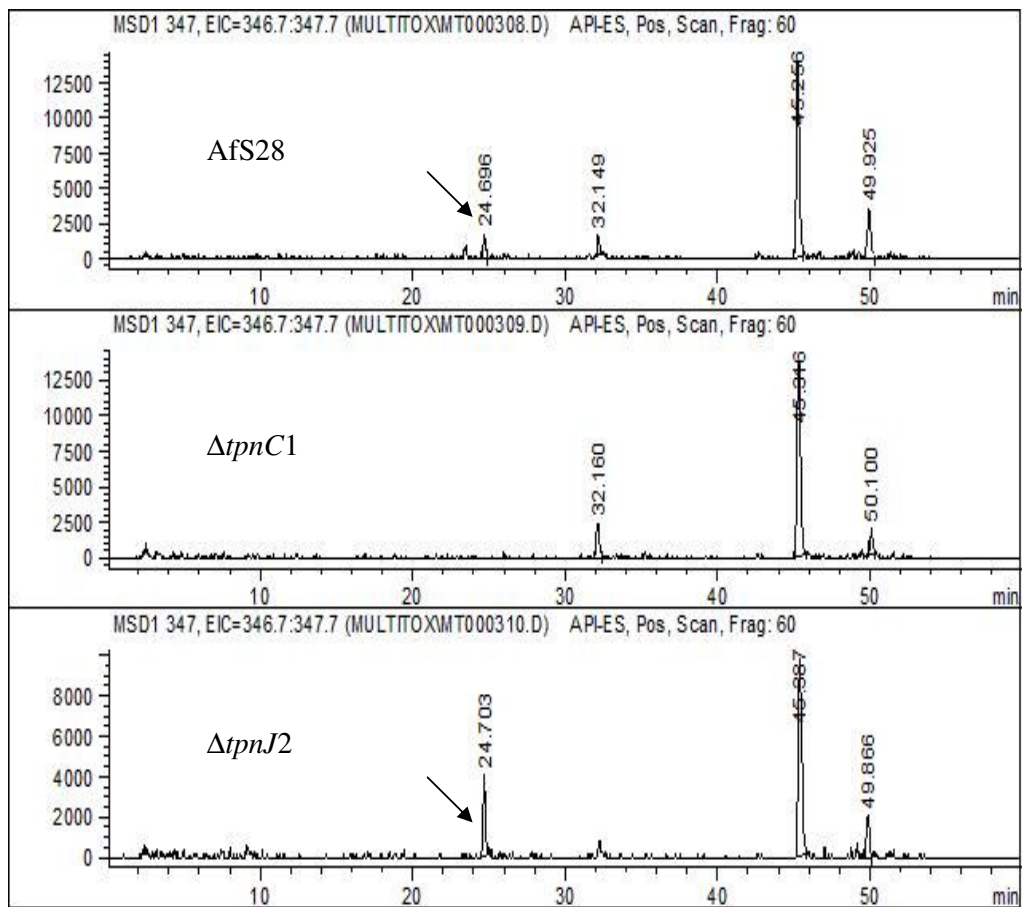


Figure 3.53. Chromatograms of *A. fumigatus* AfS28, $\Delta tpnC1$, and $\Delta tpnJ2$ extracts when searched for the presence of monomethylsulochrin having a molecular weight of 346.

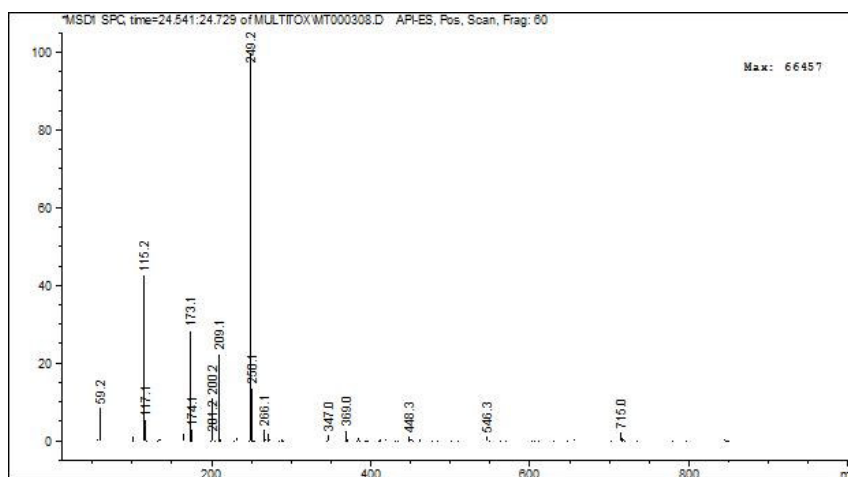


Figure 3.54. Mass spectrum of the compound eluted at 24.7 min.

3.4.3. Phenotypic Assays

As most of the fungal secondary metabolites, trypacidin and monomethylsulochrin are bioactive compounds. Trypacidin is an antibiotic first reported by Balan *et al.* (1963). It was isolated from *Aspergillus fumigatus* and was shown to be active against some protozoa, including *Trypanosoma cruzi* and *Toxoplasma gondii* (Parker and Jenner, 1968). Monomethylsulochrin has been shown to inhibit eosinophils, which may play important roles in allergic diseases (Ohashi *et al.*, 1999). Monomethylsulochrin has also been shown to have anti-*Helicobacter pylori* activity with a MIC (minimum inhibitory concentration) of 10.0 µg/ml, which is comparable to the promisingly potent anti-*H. pylori* natural products (Li *et al.*, 2005). To analyze the importance of these compounds for the fungus itself, different phenotypic assays were performed.

3.4.3.1. Analysis of the Effect of Carbon Sources

To analyze the effect of carbon sources, the strains were grown in Minimal Medium agar plates containing ethanol, fructose, galactose, glycerol, lactose, maltose or sorbitol at a concentration of 100 mM instead of glucose for 3 days at 37°C. The

result of the assays did not show a different phenotype in deletion strains with respect to the carbon source (Figure 3.55).

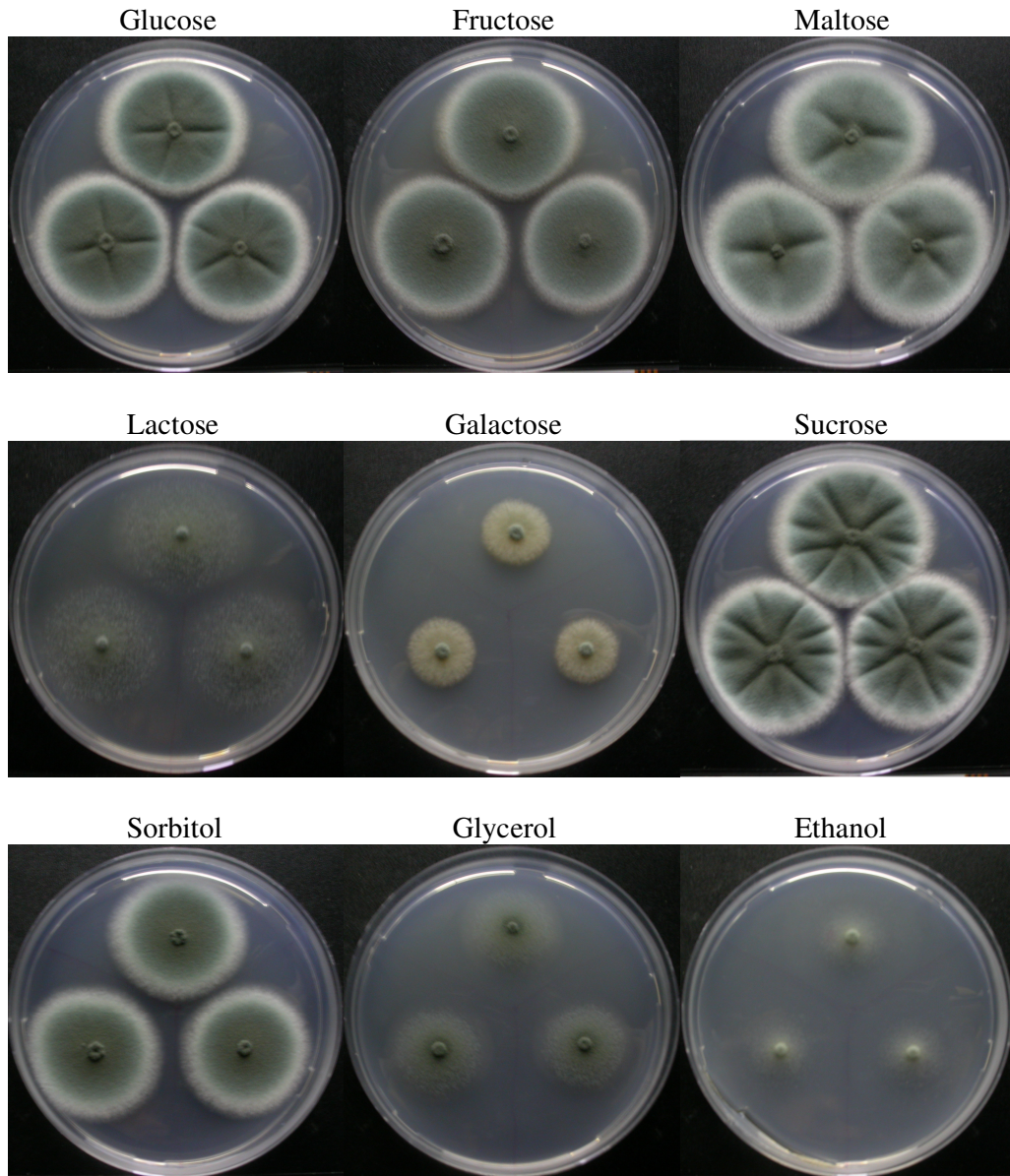


Figure 3.55. Effects of different carbon sources on growth of *A. fumigatus* AfS28 and deletion strains. The strain at the upper side of the plate is AfS28, at the lower left side of the plates is $\Delta tpnJ2$, the lower right side of the plate is $\Delta tpnC1$.

3.4.3.2. Analysis of the Effect of Nitrogen Sources

To examine the effect of nitrogen sources, the strains were grown in Minimal Medium agar plates containing glutamine, alanine, proline, ammonium chloride or sodium glutamate at a concentration of 10 mM instead of sodium nitrate for 3 days at 37°C. The result of the assays did not show a different phenotype in deletion strains with respect to the nitrogen source (Figure 3.56).

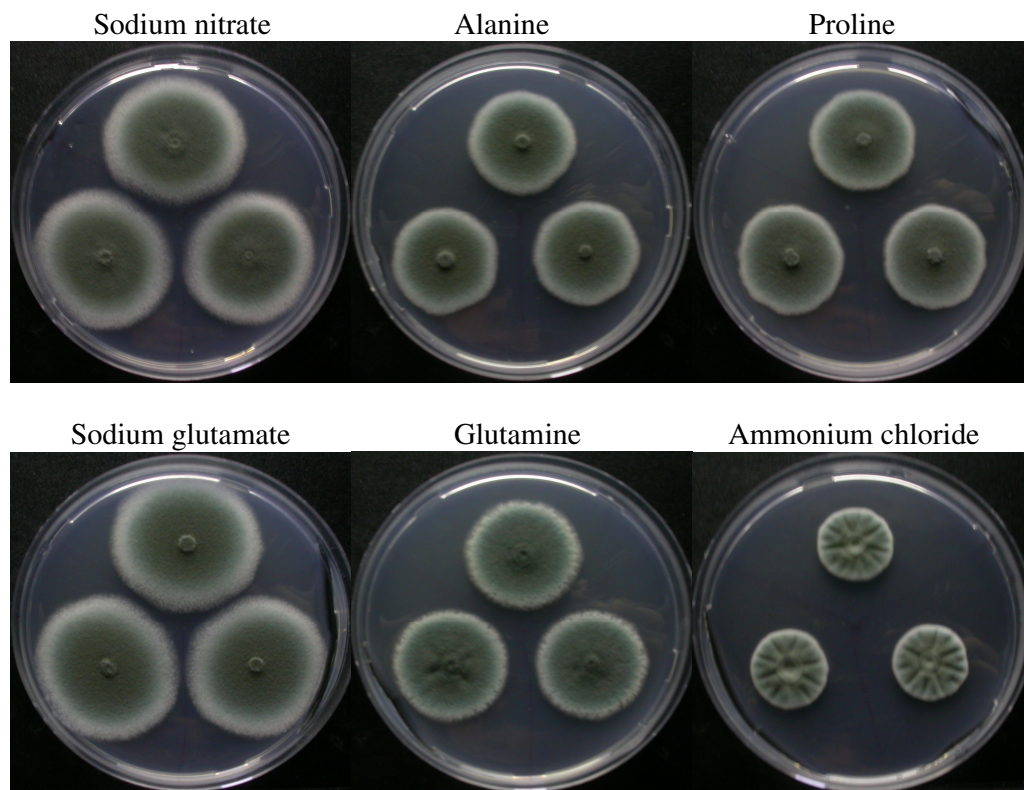


Figure 3.56. Effects of different nitrogen sources on growth of *A. fumigatus* AfS28 and deletion strains. The strain at the upper side of the plate is AfS28, at the lower left side of the plates is $\Delta tpnJ2$, the lower right side of the plate is $\Delta tpnC1$.

3.4.3.3. Analysis of the Effect of Temperature

To examine the effect of temperature, Minimal Medium agar plates inoculated with fungal strains were incubated at 25°C, 37°C and 45°C for 3 days. The result of the assay did not show a different phenotype in deletion strains with respect to the growth temperature (Figure 3.57).

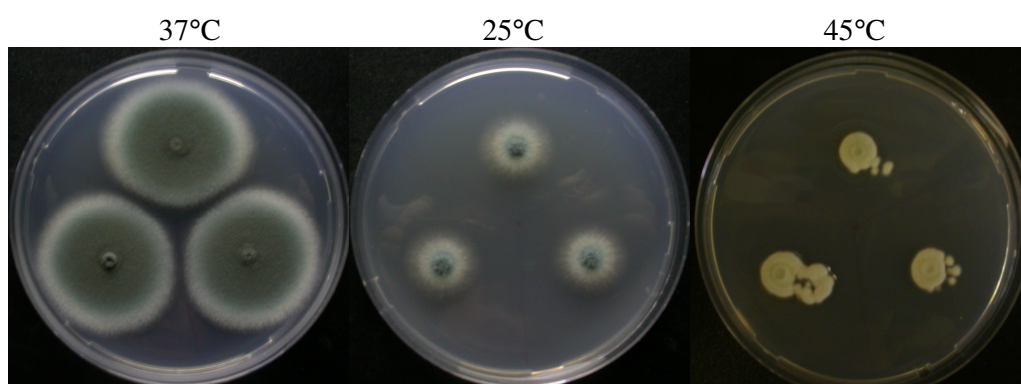


Figure 3.57. Effect of temperature on growth of *A. fumigatus* AfS28 and deletion strains. The strain at the upper side of the plate is AfS28, at the lower left side of the plates is $\Delta tpnJ2$, the lower right side of the plate is $\Delta tpnC1$.

3.4.3.4. Analysis of the Effect of Oxidative and Osmotic Stress on Growth

To examine the effect of oxidative and osmotic stress on growth, Minimal Medium agar plates supplemented with H₂O₂ (2 mM) and NaCl (1.5 M), respectively, were inoculated with fungal strains and incubated at 37°C for 3 days. Neither oxidative nor osmotic stress lead to a different phenotype in deletion strains (Figure 3.58).

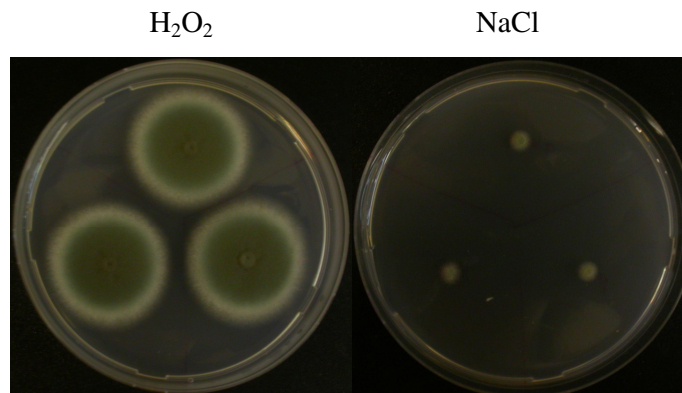


Figure 3.58. Effect of oxidative and osmotic stress on growth, the medium was supplemented with H₂O₂ (2 mM) and NaCl (1.5 M), respectively. The strain at the upper side of the plate is AfS28, at the lower left side of the plates is $\Delta tpnJ2$, the lower right side of the plate is $\Delta tpnC1$.

3.4.3.5. Analysis of the Effect of Cell Wall Inhibitor Agents on Growth

To examine any defect in the cell walls of deletion strains, the strains were grown in Minimal Medium agar plates supplemented with the cell wall inhibitor agents, SDS (0.01%) and congo red (80 µg/ml), at 37°C for 3 days. The result of the assay did not show a different phenotype in deletion strains (Figure 3.59).

3.4.3.6. Analysis of the Effect of Antifungal Agents on Growth

To examine the effect of antifungal agents on growth, , the strains were grown in Minimal Medium agar plates containing amphotericin B (0.2 µg/ml) and voriconazole (0.2 µg/ml) at 37°C for 3 days. The result of the assay did not show any difference between *A. fumigatus* AfS28 and deletion strains (Figure 3.60).

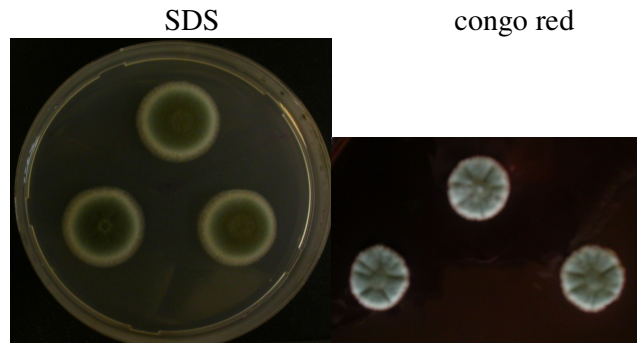


Figure 3.59. Effect of cell wall inhibitor agents, SDS and congo red, on growth. The strain at the upper side of the plate is Afs28, at the lower left side of the plates is $\Delta tpnJ2$, the lower right side of the plate is $\Delta tpnC1$.

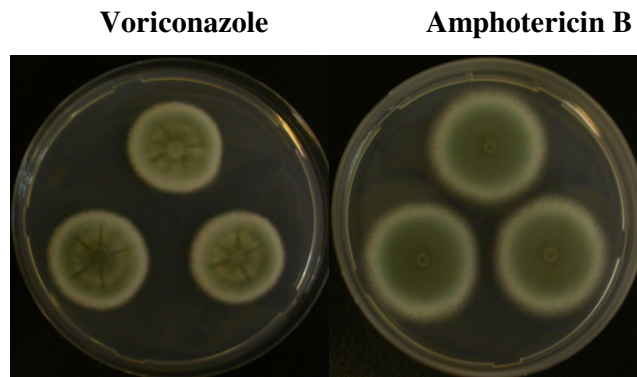


Figure 3.60. Effect of antifungal agents, voriconazole and amphotericin B on growth. The strain at the upper side of the plate is Afs28, at the lower left side of the plates is $\Delta tpnJ2$, the lower right side of the plate is $\Delta tpnC1$.

None of the analyzed conditions led to a different phenotype. The reason of production of these compounds by *A. fumigatus* could be to compete with other organisms in its natural ecological niche, wherein it survives and grows on organic debris. These compounds can also have roles in *A. fumigatus* pathogenicity. The strains can also be used in virulence assays in future studies to see the effect of deletions in pathogenicity.

CHAPTER 4

CONCLUSION AND FUTURE WORK

This study was aimed at the characterization and functional analysis of a novel polyketide biosynthesis gene cluster of *A. fumigatus* by deleting the polyketide synthase gene and a multi-copper oxidase gene within the cluster identified for the first time in this study.

Analysis of the *A. fumigatus* genome for laccases revealed several putative laccase and multicopper oxidase gene sequences, one of which, Afu4g14490 (*tpnJ*), was selected for further characterization. After sequence alignment and characterization studies, *tpnJ* was predicted to be 2128 bp long containing six introns, which makes the protein 606 amino acids long. The predicted amino acid sequence showed 63% identity with the dihydrogeodin oxidase of *Aspergillus terreus*, which is involved in the biosynthesis of an antifungal geodin.

The multicopper oxidase gene *tpnJ* was later found to be part of an uncharacterized gene cluster containing 13 genes including a polyketide synthase having a minimal domain structure (KS-AT-ACP). In this study, it is shown that this gene cluster is involved in the biosynthesis of the *A. fumigatus* metabolites, trypacidin and monomethylsulochrin. By a comparative genomics approach, a putative geodin biosynthesis gene cluster containing 13 genes, including dihydrogeodin oxidase, in *A. terreus* and a putative trypacidin biosynthesis gene cluster containing 13 genes in *N. fischeri* were also established.

Considering the nature of the reactions involving the conversion of dihydrogeodin to geodin in *A. terreus* and sulochrin to bisdechlorogeodin in *P. frequentans*, it was hypothesized in this study that a similar reaction, monomethylsulochrin to trypacidin conversion, takes place in *A. fumigatus* catalyzed

by the multicopper oxidase, TpnJp. In this respect, TpnJp was hypothesized to be a monomethylsulochrin oxidase.

Moreover, based on the studies involving aflatoxin and geodin biosynthesis pathways and genes found in geodin and trypacidin clusters in this study, possible gene products in the biosynthesis of geodin in *A. terreus* and proposed biosynthetic pathway of trypacidin and monomethylsulochrin in *A. fumigatus* and *N. fischeri* were determined.

In order to prove the hypothesized functions of the polyketide synthase (*tpnC*) and multicopper oxidase (*tpnJ*) genes, targeted gene deletion studies were performed. LC-MS analysis of extracts from *A. fumigatus* AfS28 and deletion strains confirmed the hypothesis that TpnCp is involved in trypacidin and monomethylsulochrin biosynthesis in *A. fumigatus*. This is the first fungal minimal polyketide synthase having only three domains whose biological function is identified. Moreover, the fact that LC-MS analysis of Δ *tpnJ* strain showed the absence of trypacidin and the presence of a higher amount of monomethylsulochrin in Δ *tpnJ* strain, confirmed the hypothesized monomethylsulochrin oxidase function of the enzyme, TpnJp. The strains were also analyzed by phenotypic assays, however, a different phenotype was not observed in either deletion strain. The strains can also be used in virulence assays in future studies to see the effect of deletions in pathogenicity.

Monomethylsulochrin oxidase gene, *tpnJ*, was also cloned onto pAN52-1 and pAN52-4 vectors for heterologous expression in *Aspergillus sojae*. However, although integration into the genome was confirmed by Southern Blot analysis and transcription was detected by RT-PCR; activity assays using dihydrogeodin and sulochrin as the substrates failed to show an oxidation product. Enzyme assays using monomethylsulochrin as the substrate could not be performed in this study since it is not commercially available; however, it can be purified from *A. fumigatus* and used in activity assays in future studies.

REFERENCES

Abe Y. *et al.* (2002) Effect of increased dosage of the ML-236B (compactin) biosynthetic gene cluster on ML-236B production in *Penicillium citrinum*. *Molecular and General Genetics*. 268, 130–137.

Ahn J., Cheng Y., Walton J. (2002) An extended physical map of the TOX2 locus of *Cochliobolus carbonum* required for biosynthesis of HC-toxin. *Fungal Genetics and Biology*. 35, 31–38.

Balajee S.A., Gribskov J.L., Hanley E., Nickle D., Marr K.A. (2005) *Aspergillus lentulus* sp nov, a new sibling species of *A. fumigatus*. *Eukaryotic Cell*. 4, 635-632.

Balan J., Ebringer L., Nemeč P., Kovac S., Dobias J. (1963) Antiprotozoal antibiotics. II. Isolation and characterization of trypacidin, a new antibiotic, active against *Trypanosoma cruzi* and *Toxoplasma gondii*. *Journal of Antibiotics* (Tokyo). 16, 157–160.

Bennett J.W., Bentley R. (1989) What's in a name? Microbial secondary metabolism. *Advances in Applied Microbiology*. 34, 1–28.

Bernardo P.H., Chai C.L.L., Deeble G.J., Lui X.M., Waring P. (2001) Evidence for gliotoxin-glutathione conjugate adducts. *Bioorganic & medicinal chemistry letters*. 11, 483–485.

Bok J., Keller N. (2004) *LaeA*, a regulator of secondary metabolism in *Aspergillus*. *Eukaryotic Cell*. 3, 527–535.

Bok J.W., Balajee S.A., Marr K.A., *et al.* (2005) *LaeA*, a regulator of morphogenetic fungal virulence factors. *Eukaryotic Cell*. 4, 1574-1582.

Bok J.W., Chung D., Balajee S.A., Marr K.A., Andes D., Nielsen K.F., Frisvad J.C., Kirby K.A., Keller N.P. (2006). GliZ, a transcriptional regulator of gliotoxin biosynthesis, contributes to *Aspergillus fumigatus* virulence. *Infection and Immunity*. 74, 6761–6768.

Brakhage A.A. (1998) Molecular regulation of β -lactam biosynthesis in filamentous fungi. *Microbiology and Molecular Biology Reviews*. 62, 547–585.

Brakhage A.A., Langfelder K. (2002) Menacing mold: The molecular biology of *Aspergillus fumigatus*. *Annual Review of Microbiology*. 56, 433-455.

Brakhage A.A., Liebmann B. (2005) *Aspergillus fumigatus* conidial pigment and cAMP signal transduction: significance for virulence. *Medical Mycology*. 43, S75-S82.

Brown D. *et al.* (1996) Twenty-five co-regulated transcripts define a sterigmatocystin gene cluster in *Aspergillus nidulans*. *Proceedings of National Academy of Sciences, USA* 93, 1418–1422.

Cary J.W., Ehrlich K.C., Bland J.M., Montalbano B.G. (2006) The aflatoxin biosynthesis cluster gene, *afIX*, encodes an oxidoreductase involved in conversion of versicolorin A to demethylsterigmatocystin. *Applied and Environmental Microbiology*. 72, 1096-1101.

Catlett N.L., Lee B, Yoder O.C., Turgeon B.G. (2002) Split-marker recombination for efficient targeted deletion fungal genes. *Fungal Genetics Newsletter*. 50, 9-11.

Clutterbuck A.J. (1972) Absence of laccase from yellow-spored mutants of *Aspergillus nidulans*. *Journal of Gen. Microbiol.* 70, 423-435.

Cole R.J., Cox R.H. (1981) Handbook of Toxic Fungal Metabolites. New York, Academic Press.

Cole R.J., Jarvis B.B., Schweikert M.A. (2003) Handbook of Secondary Fungal Metabolites, vol. III. Amsterdam, Academic Press.

Cole R.J., Schweikert M.A. (2003a) Handbook of Secondary Fungal Metabolites, vol. I. Amsterdam, Academic Press.

Cole R.J., Schweikert M.A. (2003b) Handbook of Secondary Fungal Metabolites, vol. II. Amsterdam: Academic Press.

Cramer R.A., Jr, Gamcsik, M.P., Brooking R.M., *et al.* (2006a) Disruption of a nonribosomal peptide synthetase in *Aspergillus fumigatus* eliminates gliotoxin production. *Eukaryotic Cell*. 5, 972–980.

Cramer R.A., Jr, Stajich J.S., Yamanaka Y., Dietrich F.E., Steinbach W.J. & Perfect J.R. (2006b) Phylogenomic analysis of non-ribosomal peptide synthetases in the genus *Aspergillus*. *Gene*. 383, 24–32.

Cui C.B., Kakeya H., Okada G., Onose H. (1996a) Novel Mammalian Cell Cycle Inhibitors, Tryprostatins A, B and Other Diketopiperazines Produced by *Aspergillus fumigatus* I. Taxonomy, Fermentation, Isolation and Biological Properties. *Journal of Antibiotics*. 49, 527-533.

Cui C.B., Kakeya H., Osada H. (1996b) Novel Mammalian Cell Cycle Inhibitors, Tryprostatins A, B and Other Diketopiperazines Produced by *Aspergillus fumigatus* II. Physico-chemical Properties and Structures. *Journal of Antibiotics*. 49, 534-540.

Ehrlich K.C., Montalbano B., Boue S.M., Bhatnagar D. (2005) An aflatoxin biosynthesis cluster gene encodes a novel oxidase required for conversion of versicolorin A to sterigmatocystin. *Applied and Environmental Microbiology*. 71, 8963-8965.

Finking R., Marahiel M.A. (2004) Biosynthesis of nonribosomal peptides. *Annual Review of Microbiology*. 58, 453-488.

Fischbach M.A., Walsh C.T. (2006) Assembly-line enzymology for polyketide and nonribosomal peptide antibiotics: Logic, machinery, and mechanisms. *Chemical Reviews*. 106, 3468-3496.

Fujii I., Iijima H., Tsukita S., Ebizuka Y., Sankawa U. (1987) Purification and Properties of Dihydrogeodin Oxidase from *Aspergillus terreus*. *Journal of Biochemistry (Tokyo)*. 101, 11-18.

Fujii I., Watanabe A., *et al* (1998) Structures and functional analyses of fungal polyketide synthase genes. *Actinomycetologica*. 12, 1–14.

Fujii I., Watanabe A., *et al* (2001) Identification of a Claisen cyclase domain in fungal polyketide synthase WA, a naphthopyrone synthase of *Aspergillus nidulans*. *Chemical Biology*. 8, 189–197.

Galagan J.E., Calvo S.E., Cuomo C., *et al.* (2005) Sequencing of *Aspergillus nidulans* and comparative analysis with *A. fumigatus* and *A. oryzae*. *Nature*. 438, 1105-1115.

Gardiner D., Cozijnsen A., Wilson L., Pedras M., Howlett, B. (2004) The sirodesmin biosynthetic gene cluster of the plant pathogenic fungus *Leptosphaeria maculans*. *Molecular Microbiology*. 53, 1307–1318.

Gardiner D.M., Howlett B.J. (2005) Bioinformatic and expression analysis of the putative gliotoxin biosynthetic gene cluster of *Aspergillus fumigatus*. *FEMS Microbiology Letters*. 248, 241–248.

Geiser D.M., Frisvad J.C., Taylor J.W. (1998) Evolutionary relationships in *Aspergillus* section *Fumigati* inferred from partial β -tubulin and hydrophobin DNA sequences. *Mycologia*. 90, 831–845.

Girardin H., Monod M., Latge J.P. (1995) Molecular characterization of the foodborne fungus *Neosartorya fischeri*. *Applied and Environmental Microbiology*. 61, 1378–1383.

Gokhale R.S., Saxena P., Chopra T., Mohanty D. (2007) Versatile polyketide enzymatic machinery for the biosynthesis of complex mycobacterial lipids. *Natural Product Reports*. 24, 267-277.

Gomi M., Sonoyama M., Mitaku S. (2004) High performance system for signal peptide prediction: SOSUIsignal. *Chem-Bio Informatics Journal*. 4, 142-147.

Gutierrez S., Velasco J., Fernandez F.J., Martin J.F. (1992) The *cefG* gene of *Cephalosporium acremonium* is linked to the *cefEF* gene and encodes a deacetylcephalosporin C acetyltransferase closely related to homoserine O-acetyltransferase. *Journal of Bacteriology*. 174, 3056–3064.

Hakulinen N., Kiiskinen L., Kruus K., Saloheimo M., Paananen A., Koivula A., Rouvinen J. (2002) Crystal structure of a laccase from *Melanocarpus albomyces* with an intact trinuclear copper site. *Nature Structural Biology*. 9, 601-605.

Hayashi A., Fujioka S., Nukina M., et al. (2007) Fumiquinones A and B, nematicidal quinones produced by *Aspergillus fumigatus*. *Bioscience Biotechnology and Biochemistry*. 71, 1697-1702.

Hayes J.D., Pulford D.J. (1995) The glutathione S-transferase supergene family: regulation of GST and the contribution of the isoenzymes to cancer chemoprotection and drug resistance. *Critical Reviews of Biochemistry and Molecular Biology*. 30, 445-600.

Hayes J.D., and Strange R.C. (1995) Potential contribution of the glutathione S-transferase supergene family to resistance to oxidative stress. *Free Radical Research*. 22, 193-207.

Heerikhuisen M., van den Hondel C.A., Punt P.J., van Biezen N., Albers A., Vogel K. (2001) Novel means of transformation of fungi and their use for heterologous protein production. World Patent Application WO01/09352.

Henry K.M., Townsend C.A. (2005) Ordering the reductive and cytochrome P450 oxidative steps in demethylsterigmatocystin formation yields general insights into the biosynthesis of aflatoxin and related fungal metabolites. *Journal of American Chemical Society*. 127, 3724-3733.

Herman J.P., de Winde J.H., Archer D., et al. (2007) Genome sequencing and analysis of the versatile cell factory *Aspergillus niger* CBS 513.88. *Nature Biotechnology*. 25, 221-231.

Hoegger P.J., Kilaru S., James T.Y., Thacker J.R., Kues U. (2006) Phylogenetic comparison and classification of laccase and related multicopper oxidase protein sequences. *FEBS Journal*. 273, 2308-2326.

Horie Y., Yamazaki M. (1981) *Transactions of the Mycological Society of Japan*. 22, 113-119.

Huang K., Fujii I., Ebizuka Y, Gomi K., Sankawa U. (1995) Molecular cloning and heterologous expression of the gene encoding dihydrogeodin oxidase, a multicopper blue enzyme from *Aspergillus terreus*. *The Journal of Biological Chemistry*. 270, 21495-21502.

Huang K., Yoshida Y., Mikawa K., Fujii I., Ebizuka Y, Sankawa U. (1996) Purification and characterization of sulochrin oxidase from *Penicillium frequentans*. *Biological and Pharmaceutical Bulletin*. 19, 42-46.

Hutchinson C.R., Kennedy J., Park C., Kendrew S., Auclair K., Vederas J., (2000) Aspects of the biosynthesis of non-aromatic fungal polyketides by iterative polyketide synthases. *Antonie van Leeuwenhoek*. 78, 287–295.

Jarv H., Lehtmaa J., Summerbell R.C., *et al.* (2004) *Neosartorya pseudofischeri* isolated from blood - first hint of pulmonary aspergillosis. *Journal of Clinical Microbiology*. 42, 925-928.

Kallow W., Kennedy J., Arezi B., Turner G. & von Doehren H. (2000) Thioesterase domain of δ -(L- α -aminoadipyl)-L-cysteinyl-D-valine synthetase: alteration of stereospecificity by site-directed mutagenesis. *Journal of Molecular Biology*. 297, 395–408.

Keller N., Hohn T. (1997) Metabolic pathway gene clusters in filamentous fungi. *Fungal Genetics and Biology*. 21, 17–29.

Keller N.P., Turner G., Bennett J.W. (2005) Fungal secondary metabolism - From biochemistry to genomics. *Nature Reviews Microbiology*. 3, 937-947.

Kennedy J. *et al.* (1999) Modulation of polyketide synthase activity by accessory proteins during lovastatin biosynthesis. *Science*. 284, 1368–1372.

Kimura N., Tsuge T. (1993) Gene cluster involved in melanin biosynthesis of the filamentous fungus *Alternaria alternata*. *Journal of Bacteriology*. 175, 4427–4435.

Krappman S., Sasse C., Braus G.H. (2006) Gene targeting in *Aspergillus fumigatus* by homologous recombination is facilitated in a nonhomologous end-joining-deficient genetic background. *Eukaryotic Cell*. 5, 212-215.

Kroken S., Glass N.L., Taylor J.W., Yoder O.J., Turgeon B.G. (2003) Phylogenomic analysis of type I polyketide synthase genes in pathogenic and saprobic ascomycetes. *Proceedings of National Academy of Sciences*. 100, 15670-15675.

Kupfahl C., Heinekamp T., Geginat G., Ruppert T., Hartl A., Hof H., Brakhage A.A. (2006) Deletion of the *gliP* gene of *Aspergillus fumigatus* results in loss of gliotoxin production but has no effect on virulence of the fungus in a low-dose mouse infection model. *Molecular Microbiology*. 62, 292–302.

Lawrence J.G., Roth J.R. (1996) Selfish operons: horizontal transfer may drive the evolution of gene clusters. *Genetics*. 143, 1843–1860.

Lawrence J.G. (1997) Selfish operons and speciation by gene transfer. *Trends in Microbiology*. 5, 355–359.

Lawrence J.G. (1999) Gene transfer, speciation, and the evolution of bacterial genomes. *Current Opinion in Microbiology*. 2, 519–523.

Larsen T.O., Smedsgaard J., Nielsen K.F., Hansen M.A.E., Samson R.A., Frisvad J.C. (2007) Production of mycotoxins by *Aspergillus lentulus* and other medically important and closely related species in section *Fumigati*. *Medical Mycology*. 45, 225-232.

Langfelder K., Jahn B., Gehringer H., Schmidt A., Wanner G., Brakhage A.A. (1998) Identification of a polyketide synthase gene (*pksP*) of *Aspergillus fumigatus* involved in conidial pigment biosynthesis and virulence. *Medical Microbiology and Immunology*. 187, 79-89.

Latge J. (1999) *Aspergillus fumigatus* and aspergillosis. *Clinical Microbiology Reviews*. 12, 310-350.

Latge J. (2001) The Pathobiology of *Aspergillus fumigatus*. *Trends in Microbiology*. 9, 382-389.

Lee D.Y., Teyssier C., Strahl B.D., Stallcup M.R. (2005) Role of protein methylation I regulation of transcription. *Endocrine Reviews*. 26, 147–170.

Li Y., Song Y.C., Liu J.Y., Ma Y.M., Tan R.X. (2005) Anti-*Helicobacter pylori* substances from endophytic fungal cultures. *World Journal of Microbiology and Biotechnology*. 21, 553-558.

Machida, M., Asai K., Sano M., *et al.* (2005) Genome sequencing and analysis of *Aspergillus oryzae*. *Nature*. 438, 1157-1161.

Maiya S., Grundmann A., Li S.M. & Turner, G. (2006) The fumitremorgin gene cluster of *Aspergillus fumigatus*: identification of a gene encoding brevianamide F synthetase. *ChemBioChem*. 7, 1062–1069.

Mitchell C.G., Slight J., Donaldson K. (1997) Diffusible component from the spore surface of the fungus *Aspergillus fumigatus* which inhibits the macrophage oxidative burst is distinct from gliotoxin and other hyphal toxins. *Thorax*. 52, 796-801.

Mootz H.D., Schwarzer D. & Marahiel M.A. (2002) Ways of assembling complex natural products on modular nonribosomal peptide synthetases. *ChemBioChem*. 3, 490–504.

Nakamura K., Go N. (2005) Function and molecular evolution of multicopper blue proteins. *Cellular and Molecular Life Sciences*. 62, 2050-2066.

Neville C.M., Murphy A., Kavanagh K. & Doyle S. (2005) A 4-phosphopantetheinyl transferase mediates non-ribosomal peptide synthetase activation in *Aspergillus fumigatus*. *ChemBioChem*. 6, 679–685.

Nierman W.C., May G., Kim H.S., Anderson M.J. Chen D., Denning D.W. (2005b) What the *Aspergillus* genomes have told us. *Medical Mycology*. 43, S3-S5.

Nierman W.C., Pain A., Anderson M.J., *et al.* (2005a) Genomic sequence of the pathogenic and allergenic filamentous fungus *Aspergillus fumigatus*. *Nature*. 438, 22-29.

Nordlov H., Gatenbeck S. (1982) Enzymatic synthesis of (+)- and (-)-bisdechlorogodin with sulochrin oxidase from *Penicillium frequentans* and *Oospora sulphurea-ochracea*. *Archives of Microbiology*. 131, 208-211.

O'Hara E.B., Timberlake W.E. (1989) Molecular characterization of the *Aspergillus nidulans* yA locus. *Genetics*. 121, 249-254.

Ohashi H., Akiyama H., Nishikori K., Mochizuki Z.I. (1992) Asterric acid, a new endothelin binding inhibitor. *Journal of Antibiotics*. 45, 1684-1685.

Ohashi H., Ueno A., Nakao T., Ito J., Kimura K., Ishikawa M., Kawai H., Iijima H., Osawa T. (1999) Effects of ortho-substituent groups of sulochrin on inhibitory activity to eosinophil degranulation. *Bioorganic and Medicinal Chemistry Letters*. 9, 1945-1948.

Packter N.M, Glover J. (1965) Biosynthesis of [14C]fumigatin in *Aspergillus fumigatus* Fresenius. *Biochimica Et Biophysica Acta*. 100, 50.

Packter N.M. (1966) Studies on biosynthesis of phenols in Fungi - Conversion of [14C]orsellinic acid and [14C]orcinol into fumigatol by *Aspergillus Fumigatus* IMI 89353. *Biochemical Journal* 98, 353-359.

Padhye A.A., Godfrey J.H., Chandler F.W., Peterson S.W. (1994) Osteomyelitis caused by *Neosartorya pseudofischeri*. *Journal of Clinical Microbiology*. 32, 2832-2836.

Parker G.F., Jenner P.C. (1968) Distribution of trypacidin in cultures of *Aspergillus fumigatus*. *Applied Microbiology*. 16, 1251-1252.

Peterson S.W. (1992) *Neosartorya pseudofischeri* sp nov. and its relationship to other species in *Aspergillus* section *Fumigati*. *Mycological Research*. 96, 547-554.

Pettersson G. (1964) Biosynthesis of spinulosin in *Aspergillus fumigatus*. *Acta Chemica Scandinavica*. 18, 335.

Proctor R.H., Brown D.W., Plattner R.D., Desjardins A.E. (2003) Co-expression of 15 contiguous genes delineates a fumonisin biosynthetic gene cluster in *Gibberella moniliformis*. *Fungal Genetics and Biology*. 38, 237-249.

Punt P.J., Oliver R.P., Dingemanse M.A., Pouweisa P.H., van den Hondel C.A. (1987) Transformation of *Aspergillus* based on the hygromycin B resistance marker from *Eschericia coli*. *Gene*. 56, 117-124.

Raper K.B., Fennell D.I. (1965) The Genus *Aspergillus*. Baltimore, Williams &Wilkins.

Rosewich U., Kistler H. (2000) Role of horizontal gene transfer in the evolution of fungi. *Annual Reviews of Phytopathology*. 38, 325–363.

Rawlings B.J. (1999) Biosynthesis of polyketides (other than actinomycete macrolides). *Natural Product Reports*. 16, 425–484.

Record E., Punt P.J., Chamka M., Labat M., van den Hondel C.A., Asther M. (2002) Expression of the *Pycnoporus cinnabarinus* laccase gene in *Aspergillus niger* and characterization of the recombinant enzyme. *European Journal of Biochemistry*. 269, 602-609.

Reeves C.D. (2003) The enzymology of combinatorial biosynthesis. *Critical Reviews in Biotechnology*. 23 (2), 95-147.

Reeves E.P., Reiber K., Neville C., Scheibner O., Kavanagh K., Doyle S. (2006) A nonribosomal peptide synthetase (Pes1) confers protection against oxidative stress in *Aspergillus fumigatus*. *FEBS Journal*. 273, 3038–3053.

Reiber K., Reeves E.P., Neville C., Winkler R., Gebhardt P., Kavanagh K., Doyle S. (2005) The expression of three nonribosomal peptide synthetases in *Aspergillus fumigatus* is mediated by the availability of free iron. *FEMS Microbiology Letters*. 248, 83–91.

Rementería A., Lopez-Molina N., Ludwig A., et al. (2005) Genes and molecules involved in *Aspergillus fumigatus* virulence. *Revista Iberoamericana de Micología*. 22, 1-23.

Samson R.A. (1999) The genus *Aspergillus* with special regard to the *Aspergillus fumigatus* group; in Brakhage A.A., Jahn B., Schmidt A. (eds) *Aspergillus fumigatus*. Biology, clinical aspects and molecular approaches to pathogenicity. In Contributions to Microbiology, Basel, Karger. Vol 2, 5-20.

Samson R.A., Hong S., Frisvad J.C. (2006) Old and new concepts of species differentiation in *Aspergillus*. *Medical Mycology*. 44, S133-S148.

Scherer M., Fischer R. (2001) Molecular characterization of a blue-copper laccase, TILA, of *Aspergillus nidulans*. *FEMS Microbiology Letters*. 199, 207-213.

Schümann J., Hertweck C. (2006) Advances in cloning, functional analysis and heterologous expression of fungal polyketide synthase genes. *Journal of Biotechnology*. 124, 690-703.

Shen B. (2003) Polyketide biosynthesis beyond the type I, II and III polyketide synthase paradigms. *Current Opinion in Chemical Biology*. 7, 285–295.

Sheppard D.C., Doedt T., Chiang L.Y., Kim H.S., Chen D., Nierman W.C., Filler S.G. (2005) The *Aspergillus fumigatus* StuA protein governs the up-regulation of a discrete transcriptional program during the acquisition of developmental competence. *Molecular Biology of the Cell*. 16, 5866–5879.

Smith D.J., Earl A.J., Turner G. (1990a) The multifunctional peptide synthetase performing the first step of penicillin biosynthesis in *Penicillium chrysogenum* is a 421073 dalton protein similar to *Bacillus brevis* peptide antibiotic synthetases. *EMBO Journal*. 9, 2743–2750.

Smith D.J. *et al.* (1990b) β -lactam antibiotic biosynthetic genes have been conserved in clusters in prokaryotes and eukaryotes. *EMBO Journal*. 9, 741–747.

Smith J.E., 1994. *Aspergillus*. Plenum Press, New York.

Smith M.W., Feng D.F., Doolittle R.F. (1992) Evolution by acquisition: the case for horizontal gene transfers. *Trends in Biochemical Science*. 17, 489–493.

Solomon E.I., Sundaram U.M., Machonkin T.E. (1996) Multicopper oxidases and oxygenases. *Chemical Reviews*. 96, 2563-2605.

Stack D., Neville C., Doyle S. (2007) Nonribosomal peptide synthesis in *Aspergillus fumigatus* and other fungi. *Microbiology*. 153, 1297–1306.

Staunton J., Weissman K.J. (2001) Polyketide biosynthesis: a millennium review. *Natural Product Reports*. 18, 380-416.

Suresh Kumar S.V., Phale P.S., Durani S., Wangikar P.P. (2003) Combined sequence and structure analysis of the fungal laccase family. *Biotechnology and Bioengineering*. 83, 386-394.

- Trapp S., Hohn T., McCormick S., Jarvis B. (1998) Characterization of the gene cluster for biosynthesis of macrocyclic trichothecenes in *Myrothecium roridum*. *Molecular and General Genetics*. 257, 421–432.
- Tsai H., Yun C.C., Washburn R.G., Wheeler M.H., Kwon-Chung K.J. (1998) The developmentally regulated *alb1* gene of *Aspergillus fumigatus*: its role in modulation of conidial morphology and virulence. *Journal of Bacteriology*. 180, 3031–3038.
- Tsai H., Wheeler M.H., Chang Y.C., Kwon-Chung K.J. (1999) A developmentally regulated gene cluster involved in conidial pigment biosynthesis in *Aspergillus fumigatus*. *Journal of Biotechnology*. 181, 6469-6477.
- Tsai H., Fujii I., Watanabe A., *et al.* (2001) Pentaketide-melanin biosynthesis in *Aspergillus fumigatus* requires chain-length shortening of a heptaketide precursor. *Journal of Biological Chemistry*. 276, 29292-29298.
- Tudzynski, B. (1999) Biosynthesis of gibberellins in *Gibberella fujikuroi*: biomolecular aspects. *Applied and Environmental Microbiology*. 52, 298–310.
- Tudzynski, P. *et al.* (1999) Evidence for an ergot alkaloid gene cluster in *Claviceps purpurea*. *Molecular and General Genetics*. 261, 133–141.
- Tudzynski B., Hedden P., Carrera E., Gaskin P. (2001) The 450–4 gene of *Gibberella fujikuroi* encodes entkaurine oxidase in the gibberellin biosynthesis pathway. *Applied and Environmental Microbiology*. 67, 3514–3522.
- Turner W.B. (1965) The production of tryptacidin and monomethylsulochrin by *Aspergillus fumigatus*. *Journal of Chemical Society*. 6658-6659.
- Turner W.B. (1971) *Fungal Metabolites*. London, Academic Press.
- Turner W.B., Aldridge D.C. (1983) *Fungal Metabolites II*. London, Academic Press.
- Walton J.J. (2000) Horizontal gene transfer and the evolution of secondary metabolite gene clusters in fungi: an hypothesis. *Fungal Genetics and Biology*. 30, 167–171.

Watanabe A., Fujii I., Tsai H., Chang Y.C., Kwon-Chung J., Ebizuka Y. (2000) *Aspergillus fumigatus alb1* encodes naphthopyrone synthase when expressed in *Aspergillus oryzae*. *FEMS Microbiology Letters*. 192, 39-44.

Williams R.M., Stocking E.M., Sanz-Cervera J.F. (2000) Biosynthesis of Prenylated Alkaloids Derived from Tryptophan. *Topics in Current Chemistry*. 209, 97-173.

Wirsel S., Turgeon, B.G., Yoder, O.C. (1996) Deletion of the *Cochliobolus heterostrophus* mating-type (MAT) locus promotes the function of MAT transgenes. *Current Genetics*. 29, 241-249.

Wortman J.R., Federova N., Crabtree J., Joardar V., Maiti R., Haas B.J., Amedeo P., Lee E., Angiuoli S.V., Jiang B., Anderson M.J., Denning D.W., White O.R., Nierman C. (2006) Whole genome comparison of the *A. fumigatus* family. *Medical Mycology*. 44, S3-S7.

Yamamoto Y., Kiriya N., Arahata S.A. (1968) Studies on the metabolic products of *Aspergillus fumigatus* (3-4). Chemical structures of metabolic products. *Chemical and Pharmaceutical Bulletin*. 16, 304-310.

Yamazaki M., Suzuki S. Miyaki K. (1971) Tremorgenic toxins from *Aspergillus fumigatus* Fres. *Chemical and Pharmaceutical Bulletin*. 19, 1739-1740.

Young C., McMillan L., Telfer E., Scott, B. (2001) Molecular cloning and genetic analysis of an indole-diterpene gene cluster from *Penicillium paxilli*. *Molecular Microbiology*. 39, 754-764.

Yu J., Chang P.K., Ehrlich K.C., *et al.* (2004) Clustered pathway genes in aflatoxin biosynthesis. *Applied and Environmental Microbiology*. 70, 1253-1262.

APPENDIX A

CHEMICALS, ENZYMES AND THEIR SUPPLIERS

Chemical or Enzyme	Supplier
β -mercaptoethanol	Merck
ABTS	Sigma
Acrylamide	Sigma
Agar	Difco
Agarose	Applichem
$\text{CaCl}_2 \cdot 2\text{H}_2\text{O}$	Merck
Calf intestine alkaline phosphatase	Fermentas
Casein Hydrolysate	Difco
Chloroform	Merck
Digoxygenin system	Roche
Dimethylsulfoxide (DMSO)	Merck
DNA Ladder	Genemark
EDTA	Merck
$\text{FeSO}_4 \cdot 7\text{H}_2\text{O}$	Merck
Formaldehyde	Merck
Gel elution kit	Gememark
Glacial Acetic Acid	Merck
Glucose	Merck
Hydrochloric Acid	Merck
Hygromycin	Applichem
Isoamylalcohol	Merck
Isopropanol	Merck

K ₂ HPO ₄	Merck
KH ₂ PO ₄	Merck
Lambda DNA/EcoR I+Hind III	Genemark
Ligation kit	Sigma
Long PCR kit	Fermentas/Qiagen
Lysing enzymes from <i>Trichoderma harzianum</i>	Sigma
Maleic Acid	Merck
Maltose	Difco
MgCl ₂ .7.H ₂ O	Merck
NaOH	Merck
PDA	Merck
Pfu polymerase	Genemark
Plant genomic DNA purification kit	Genemark
Plasmid miniprep purification kit	Genemark
Protein ladder	Genemark
Restriction enzymes	Fermentas
SDS	Merck
Sorbitol	Sigma
Superscript first strand synthesis system for RT-PCR	Invitrogen
Taq DNA Polymerase	Fermentas/Genemark
TEMED	Applichem
Transformation and storage solution (SSCS)	Genemark
Tris	Merck
Trisolution reagent plus	Genemark
Tryptone	Difco
Uracil	Sigma
Uridine	Sigma
Yeast Extract	Merck

APPENDIX B

PREPARATIONS OF GROWTH MEDIA, BUFFERS AND SOLUTIONS

2TY agar

Dissolve 16 g tryptone, 10 g yeast extract, 5 g NaCl and 20 g agar in 1000 ml of water. Autoclave and pour into petri dishes.

Agarose (0.8%)

0.8 g agarose is dissolved in 100 ml TAE buffer by heating and stirring.

Antibody Solution

Anti-digoxygenin-AP is centrifuged for 5 min at 10,000 rpm prior to each use and the necessary amount is carefully pipetted from the surface. Antibody solution is freshly prepared by diluting anti-digoxygenin-AP 1:10,000 (75 mU/ml) in blocking solution.

APS (Ammonium persulfate) (25%)

Dissolve 0.125 g in 0.5 ml water. Prepare fresh.

Blocking Solution

Dilute 10x Blocking Solution 1:10 with Maleic Acid Buffer

Complete Medium (1L)

Dissolve 5.95 g NaNO₃, 0.52 g KCl, 1.5 g KH₂PO₄, 5 g yeast extract, 2 g casein digest and 1 ml trace element solution (1000X). Adjust pH to 6.5 with KOH and

autoclave. After the autoclave, add 2 ml 1 M MgSO₄, 25 ml 40% glucose and 1 ml vitamin solution (1000X).

Czapek-Yeast Autolysate Agar (CYA)

0.3% NaNO₃, 0.5% yeast extract, 3% sucrose, 0.13% K₂HPO₄·3H₂O, 0.05% MgSO₄·7H₂O, 0.05% KCl, 0.001% FeSO₄·7H₂O, 0.0005% CuSO₄·5H₂O, 0.001% ZnSO₄·7H₂O, 1.5% agar.

Denaturation solution

0.5 M NaOH, 1.5 M NaCl

Detection Buffer

0.1 M Tris-HCl, 0.1 M NaCl, pH 9.5

Developing Solution (100 ml)

Measure 2.25 g potassium carbonate, add 2 ml from previously kept pretreatment solution and 75 µl of formaldehyde. Complete the volume to 100 ml with water.

Fixer Solution (100 ml)

50 ml methanol, 12 ml acetic acid, 50 µl 37% formaldehyde. Make up volume to 100 ml with water.

Gel Buffer (100 ml)

Dissolve 18.5 g Tris and 0.4 g SDS in 80 ml water. Adjust pH to 8.9 with concentrated HCl. Make up volume to 100 ml. Filter-sterilize and store at 4°C.

High Stringency Buffer

0.5x SSC containing 0.1% SDS

Hygromycin Agar

Dissolve 1 g yeast extract, 1 g casein digest and 20 g agar in 975 ml water. After the autoclave, add 25 ml 40% glucose and hygromycin making the final concentration 266 µg/ml.

Hygromycin Top Agar

1% agar containing 532 µg/ml hygromycin.

LB ampicillin agar

Dissolve 10 g NaCl, 10 g tryptone, 5 g yeast extract and 20 g agar in 1 l H₂O. After adjusting pH to 7.0 with NaOH, the medium is autoclaved. 100 µg/ml ampicillin is added when it cools to 55°C, and poured to petri dishes (~25 ml/100 mm plate). The plates are covered with foil and stored at 4°C.

LB tetracycline agar

Dissolve 10 g NaCl, 10 g tryptone, 5 g yeast extract and 20 g agar in 1 l H₂O. After adjusting pH to 7.0 with NaOH, the medium is autoclaved. 1.5 ml of 10 mg/ml tetracycline is added when it cools to 55°C, and poured to petri dishes (~25 ml/100 mm plate). The plates are covered with foil and stored at 4°C.

Low Stringency Buffer

2x SSC containing 0.1% SDS

Lytic Solution

20.45 g NaCl was added to 400 ml of water and mixed until dissolved. Then 21.91 g CaCl₂·2H₂O was added and mixed until dissolved. The pH of the solution was adjusted to 5.8 with dilute HCl and autoclaved.

Maleic Acid Buffer

0.1 M Maleic acid, 0.15 M NaCl; adjust with NaOH (solid) to pH 7.5

Malt Extract Autolysate Agar (MEA)

3% malt extract, 0.1% peptone, 2% glucose, 0.0005% $\text{CuSO}_4 \cdot 5\text{H}_2\text{O}$, 0.001% $\text{ZnSO}_4 \cdot 7\text{H}_2\text{O}$, 2% agar.

MgSO₄ (1 M)

Dissolve 24.6 g $\text{MgSO}_4 \cdot 7\text{H}_2\text{O}$ in 100 ml water, autoclave.

Minimal Medium Agar

Complete medium without yeast extract and casein digest + 20% agar

Modified Czapek-Dox Medium

Dissolve 40 g glucose, 1 g NaNO_3 , 1 g KH_2PO_4 , 0.5 g KCl , 0.5 g $\text{MgSO}_4 \cdot 7\text{H}_2\text{O}$, 0.01 g $\text{FeSO}_4 \cdot 7\text{H}_2\text{O}$, 0.01 g $\text{CuSO}_4 \cdot 5\text{H}_2\text{O}$ and 1 g yeast extract in 1000 ml water.

Neutralization solution

0.5 M Tris-HCl (pH 7.5), 1.5 M NaCl

PEG solution

25% PEG-6000, 0.01 M Tris, pH 7.5, 50 mM CaCl_2

Phosphate Buffer (0.5 M, pH 6)

Dissolve 5.648 g KH_2PO_4 , 1.48 g K_2HPO_4 in 100 ml of water.

Pretreatment Solution (100 ml)

Dissolve 0.02 g sodium thiosulfate ($\text{Na}_2\text{S}_2\text{O}_3 \cdot 5\text{H}_2\text{O}$) in 100 ml water. Take 2 ml for further use in developing solution preparation.

Regeneration Medium

Flask A: Dissolve 0.2 g yeast extract, 0.2 g casein digest and 3.2 g agar in 100 ml water. Flask B: Dissolve 68.1 g sucrose in 100 ml water. Autoclave two flasks separately, combine after autoclave.

Running Buffer (1X)

0.25 M Tris, 1.91 M glycine, 1% SDS

Saline/Tween Solution

0.5 NaCl was added to 95 ml of distilled water. While stirring, 2 ml 1% tween solution was added. Distilled water was added up to 100 ml, divided into 10 glass tubes and autoclaved.

Sample Buffer (4X) (5 ml)

Mix 2 ml of 20% SDS, 1 ml of 1M Tris-HCl, pH 7, 1 ml of glycerol and few grains of bromophenol blue. Store at room temperature. Before use, add mercaptoethanol such that the final concentration is 20%.

Silver Nitrate Solution (100 ml)

Dissolve 0.2 g silver nitrate in 100 ml water and add 75 μ l formaldehyde.

SSC (20X)

3 M NaCl, 300 mM sodium citrate, pH 7.0

Stabilized minimal medium top agar

Minimal medium + 0.95 M sucrose and 0.6% agar

Stacking Gel Buffer (100 ml)

Dissolve 5.1 g Tris and 0.4 g SDS in 80 ml water. Adjust pH to 6.7 with concentrated HCl. Make up volume to 100 ml. Filter-sterilize and store at 4°C.

STC solution

1.33 M sorbitol, 0.01 M Tris pH 7.5, 50 mM CaCl₂

TAE buffer (50X)

242 g of Tris base is dissolved in 600 ml of distilled water. The pH is adjusted to 8.0 with approximately 57 ml of glacial acetic acid. Then 100 ml of 0.5 M EDTA (pH 8.0) is added and the volum is adjusted to 1 liter.

Trace Element Solution (1000X)

76 mM ZnSO₄, 178 mM H₃BO₃, 25 mM MnCl₂, 18 mM FeSO₄, 7.1 mM CoCl₂, 6.4 mM CuSO₄, 6.2 mM Na₂MoO₄, 174 mM EDTA.

Tris-HCl buffer

121.1 g Tris base is dissolved in 800 ml of distilled water. The pH is adjusted to the desired value with concentrated hydrochloric acid. The solution is cooled to room temperature before making final adjustment to pH. The volume of the solution is then adjusted to 1 liter with distilled water, dispensed into aliquots and sterilized by autoclaving.

Tween Solution (1%)

10 ml Tween 80 was added to 90 ml of distilled water, mixed well and kept at 4°C.

Vitamin Solution (1000x)

100 mg/l thiamin, 100 mg/l riboflavin, 100 mg/l nicotinamide, 50 mg/l pyridoxine, 10 mg/l panthotenic acid, 0.2 mg/l biotin.

Washing Buffer

0.1 M Maleic acid, 0.15 M NaCl; pH 7.5; 0.3% (v/v) Tween 20

Yeast Extract Sucrose Agar (YES)

2% yeast extract, 15% sucrose, 0.05% MgSO₄.7H₂O, 0.0005% CuSO₄.5H₂O, 0.001% ZnSO₄.7H₂O, 2% agar.

APPENDIX C

PLASMID MAPS

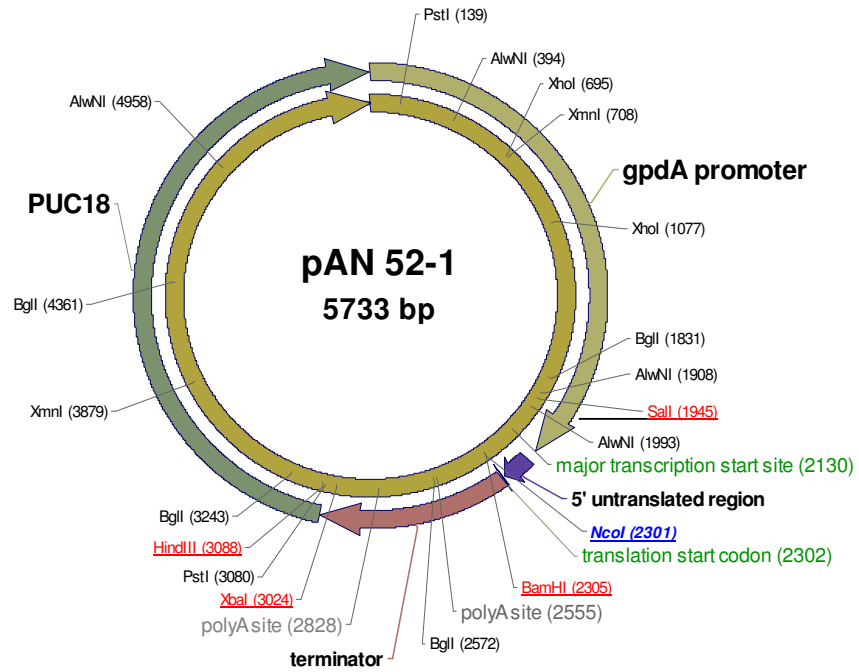


Figure C.1. Map of pAN52-1

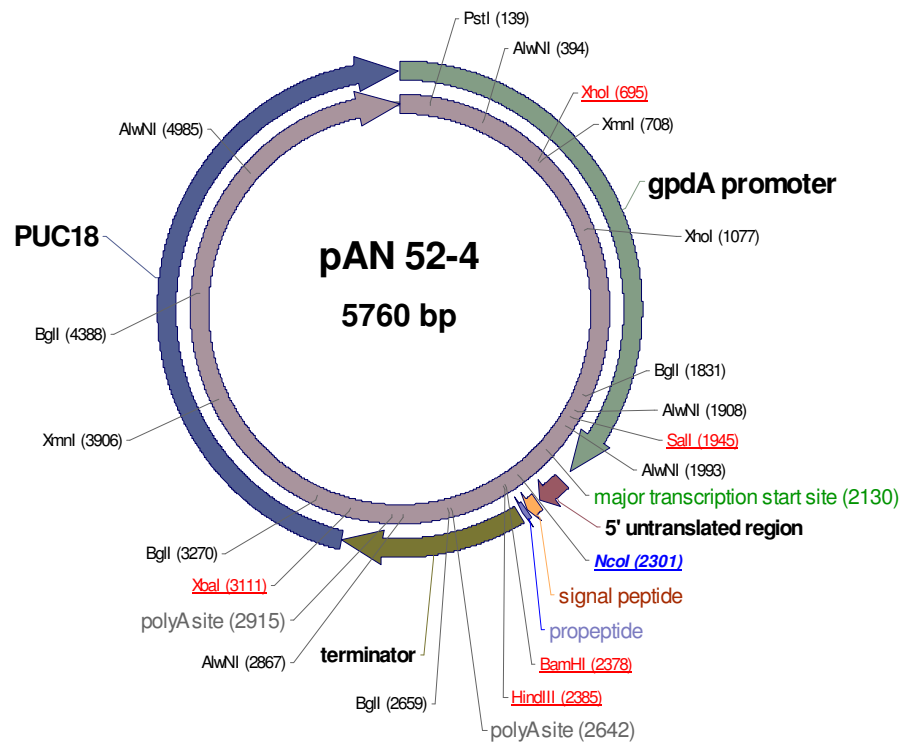


Figure C.2. Map of pAN52-4

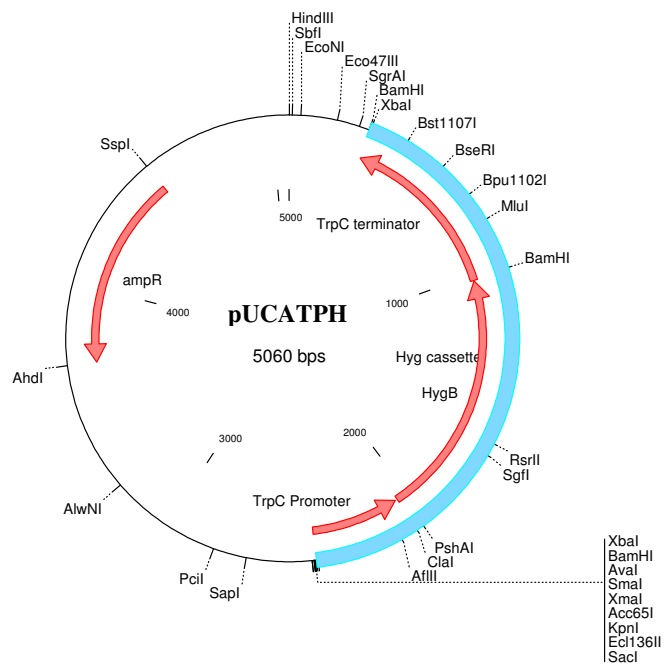


Figure C.3. Map of pUCATPH. Hygromycin cassette in the vector is composed of trpC promoter and trpC terminator sequences originated from *A. nidulans*; and hygromycin B phosphotransferase gene originated from *E. coli*.

CURRICULUM VITAE

PERSONAL INFORMATION

Surname, Name: Metin, Banu

Nationality: Turkish

Date and Place of Birth: 06.03.1978, Ankara

Marital Status: Married

Phone: +90 312 221 30 68

e-mail: banuy@metu.edu.tr

EDUCATION

- 2002 - 2007 Middle East Technical University Ankara/Turkey
PhD in Department of Food Engineering
- 1999 - 2002 Middle East Technical University Ankara/Turkey
MSc in Department of Food Engineering
- 1994 - 1999 Middle East Technical University Ankara/Turkey
BSc in Department of Food Engineering

PROFESSIONAL EXPERIENCE

2006 Sep - 2007 Jan Cornell University Ithaca, CA, USA

Visiting Scientist, Projects:

- *Functional and virulence analysis of pks19 gene of the maize pathogen Cochliobolus heterostrophus*
- *Analysis of domains of Cochliobolus heterostrophus mating type proteins by site-directed mutagenesis*

1999 - 2006 Middle East Technical University Ankara/Turkey

Teaching Assistant in Department of Food Engineering (in Food Chemistry Laboratory, Food Engineering Design (5 times), Process Control Applications in Food Engineering (2 times), Food Engineering Operations I, II, and III, Food Engineering Research (2 times), Food Engineering Laboratory (2 times))

PUBLICATIONS

Metin, B., Lu, S.W., Turgeon, B.G. (2007) Does the single Dothideomycete MAT1-1-1 protein harbor domains for activities performed by multiple MAT1-1 proteins from Sordariomycetes? 24th Fungal Genetics Conference, Asilomar, CA, USA. (Meeting Abstract)

Yalcindag (Metin), B., Ogel, Z.B. (2006) Molecular Genetics of Secondary Metabolite Biosynthesis in *Aspergillus* Species. National Congress of Fungal Infections and Clinical Mycology, Bursa, Turkey. (Chapter in the Congress Book)

Yalcindag (Metin), B., Bakir, U, Ogel, Z.B. (2006) Cloning and Heterologous Expression of a Laccase Orthologue from *Aspergillus fumigatus* and Functional Analysis of the Associated Gene Cluster. Advances Against Aspergillosis II, Athens, Greece. (Meeting Abstract)

Yalcindag (Metin), B., Ogel, Z.B., Bakir, U. (2005) Cloning and Heterologous Expression of a Laccase Orthologue from *Aspergillus fumigatus* and Functional Analysis of the Associated Gene Cluster. European Biotechnology Congress, Copenhagen, Denmark (Meeting Abstract)

Yalcindag (Metin), B., Ogel, Z.B., Bakir, U. (2005) Cloning and Heterologous Expression of a Laccase Orthologue from *Aspergillus fumigatus* and Functional Analysis of the Associated Gene Cluster. XIV. National Biotechnology Congress, Eskisehir, Turkey. (Meeting abstract)

Yalcindag (Metin), B., Ogel, Z.B., Bakir, U. (2005) Functional analysis of a laccase gene of the mycotoxin producing human parhogen *Aspergillus fumigatus*. II. National Mycotoxin Symposium, Istanbul, Turkey. (Meeting abstract)

Yalcindag (Metin), B., Ogel, Z.B., Bakir, U. (2004) Functional genomic studies on laccases of *Aspergillus fumigatus*. Advances Against Aspergillosis I, San Francisco, California, USA. (Meeting abstract)

Yalcindag (Metin), B., Ogel, Z.B., Bakir, U. (2004) Functional analysis of a laccase gene of the mycotoxin producing human pathogen *Aspergillus fumigatus*. II. National Bioinformatics Congress, Istanbul, Turkey. (Meeting abstract)

Yalçındağ (Metin), Banu. (2002) Alpha-galactosidase gene cloning from *Aspergillus fumigatus*. Middle East Technical University, Ankara/Turkey. (MSc thesis)

Yalçındağ (Metin), B., Ögel, Z.B., Bakır, U., Biely, P. (2002). Alpha-galactosidase gene cloning from *Aspergillus fumigatus*. International Mycological Congress, Oslo, Norway. (Meeting abstract)

Yalcindag (Metin), B., Ogel, Z.B., Bakir, U., Biely, P. (2001). Cloning of alpha-galactosidase gene of *Aspergillus fumigatus*. XII. National Biotechnology Congress, Ayvalik, Balikesir-Turkey. (Meeting abstract)

SCHOLARSHIPS OR FELLOWSHIPS

- 24th Fungal Genetics Conference (Asilomar, CA, USA, 2007): Registration fee.
- The Scientific and Technological Research Council of Turkey, 2006: 4 month period of research fellowship in Cornell University, USA.
- Advances Against Aspergillosis Congress II (Athens, Greece, 2006): Registration fee, accommodation, food expenses, congress dinner
- Advances Against Aspergillosis Congress I (San Francisco, USA, 2004): Registration fee, travel expenses, accommodation, food expenses, congress dinner.
- International Mycological Congress (Oslo, Norway, 2002): Registration fee, travel expenses, accommodation, food expenses, congress dinner.

HOBBIES

Painting, yoga, travelling, shopping